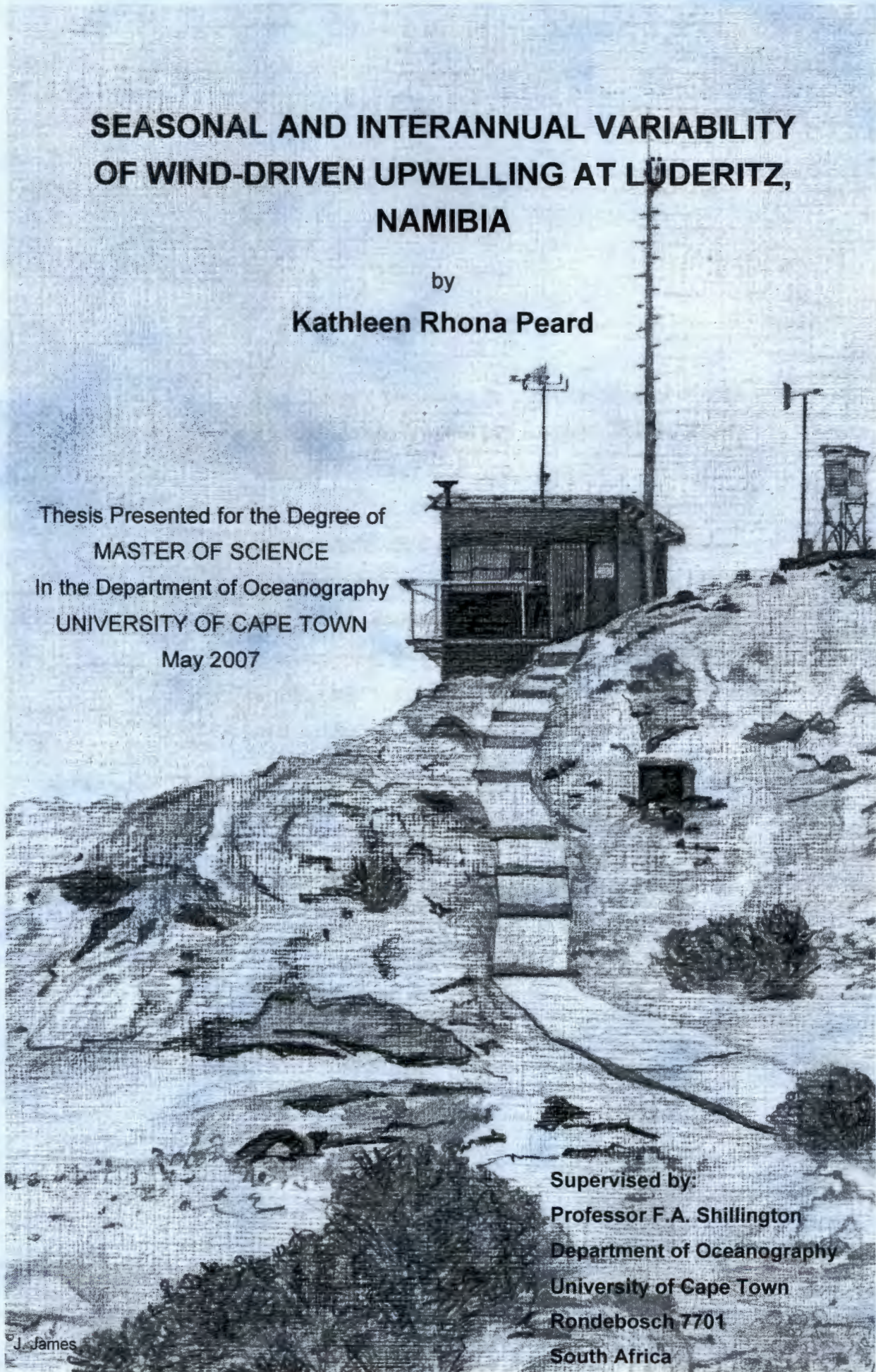


**SEASONAL AND INTERANNUAL VARIABILITY  
OF WIND-DRIVEN UPWELLING AT LÜDERITZ,  
NAMIBIA**

by  
**Kathleen Rhona Peard**

Thesis Presented for the Degree of  
**MASTER OF SCIENCE**  
In the Department of Oceanography  
**UNIVERSITY OF CAPE TOWN**  
May 2007

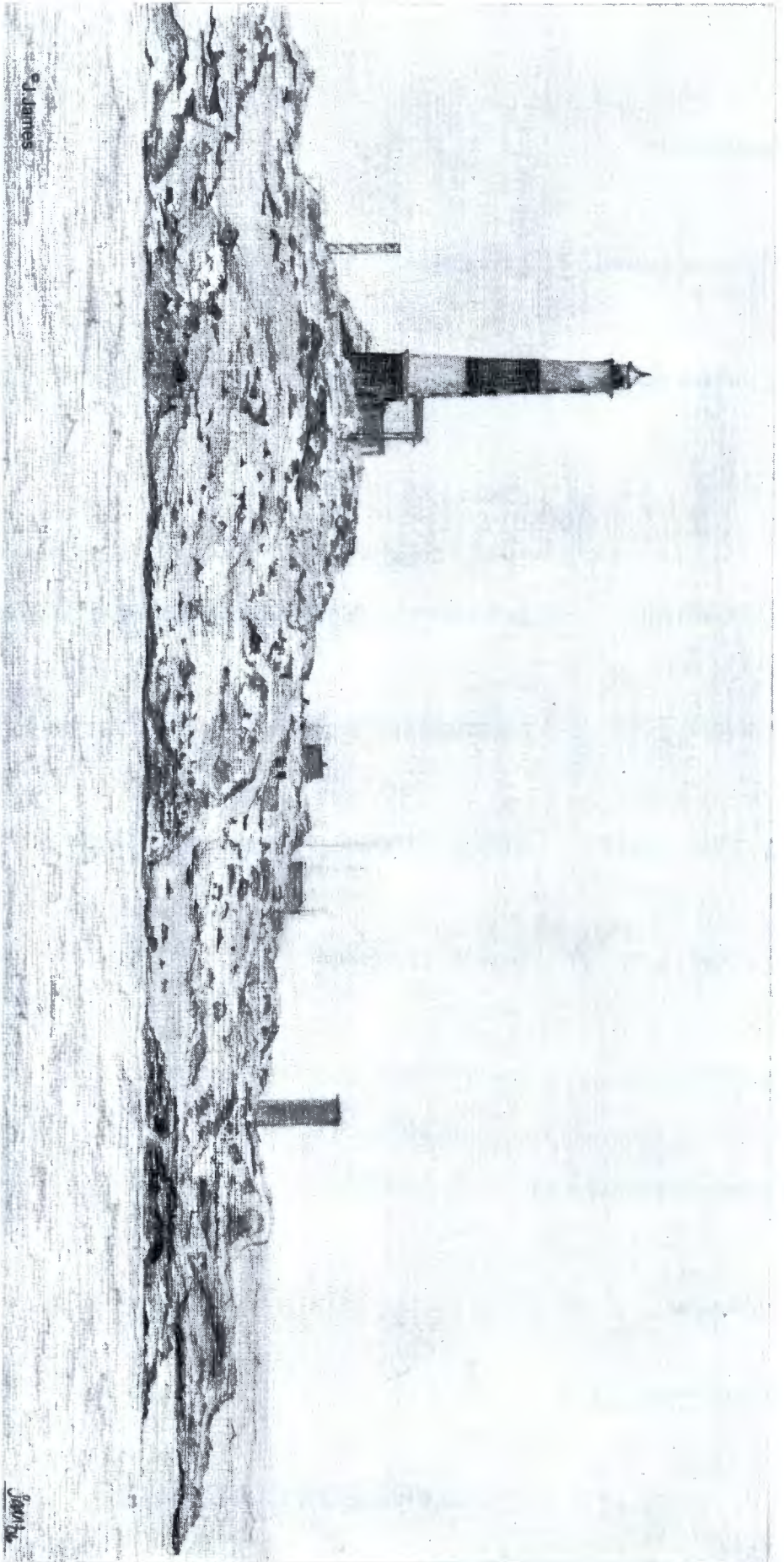
Supervised by:  
**Professor F.A. Shillington**  
Department of Oceanography  
University of Cape Town  
Rondebosch 7701  
South Africa



The copyright of this thesis vests in the author. No quotation from it or information derived from it is to be published without full acknowledgement of the source. The thesis is to be used for private study or non-commercial research purposes only.

Published by the University of Cape Town (UCT) in terms of the non-exclusive license granted to UCT by the author.

This thesis is dedicated to a unique band of people, the last of their era, the Lightkeepers at Dias Point Lighthouse. They lived and worked in an extreme environment of wind, sand and isolation in a spirit of camaraderie - to Carla and Frank, Orti and Crispin, Sylvi and their canine friends, Beriley, Bella, Mabel and Monty. You were there at any time of the night to tell us how strong the wind was, to keep the light shining and to listen out for those in peril on the sea. In the data you and those before you recorded, your work lives on.



© James

Dias Point Lighthouse

James

## TABLE OF CONTENTS

CHAPTER TITLE	PAGES
<b>Abstract</b> .....	i
<b>Acknowledgements</b> .....	iii
<b>Chapter One</b> Introduction and Key Questions.....	1
<b>Chapter Two</b> Data and Methods.....	11
<b>Chapter Three</b> Diurnal variability in the wind at Lüderitz.....	25
<b>Chapter Four</b> Seasonal variability in wind-driven upwelling at Lüderitz.....	35
<b>Chapter Five</b> The influence of wind stress on sea surface temperature and on the temperature dynamics in the water column at Lüderitz.....	49
<b>Chapter Six</b> Long term variability in the wind regime at Lüderitz.....	71
<b>Chapter Seven</b> Conclusion.....	95
<b>References</b> .....	101

## Abstract

**Author:** Kathleen Rhona Peard

**Title:** Seasonal and Interannual variability of wind-driven upwelling at Lüderitz, Namibia

**Date:** May 2007

The aim of this study is to examine the variability in the wind regime at diurnal, seasonal, interannual and interdecadal time scales. Meteorological measurements including wind speed, wind direction and air pressure collected at Dias Point Lighthouse ( $26^{\circ} 38.094'S$   $15^{\circ} 05.612'E$ ) at hourly to eight-hourly intervals from 1960 to 2006 are analysed. Known instrument changes in the time series are validated where possible.

Predominant winds at Lüderitz blow parallel to the South to North alignment of the coast. Ekman divergence in response to longshore, equatorward wind stress drives coastal upwelling at Lüderitz, the main centre of upwelling in the Benguela Current System. Wind stress is proportional to the square of the wind speed parallel to the coast and is a proxy for upwelling.

A diurnal intensification of wind speeds occurred in all seasons at Lüderitz with a concomitant change in wind direction from south in the early morning to southwest in the afternoon. Pressure changes over the continent due to daytime heating and night-time cooling of the land underlie this variability.

Southwesterly winds predominate throughout the year at Lüderitz. Maximum wind stress occurs in the austral summer with a fourfold decrease in wind stress during the austral winter. Highest wind stress was recorded from November to January and lowest wind stress from May to July. The wind mixing index, a measure of turbulent mixing calculated from total wind speed cubed, follows the same seasonal pattern

indicating the predominance of southerly winds. The wind minimum at Lüderitz is caused by weakened pressure gradients due to the latitudinal northwesterly shift in the position of the South Atlantic Anticyclone in winter combined with a pressure increase over the continent.

A significant relationship was established between pulses of southerly wind at Lüderitz and lowered Sea Surface Temperature in all seasons. During intermittent periods of calm or northerly winds surface layers warmed, particularly in summer, and a stable stratified structure developed in the water column. Resumption of southerly winds caused stratification to break down within two days, vertical temperature profiles after upwelling indicating replacement of surface water with colder bottom water. The Temperature - Salinity properties of surface and sub-thermocline water sampled during and after strong wind stress indicate Central Water origin.

Periods of almost consistently below-average (1960 to 1975, 1988 to 2006) or above-average wind stress (1975 to 1988) were identified in the Lüderitz time series, with turning points in 1975 and 1988. A significant increase in the frequency of occurrence of northerly winds and calm occurred in the South-North sector, but no trend in the occurrence of southerly winds. Westerly winds also increased in frequency. The cause of this interdecadal variability is unknown but large-scale atmospheric pressure changes are hypothesized. As the main upwelling cell at Lüderitz is the source of nutrients for the downstream Northern Benguela system, the consequent variability in productivity of the ecosystem is of extreme significance.

Variability in the wind regime at Lüderitz could provide the key to understanding the dynamics and variability of the Northern Benguela ecosystem therefore the continuation of the time series is of national importance particularly to the Fisheries sector.

## Acknowledgements

The data analysed in this study was largely collected and recorded by Lightkeepers at Dias Point Lighthouse. Their mainly anonymous contribution is gratefully acknowledged as is the dedication and commitment of Carla Jooste, Orti Clay and Frank Jooste, Lightkeepers responsible for meteorological data collection at Dias Point between 1989 and 1998.

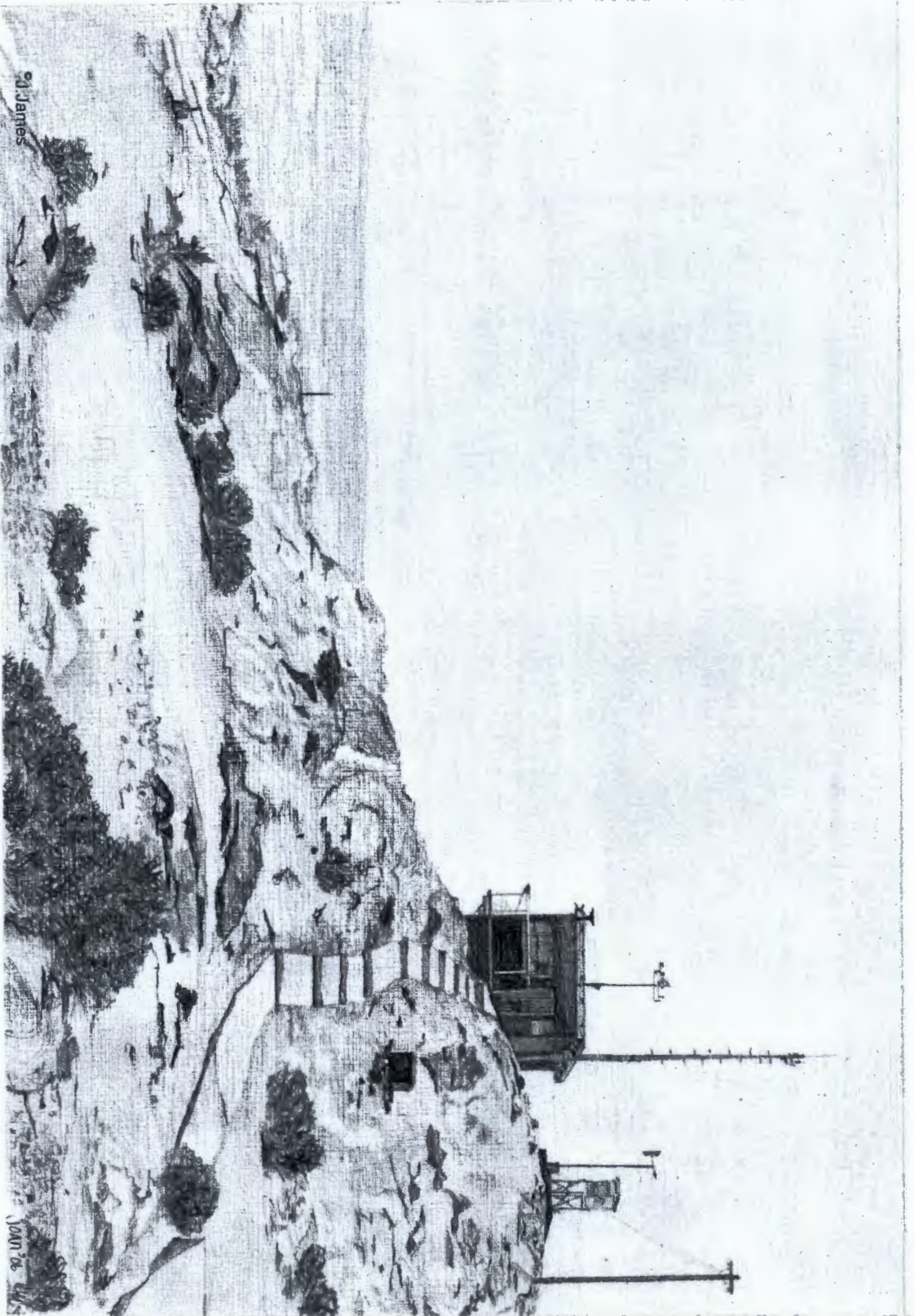
The data collection from 1998 was completed while employed in the Environment Subdivision at Lüderitz Marine Research by the Namibian Ministry of Fisheries and Marine Resources (MFMR). Funding of weather station equipment at Dias Point from 1996 to 2006 was provided by BENEFIT / GTZ through the Inshore Monitoring Project. The logistical support of the BENEFIT Secretariat ensured that the time series was maintained without any interruptions in data collection. BENEFIT is also thanked for funding my registration fees for 3 years. Alan Kemp (then MFMR) and Neil Needham (then SFRI, RSA) are thanked for technical expertise in setting up the automatic weather station. NAMDEB assisted with surveying the site. NAMPORT made the Lightkeeper's watch office available as a locality for the automatic weather station, thus ensuring valuable continuity in the measurement site at Dias Point. Richard Callard is acknowledged for computerizing the 1960 to 1989 Lighthouse wind database.

The end would never have been reached without the tireless enthusiasm and encouragement of my colleague Dr Jean-Paul Roux, who is very sincerely thanked for many discussions and take-away doodlegrams. Statistical advice from Prof Les Underhill was also most helpful. Thanks to Alex Hendricks for technical assistance. The captain, Mr. S. Jason, and crew of the *RV Kuiseb* are thanked for Dias Point monitoring cruises and the contribution of MFMR staff who assisted on these cruises is acknowledged.

Special thanks to Joan James for her wonderful pencil sketches, drawn from photographs by Rian Jones - both are thanked for their Mercury Island perspective. Dr Jessica Kemper's invaluable spheniscid-inspired advice was gratefully received during long dog walks with our sister pups. Bronwen Currie's support is also specially acknowledged.

My parents are thanked for their encouragement and for making my academic studies and a wonderful career choice possible; and my husband Gino Noli for his unwavering support.

Finally, my supervisor Prof Frank Shillington is thanked for his patience with a long-distance, part-time student and for his scientific guidance.



© J. James

Dias Point Lightkeeper's Watch Office

1900-20

# Chapter One

## Introduction and Key Questions



© J. James

# Introduction and Key Questions

## 1.1. Introduction

Descriptions in the literature of the wind on the Namibian coast are few and incidental, generally from the Pelican Point Lighthouse off Walvis Bay (Shannon and Nelson 1996, Hart and Currie 1960, Stander 1964, Boyd 1987). This is partly due to the bias of oceanographic and fisheries research focus on the northern Namibian coast as a result of the productive pelagic fishery situated downstream of the main Lüderitz upwelling cell.

In addition to Pelican Point, a time series of meteorological data was collected on the southern Namibian coast, from Dias Point Lighthouse, situated close to Lüderitz at 26° 38'S 15° 05'E. Data from this ex-South African Railways Lighthouse station (taken over by the Namibian Ports Authority, NAMPORT, in 1990) is available from mid-1960 until the close of the manned Lighthouse station in 1998. The Namibian Ministry of Fisheries and Marine Resources (MFMR) installed an automatic weather station in 1998, with ongoing data collection. During the period when Dias Point Lighthouse was manned, Lightkeepers were on watch around the clock and their duties included meteorological observations at least three times per day, which were recorded in logbooks and transmitted by telephone to the Weather Bureau. Meteorological observations and measurements related to wind speed, wind direction, air pressure, air temperature, clouds, visibility, precipitation and sea state were recorded. Weather logs were not kept indefinitely at the station, thus wind data was retrievable from 1960 but sea level pressure only from 1978.

Bailey (1979) has described the major features of the Dias Point wind field in relation to hydrographical data collected from 1976 to 1977 between 24°S and 28°S and up to 100 miles offshore. Using Dias Point Lighthouse wind records from 1971 to 1977 Bailey (1979) found that southerly winds were strongest and most frequent, favouring coastal upwelling due to the interaction of the equatorward wind blowing parallel to the coast and the rotation of the earth by Coriolis force. Diurnal changes in

wind speed and direction were analysed and the coastal wind regime found to be under the influence of diurnal heating and cooling of the continental landmass. Bailey was able to relate the dynamic response of the water column in terms of temperature, salinity, oxygen and nutrient chemistry to the Dias Point wind regime during active upwelling and downwelling events.

### **1.1.1. Overview of meteorological and hydrographical features related to coastal upwelling at Lüderitz**

The eastern boundary of the South Atlantic subtropical gyre between latitudes 15° and 34°S and extending some 200 km offshore from the coastline is known as the Benguela Current system (Shannon 1970, Nelson and Hutchings 1983). The oceanography of this highly dynamic current is dominated by coastal upwelling initiated by an equatorward, longshore wind regime (Shannon 1985).

A combination of atmospheric forcing factors gives rise to the longshore wind regime off Lüderitz. These include the atmospheric high pressure cell situated over the South Atlantic, forming part of the discontinuous high pressure belt that circles the southern hemisphere at about 30°S, and associated anticyclonic air flow (Tyson and Preston-Whyte 2000). A strong pressure gradient is set up by the juxtaposition of the South Atlantic Anticyclone (SAA) and the continental heat-induced low pressure system over the land. The air flow around the SAA is guided by the northeast coastline orientation of southern Africa and by the arid nature of the western coast interior, which further enhances longshore flow by setting up a thermal cross-flow barrier (Nelson and Hutchings 1983, Shannon and Nelson 1996). In addition, as illustrated by Boyd (1987), the landmass at Lüderitz (26° 38'S) and Cape Frio (18° 24'S), extends westwards away from the mean coastline orientation, thus being more exposed to the energy of the SAA and southeast Atlantic water masses than other coastline stretches. It is offshore of these two areas that the two main upwelling cells in the northern Benguela are located (Boyd 1987). The Walvis Bay region by comparison forms a sheltered concave bight with a local minimum in offshore Ekman transport, thus a relatively low turbulence environment due to lower wind stress (Bakun 1996). A local maximum in the offshore Ekman transport has

been reported for the Lüderitz area (Boyd 1987) and upwelling is considered to be perennial at Lüderitz (Bailey 1979, Boyd 1987). From Dias Point Lighthouse wind records for the period 1971 to 1977, Bailey (1979) found the maximum in occurrence of upwelling-favourable winds between August and February. The period of most active upwelling in the Lüderitz region has been reported from other studies as being May to January (Cushing 1969 as cited in Bailey 1979), September to December (Schell 1968 as cited in Bailey 1969) and July to September / October (Stander 1964, Hagen *et al.* 2001).

The southerly upwelling-favourable winds off Lüderitz are subject to periodic modulation by the passage in the westerly wind belt between 35°S and 45°S of eastward-moving low pressure cells (Nelson and Hutchings 1983). In summer, these cyclonic cells pass south of the subcontinent, causing weakening of the SAA and an abatement of the southerly winds. In winter, due to the more northerly position of the SAA and higher pressure over the subcontinent (Tyson and Preston-Whyte 2000), the low pressure systems shift further north within the more northerly passage of the westerlies over the southern Cape. The winter northward migration of the pressure systems induces a strong seasonality upon the wind-induced upwelling regime of the southern Benguela (Shannon 1985). Upwelling-favourable south-easterlies constitute less than 10% of the winds in the southern Benguela in winter, compared with 50 to 70% in summer (Andrews and Hutchings 1980).

Associated with the passage of low pressure cells in the westerly wind belt as described above is the development of coastal lows off 25°S, north of Lüderitz. These systems have important consequences as they result in the periodic "switching off" of the southerly wind regime at Lüderitz. Northerly winds predominate during the passage of the low, causing downwelling of surface water against the shore. The formation of a coastal low is preceded by the intensification of the wind at Lüderitz as the SAA approaches the land behind a cold front low pressure system in the westerlies trailing across or to the south of the Cape. Depending on the intensity of the low the SAA may be entrained eastward toward Cape Town (termed ridging – an elongated local region of high pressure). As a result, high pressure becomes established over the southeastern part of the African continent. The anticyclonic air

circulation around the high causes easterly winds that, on descending the escarpment, attain cyclonic vorticity due to vertical expansion of the air column, resulting in a low pressure cell over the coast (Tyson and Preston-Whyte 2000). As the ridging process continues further eastward, offshore flow extends further south on the west coast and hence coastal low propagation is induced, travelling southwards at 4 to 5 degrees of latitude per day towards the Cape Peninsula (Reason and Jury 1990). The modulation of the southerly wind regime at Lüderitz is thus under atmospheric control and occurs at a synoptic scale of 3 to 10 days (Shannon and Nelson 1996).

From the early descriptions of the Benguela current, it was characterised as a cold coastal current flowing in a northwesterly direction, and the patchy nature of the cold water was soon recognised (Rennell 1832 and Bourke 1878 as cited by Hart and Currie 1960). The origin of the lowered coastal water temperatures from upwelling was confirmed in the early 20<sup>th</sup> century, and the coastal area off Lüderitz was identified as a centre of upwelling (Schott *et al.* 1914 as cited in Hart and Currie 1960, Copenhagen 1953). Lower surface temperatures were recorded between the Orange River and north of Lüderitz (Stander 1964) and at other localities along the Namibian coast including Cape Frio to Kunene River mouth (Hart and Currie 1960). The Lüderitz upwelling cell is now recognised as being the principal centre of upwelling in the Benguela (Shannon 1985) and is possibly the strongest coastal upwelling centre in the world (Bakun 1996).

Ekman divergence, in response to longshore wind stress on the ocean surface, is the primary driving mechanism for coastal upwelling in eastern boundary currents such as the Benguela (Nelson 1992). It causes offshore surface flow due to Coriolis force and the displacement of surface water causes a lowering of the sea surface at the coast. A pressure gradient is established and the mass imbalance is quickly replaced from below the surface (Bakun 1996). The upward movement (upwelling) of subsurface water entrains bottom water flowing towards the coast along the sea floor contour, thus replacing the displaced surface water near the coast. The response time of the water column to the onset of upwelling-favourable winds described from changes in temperature, salinity and nutrients off the Cape Peninsula was almost

immediate in the surface layers compared with a slower response time in deep water (Andrews and Hutchings 1980). Similar studies relating wind direction changes to oceanographic response in the Lüderitz upwelling cell are limited to the description by Bang (1971) as cited in Shannon (1985).

Upwelled water on the west coast south of the Orange River is of South Atlantic Central Water origin, which typically has a temperature of 11° to 12°C, salinity of < 35.0 psu, and sigma-t of 26.7 kg.m<sup>-3</sup> (Shannon 1966 as cited in Bailey 1979). Bailey (1979) found a longshore band of upwelled South Atlantic Central Water with sigma-t of 26.7 kg.m<sup>-3</sup> between just south of 25°S and 28°S during active upwelling. A broader definition of Central Water upwelling on the coast between Cape Frio and Cape Point was described and illustrated by Shannon (1985) as the linear portion of the curve connecting the approximate points 6°C, 34.5 psu and 16°C, 35.5 psu (Figure 11 in Shannon 1985). On the southern coast of Namibia (25°S to 28° 30'S) the depth from which upwelled waters originate is between 200 and 350 meters (Hart and Currie 1960, Stander 1964, Bailey 1979). Upwelling off Lüderitz is enhanced by the narrow continental shelf which is 100 to 140 km wide between 24°S and 26° 30'S and 75 km wide at 27°S (just south of Lüderitz), the latter being one of the narrowest parts of the continental shelf in the Benguela region (Shannon 1985, Boyd 1987).

Wind-induced upwelling is known to be the dominant mechanism for bringing nutrients to the coastal surface waters in the California, Peru, Canary and Benguela eastern boundary currents (Mann and Lazier 1991). Bailey (1979) in his study of the water masses, oxygen dynamics and nutrient chemistry of the Lüderitz upwelling cell, found that the horizontal concentration of nutrients within his study area (24° 30'S to 27° 56'S) generally decreased offshore, particularly in surface waters, and increased with water depth. During active upwelling high concentrations of silicate (5 – 20 µg atoms/l and up to 50 µg atoms/l inshore), nitrate (15 – 20 µg atoms/l) and phosphate (2 – 3 µg atoms/l) were sampled nearshore in the surface waters just north and south of Lüderitz, demarcating the areas where upwelling is most pronounced (Bailey 1979).

Nutrients are supplied to the surface waters by Ekman “pumping” in the Lüderitz upwelling cell, potentially enhancing the productivity of these waters during quiescent periods. However, the year round high wind speeds cause turbulent mixing which is detrimental to phytoplankton (as cells are continually removed from the photic zone), and advective losses are also high (Carr 2002). The wind speed cubed ( $W^3$ ) component is a measure of the rate of input of turbulent kinetic energy from wind to ocean (Bakun 1996) and is an index of the stability of the upper water column. High values of  $W^3$  cause both vertical motion within the water column and vertical mixing which destroys vertical stability, negatively affecting primary and secondary production (Agenbag and Shannon 1988). Thus although the maximum annual primary production in the Benguela current (calculated from satellite-measured data) is the highest of all the Eastern Boundary currents, the least productive area in the Benguela is that between 25°S and 28°S approximately the area of the Lüderitz cell. The most productive area lies between 18°S and 24°S (Carr 2002). North of 24° 30'S, downstream of the Lüderitz upwelling cell, there is a marked reduction in turbulent wind mixing (Agenbag and Shannon 1988), thus favourable conditions for phytoplankton growth enhanced by the presence of upwelled nutrients. The intense upwelling at Lüderitz is considered a biological barrier to movement of certain fish species between the northern and southern Benguela due to low food availability to phyto- and zooplankters during active upwelling. Migration through the area is only possible for these species in years of much reduced upwelling (Agenbag and Shannon 1988).

### **1.1.2. Linkages to Fisheries and Ecosystem Studies**

Lüderitz is the harbour base for the Namibian commercial spiny rock lobster (*Jasus lalandii*) fisheries. In recent years the direct effect of the wind (and swell) regime on the lobster vessels has come under scrutiny as having a significant effect on the catch per unit effort of the lobster fishing fleet (Grobler and Peard 2006). In addition the wind-driven upwelling dynamics of the Lüderitz area affects the oxygen regime of the lobster reefs (Peard and Roux 2002). Dissolved oxygen levels on the inshore reefs determine inshore - offshore migration patterns of the rock lobster (Tomalin

1993), which also affects the availability of the resource to the shallow inshore trap fishery (Grobler and Noli-Peard 1997).

Research on the population dynamics of endemic Benguela species such as the Cape Fur seal (*Arctocephalus pusillus pusillus*) and African penguin (*Spheniscus demersus*) has shown that these species are dependent on a strong wind-driven upwelling regime. There can be a direct effect on survival of young life stages in times of calm or “berg” wind (hot offshore easterly wind) conditions, as has been described for Cape Fur seal pups (de Villiers and Roux 1992) and African Penguin chicks (Kemper 2006). Low wind conditions cause high ambient temperatures that can result in hyperthermia-induced death on exposed breeding colonies. The indirect effect of interannual changes in the upwelling-favourable wind regime at Lüderitz on top predators through prey availability indicates that the entire food web is affected by such environmental variability (Roux 2003, Roux and Shannon 2004). High interannual variability in Cape Fur seal abundance at mainland colonies near Lüderitz post-1990 is related to food availability (Roux 1998), and the Lüderitz summer wind regime (weak / strong upwelling) has been used to predict seal pup growth in winter, with high pup mass in winter significantly correlated to a strong summer upwelling season (Roux *et al.* 2007).

The environment has been recognised as a contributing forcing factor for an ecosystem regime shift in the Northern Benguela. A regime shift is defined as the process whereby a large marine ecosystem that is climate-linked, undergoes a shift in state over a 10 to 30 year period (Beamish and Mahnken 1999 as cited in Cury and Shannon 2004). The structure and function of the marine ecosystem off Namibia has undergone major changes since the mid 1970s (crash of anchovy and sardine populations in 1970s, dominance of zooplanktivorous horse mackerel, mesopelagics and pelagic gobies in the 1980s, increase in jellyfish abundance) (Van der Lingen *et al.* 2006). During the 1990s most major fish stocks declined, with a concomitant reduction in biomass of top predators, and the low levels of biomass in the northern Benguela are seen as an indication of a shift to a new ecosystem regime (Cury and Shannon 2004). Environmental events through “bottom-up” control of the food web via phyto- or zooplankton are thought to have initiated these ecosystem changes,

sustained by environmental anomalies such as the 1995 Benguela Niño, and influenced by “top-down” control in the form of heavy fishing pressure. Environmental changes such as intensity of upwelling (related to wind patterns such as are described in this thesis), changes in temperature and circulation are physical mechanisms that sustain regime shifts and trigger associated biological changes in the “new” ecosystem state (Cury and Shannon 2004).

With regional programmes underway in southern Africa, such as ENVIFISH (Environmental Conditions and Fluctuations in Recruitment and Distribution of Small Pelagic Fish Stocks), IDYLE (Interactions and Spatial Dynamics of Renewable Resources in Upwelling Ecosystems), BENEFIT (Benguela Environment, Fisheries Interaction and Training) and BCLME (Benguela Current Large Marine Ecosystem) there is an increasing urgency to bring oceanographic and fisheries science closer together, and to examine data sets in tandem. With more than 100 years marine science behind South Africa, including the pre-independence participation of South African scientists based in Walvis Bay and Lüderitz, combined with Namibia's own post-independence Fisheries research programme, the information at the necessary time and spatial scales is gradually being accumulated to this end. Routine monitoring programmes and the systematic collection of accurate data sets forms the basis for long time series that are essential for retrospective analyses of trends at an interdecadal scale.

## **1.2. Key Questions**

A previous study by Bailey (1979) has described some of the features of the wind regime at Lüderitz using the Dias Point Lighthouse data. However only a limited portion of the data set was used at the time (7 years) and subsequently an additional 29 years data has been collected. This includes hourly data from an automatic weather station enabling a finer resolution of processes than was possible using 8-hourly data. The aim of this study is thus to describe the 46-year time series in further detail, particularly looking at variability in the wind field at diurnal, seasonal,

interannual and interdecadal time scales in accordance with the following key questions:

- 1) What is the diurnal variation in the sea level pressure (SLP), wind speed and wind direction at Dias Point? Does the diurnal variation exhibit a seasonal modulation?
- 2) What is the seasonal pattern in wind speed at Lüderitz?
- 3) Can the wind regime at Dias Point be used as a proxy for upwelling events close inshore and within 20 km of the coast?
- 4) What long-term changes in the wind regime have taken place on an interannual and interdecadal time scale of a) wind speed and b) wind direction?

Each key question is addressed separately in a chapter, in the manner of a paper. Within each chapter the tables and figures follow the text while references cited are combined for all chapters at the end of the thesis. A concluding chapter (Chapter Seven) provides a synthesis of the main findings of the thesis.



# Chapter Two

## Data and Methods



## Data and Methods

The aim of this chapter is to present the data source, instrumentation, validation of instrument changes, data description and methods that were used in compiling the wind and sea level pressure time series presented in this thesis. Individual chapters describe specific methods in more detail.

### 2.1. Locality

The meteorological instruments were situated at the Lighthouse Keeper's watch office at Dias Point, 26°38.094'S 15°05.612'E (Figure 2.1). The Lighthouse and associated buildings are situated on a peninsula separated from Lüderitz by a large body of water consisting of Shearwater Bay, Lüderitz Lagoon and Lüderitz Bay. The peninsula juts northward, ending in a narrow, exposed rocky headland on which the Lighthouse and associated buildings are located (Figure 2.2). The terrain is generally flat with isolated rocky ridges and outcrops interspersed with sandy flat areas (Figure 2.3).

### 2.2. Instrumentation

#### 2.2.1. Wind

Wind speed and direction readings were measured by means of a deflection (pressure) plate and wind vane situated on a rising slope 8.5 m south of the watch office from 1960 until 1990. Readings from this instrument were made on the hour three or seven times per day and recorded in weather log books along with additional meteorological measurements and observations, such as air pressure, air temperature, visibility, cloud cover and swell.

From 1990 a cup anemometer with a direction vane was used for wind measurements (Carla Jooste *pers. com.*). The anemometer was located on the roof of the watch office at a height of approximately 8 m above the roof, and

approximately 24 m above sea level. In 1996, an *Aanderaa Model 2740* cup anemometer and *Model 2750* wind direction sensor were installed by the Ministry of Fisheries at the same location. Like the previous anemometer, this system required that the wind speed and direction be manually read off a display located in the watch office. Readings were then manually recorded into the daily weather logbook.

The *Aanderaa* system was replaced in July 1998 by a *M C Systems* automatic weather station (AWS) (29 July 1998). The *M C Systems* station included a wind direction sensor (*MCS 176-2*) and two wind speed sensors (*MCS 177-3* cup anemometer). Due to corrosion of the eight-meter mast, which had supported the previous anemometers, the new sensors were placed on top of a three-meter mast on the same roof (approximately 19 m above sea level).

### **2.2.2. Air Pressure**

Prior to closure of the manned station, air pressure was measured by a temperature-compensated mercury barometer and a barograph located in the watch office. Readings from the barometer were recorded by the Lightkeepers three or seven times per day on the hour. The continuous barograph recordings were used to determine air pressure tendencies. Sea level pressure (SLP) measurements from these instruments were available from March 1978 to November 1998. The automatic weather station installed in 1998 included an air pressure sensor (*MCS 157* barometer) located inside the Lightkeeper's watch office at 15.7 m above mean sea level.

## **2.3. Instrument changes**

### **2.3.1. Validation of pressure plate wind data**

An *Aanderaa* AWS was installed by Sea Fisheries Research Institute of South Africa (now Department of Environmental Affairs and Tourism, Marine and Coastal Management) on top of a foghorn at Dias Point Lighthouse for one year (1988 - 1989) at a time when simultaneous wind measurements were being recorded from the pressure plate. The foghorn was located at 26° 37.986'S, 15° 05.579'E, 240 m

north of the pressure plate (Figure 2.2, Figure 2.3). The AWS sensors were approximately 30 m above mean sea level, situated on top of the foghorn tower some 15 m above ground.

The GMT 06h00, 12h00 and 18h00 readings from 16 November 1988 to 16 November 1989 were extracted from the foghorn AWS and compared with wind speed and direction recorded at these times by the Lightkeepers from the pressure plate outside the watch office.

#### **2.3.1.1. Wind Speed**

A paired *t* test of the mean difference between the wind speed measurements of the pressure plate compared with the anemometer wind speeds (AWS) was carried out to determine whether there was a significant difference between the two data sets during the one-year comparison period. The *t*-value of  $-1.37$  ( $p = 0.172$ ,  $n = 1084$ ) indicated that the measurements from the two instruments are not significantly different.

It was concluded that there was no systematic bias in the measurements of wind speed comparing the automatic weather station with the pressure plate wind vane and therefore the time series of directions measured by the two types of instruments could be considered as contiguous measurements. This is in agreement with findings of Bailey (1979) who found a significant correlation ( $r = 0.65$ ,  $n = 76$ ) between the wind speed measured by the pressure plate at Dias Point and those from research ship anemometers within a 30 mile radius of Dias Point during February, May, August and November 1976.

#### **2.3.1.2. Wind Direction**

The comparison of wind direction between the pressure plate (PP) wind vane and the foghorn anemometer (AWS) proved problematic. Wind directions were recorded by the Lightkeepers (in accordance with standard practice for first order weather stations) not as the absolute values but in eight main directions namely  $45^\circ$ ,  $90^\circ$ ,

135°, 180°, 225°, 270°, 315° and 360° (and calm in cases of wind speed  $< 1.5 \text{ m.s}^{-1}$ ): Once the AWS wind directions for the period 16 November 1988 to 16 November 1989 had been categorized the two data sets were compared in four sectors using the AWS readings to filter the sectors:

- $\geq 1^\circ$  to  $\leq 90^\circ$  ( $n = 17$ )
- $> 90^\circ$  to  $\leq 180^\circ$  ( $n = 444$ )
- $> 180^\circ$  to  $\leq 270^\circ$  ( $n = 397$ )
- $> 270^\circ$  to  $\leq 360^\circ$  ( $n = 108$ )

The Hotelling test for paired samples of angles (Zar 1996) was applied to the AWS and pressure plate wind directions. The hypothesis that there was no significant difference between the measurements from the two instruments could only be accepted for the sector  $\geq 1^\circ$  to  $\leq 90^\circ$  ( $F = 2.57$ ,  $p > 0.05$ ,  $n = 17$ ).

In the other three sectors the hypothesis was rejected due to the  $F$  statistic falling within significant probability limits ( $p < 0.05$ ). Using the sector  $> 90^\circ$  to  $\leq 180^\circ$  as an example, 54% of the pairs had exactly matched readings from both instruments ( $180^\circ$ ). Discrepancies of  $45^\circ$  between the instruments occurred where e.g. instead of  $180^\circ$  (AWS) the PP measured  $135^\circ$  (21% of the paired readings filtered on  $180^\circ$ ) or  $225^\circ$  (25% of the pairs). Instead of  $135^\circ$  (AWS) the PP measured  $90^\circ$  in 25% of the pairs filtered on AWS =  $135^\circ$ ,  $180^\circ$  in 10% of the pairs while in 53% of the pairs both instruments measured  $135^\circ$ . Comparing wind direction where winds in this category were  $\geq 10.29 \text{ m.s}^{-1}$  decreased the  $F$  value, but it remained significant.

In the sector  $> 180^\circ$  to  $\leq 270^\circ$ , a) filtered on  $230^\circ$ , 72% of the pairs measured the same direction ( $230^\circ$ ), AWS =  $230^\circ$ , PP =  $180^\circ$  comprised 17% of the pairs, AWS =  $230^\circ$ , PP =  $270^\circ$  (4%). b) filtered on  $270^\circ$ , 46% of the readings were the same in both instruments ( $270^\circ$ ) while AWS =  $270^\circ$ , PP =  $230^\circ$  comprised 29% of the pairs and AWS =  $270^\circ$ , PP =  $310$ , 14%.

Thus filtering the AWS time series to extract one of the following wind directions -  $135^\circ$ ,  $180^\circ$ ,  $225^\circ$ ,  $270^\circ$ ,  $315^\circ$  or  $360^\circ$  - resulted in pairs of directions (AWS and PP)

being generated, the majority having the same direction. However the remainder of the directions fell mainly either 45° higher or 45° lower than the direction filtered (i.e. centered on that direction), while very small percentages (1 to 12%) were > 90° different. Due to the large intervals between the main directions the difference between the measurements of the two types of instruments was determined to be significant based on the probability of the calculated *F* statistic.

### 2.3.2. Comparison of Anemometer data

There was no data overlap between the anemometer installed in 1990 and the replacement *Aanderaa* anemometer installed in 1996. However the *Aanderaa* and *MC Systems* automatic weather stations ran concurrently from July 1998 to June 1999, thereafter the Lighthouse was automated and Lightkeeper's watches were discontinued, thus no further readings were obtainable from the *Aanderaa* unit. In order to compare wind speeds measured by the two different anemometers at different mast heights the two data sets were plotted against each other wherever paired observations were available ( $n = 1146$ ). It was determined that a significant relationship existed ( $p < 0.001$ ). Residual plots from this regression showed that at wind speeds below 15 knots, the AWS recorded higher speeds than the Lighthouse *Aanderaa* anemometer. However, at speeds greater than 35 knots the AWS recorded lower speeds than the Lighthouse anemometer. The AWS data was transformed in accordance with the power curve trendline  $y = 1.6091x^{0.8141}$ .

The *MC Systems* anemometer is currently situated closer to the roof than the previous anemometer thus wind speeds could be slowed down due to the wind speed sensors now being situated within the turbulent boundary layer above the roof. In addition the two records differ in the duration of the observation on which they are based. The Lighthouse keepers observed the wind speed display for a few minutes around the hour before recording their observation. The AWS averages the measurements made during the hour to give an hourly average recorded on the hour. For these reasons it was decided to transform the AWS data as described above. The wind speed measurements were not adjusted to the standard 10 m above sea level (Johnson and Nelson 1999).

### 2.3.3. Validation of Sea Level Pressure Data

Sea level pressure was measured at the Lighthouse weather station by means of a temperature-compensated mercury barometer, which was replaced in 1998 with the closure of the manned weather station by a *MC Systems* barometer as part of the AWS. A period of overlap of measurements by these two different instruments occurred from 30 July 1998 to 30 November 1998. The Lightkeeper's sea level pressure measurements took place at GMT 06h00, 09h00, 12h00, 15h00 and 18h00 - the corresponding data set was extracted from the hourly AWS SLP. A significant correlation ( $r = 0.964$ ,  $p < 0.001$   $n = 536$ ) between the two data sets (sea level pressure readings of the Lighthouse barometer and that of the *MC Systems* barometer) was determined from Pearson's correlation test, and they show closely matched readings and trends (Figure 2.4). However, from a paired  $t$  test analysis the two data sets were found to be significantly different with the mean of the Lighthouse barometer readings being higher than that of the AWS ( $t = -28.01$ ,  $p < 0.01$ ). This could indicate that the adjustment of the AWS barometer to sea level is not exact. The height of the AWS barometer above mean sea level was determined from triangulation based on the distance, determined by DGPS, between the barometer and the mean sea level (MSL), the angle between the barometer and MSL was determined with a sextant. This should be checked with standard surveying equipment in future.

## 2.4. Processing of Wind Data

### 2.4.1. Composition of the wind time series

The longest data set that could be retrieved from Dias Point Lighthouse weather logs was the readings recorded daily at GMT 06h00, 12h00 and 18h00 from 1960 to 1998. To continue the time series with AWS data the readings at these times were extracted from the hourly database.

## 2.4.2. Coast alignment at Lüderitz in relation to upwelling

The forcing factor for coastal upwelling is equatorward longshore wind which results in the maximum offshore Ekman transport of surface water ( $90^\circ$  to the left of the wind direction in the southern Hemisphere) (Open University 1989). The Ekman transport equation incorporates the square of the wind speed parallel to the coast ( $v^2$ ), called wind stress in this thesis, and used as an index of upwelling (see section 2.4.3). The peninsula on which the Dias Point Lighthouse is situated was considered to be close to true North in alignment (Figure 2.5). The South-North component of the wind at Dias Point thus blows parallel to the coast and was therefore considered to be the upwelling-favourable component.

## 2.4.3. Daily average wind speed and wind stress calculations

The wind direction and speed measurements at 06h00, 12h00 and 18h00 GMT were used to calculate the South–North (longshore) and West-East (onshore-offshore) components and the daily average wind speed ( $\text{m}\cdot\text{s}^{-1}$ ) for each. A daily average wind speed was calculated for each component only if there were two or three readings per day had been recorded (1 reading per day was discarded).

Considering the longshore component, negative daily average values indicated northerly winds (downwelling) while positive average values indicated southerly winds (upwelling-favourable). In the onshore-offshore component, negative daily average values indicated easterly winds while positive average values indicated westerly winds.

A proxy for coastal upwelling intensity at Lüderitz was calculated from the wind stress component ( $\tau = r \cdot C_d \cdot v^2$ ) of Ekman transport

$$\text{Ekman transport } (M_E \text{ in } \text{kg}\cdot\text{m}\cdot\text{s}^{-1}) = r \cdot C_d \cdot v^2 / 2 \cdot \Omega \cdot \sin(\phi)$$

where:

$$r = \text{air density } (1.22 \text{ kg m}^{-3})$$

$C_d$  = drag coefficient (0.0013)

$v$  = speed of the wind component parallel to the coast ( $m \cdot s^{-1}$ ) (at Dias Point this is the South-North component)

$\Omega$  = angular rotation of earth ( $7.292 \text{ s}^{-1}$ )

$\phi$  = Latitude ( $26^\circ 38'S$  at Dias Point)

(Mann and Lazier 1991, Johnson and Nelson 1999)

Since the wind data was collected at one station, latitude and the earth's speed of rotation are constant.  $C_d$  is assumed to be constant although its actual value may vary slightly due to prevailing atmospheric conditions (Open University 1989). The remaining parameter in the Ekman transport equation, namely the square of the wind speed parallel to the coast (the South-North component), is referred to in this thesis as wind stress. The South-North (and West-East) components were first derived from the average of the wind speed measurements at 06h00, 12h00 and 18h00 GMT. The daily average South-North wind speed was squared. The square of any negative values was multiplied by  $-1$  thus if the wind direction was northerly the equation  $v^2 * -1$  was applied.

#### 2.4.4 Wind Mixing Index

Wind speed cubed is a measure of the turbulent energy input from the wind to the ocean (Boyd 1987). The total hourly wind speed  $W$  (regardless of direction i.e. not decomposed into South-North or East west components) at GMT 06h00, 12h00 and 18h00, was cubed, the sum determined and divided by 3 to calculate the daily average wind mixing index ( $W^3$ ):

$$\text{Daily average } W^3 (m^3 s^{-3}) = \frac{(W_{06})^3 + (W_{12})^3 + (W_{18})^3}{3}$$

In all cases a daily average was calculated only if there were two or three readings, one measurement per day was discarded.

#### 2.4.5. Summary of Wind Terms

The following four terms are used in this thesis to describe wind components and derived wind-driven upwelling and wind mixing indices:

- South-North wind speed  $\text{m.s}^{-1}$  (longshore wind component)
- West-East wind speed  $\text{m.s}^{-1}$  (onshore-offshore wind component)
- Wind stress – proportional to the square of the South-North wind speed, used as a proxy for upwelling intensity
- Wind mixing index ( $W^3$ ) - the cube of the total wind speed, not decomposed into longshore or on/offshore components, used as an index of turbulent wind mixing.

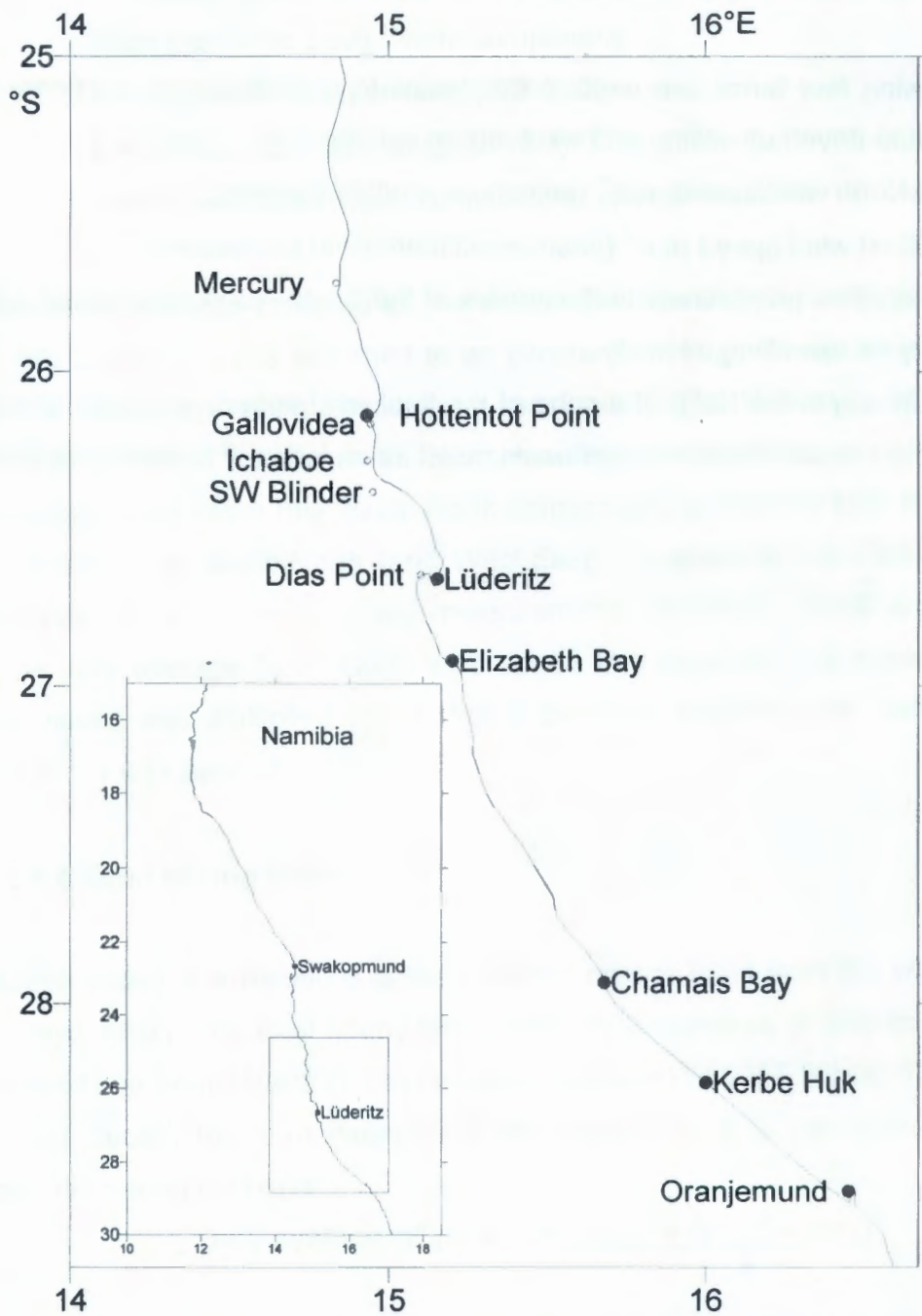


**Figure 2.1.** Map of the southern Namibian coastline showing the location of Dias Point and Lüderitz.

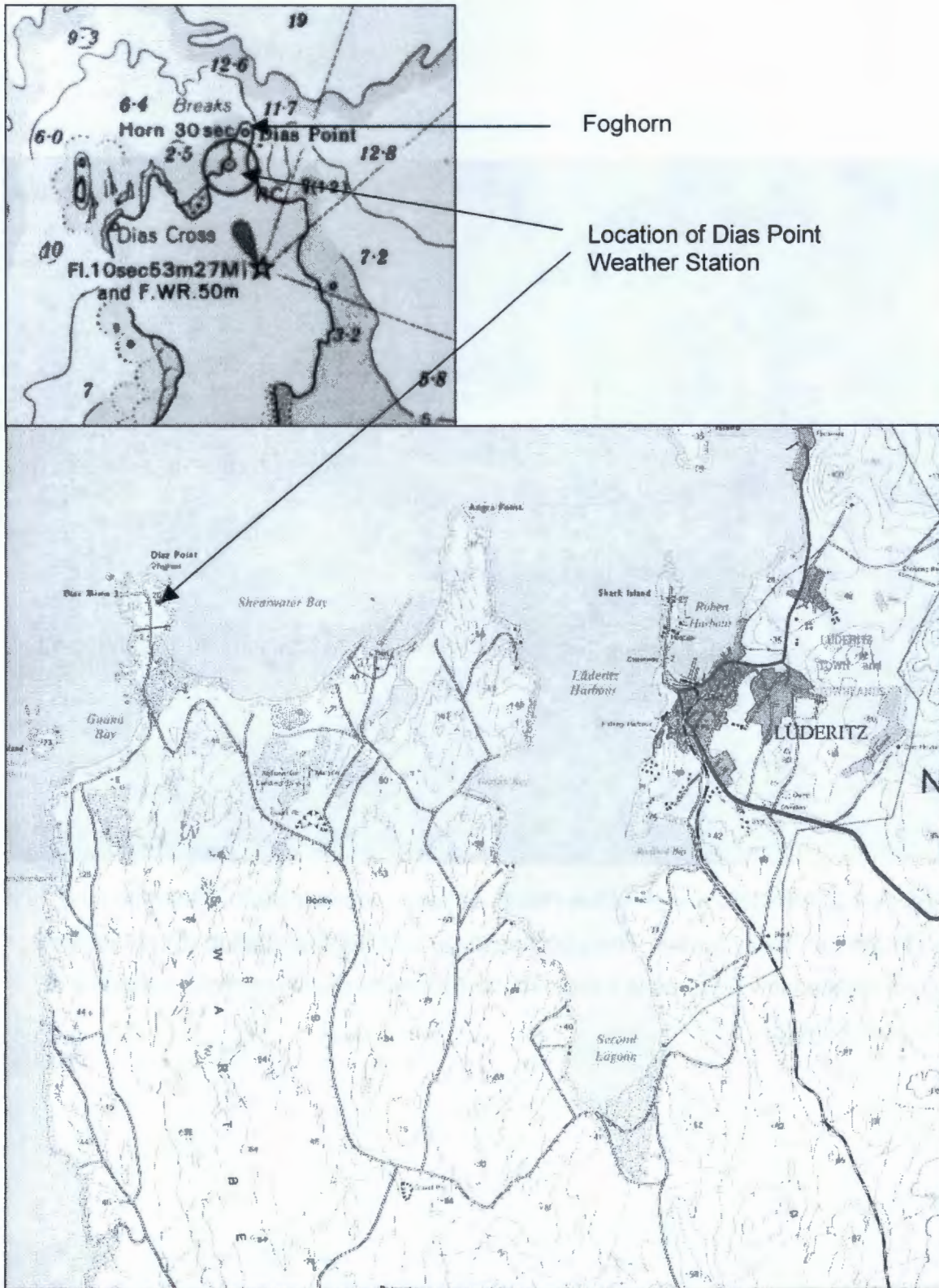


**Figure 2.2.** Locality of the Dias Point Lighthouse weather station ( $26^{\circ} 38.094'S$ ,  $15^{\circ} 05.612'E$ ) on the Lüderitz Peninsula. The Lighthouse is situated on the exposed northern tip of a rocky headland (see inset).



**Figure 2.3.** Aerial view of the Dias Point peninsula, looking south, illustrating the generally flat, rocky terrain. The Lighthouse (a) and weather station (b) are located on an isolated low ridge as is the old foghorn situated on the northern extremity of the peninsula (c).

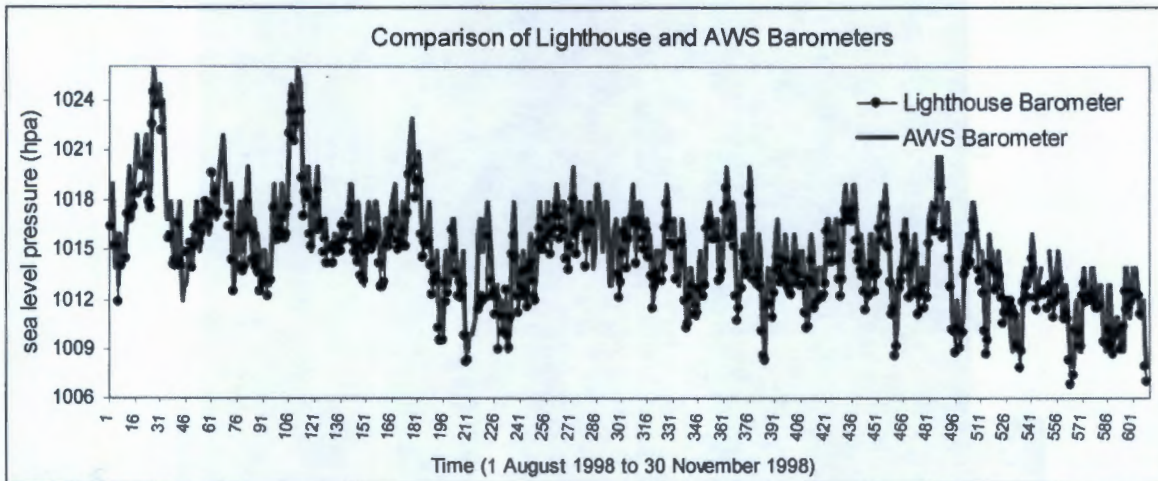


**Figure 2.4.** Comparison of sea level pressure measurements (hpa) between the Lighthouse mercury barometer and the digital barometer of the Automatic Weather Station (AWS) from 1 August 1998 to 30 November 1998.

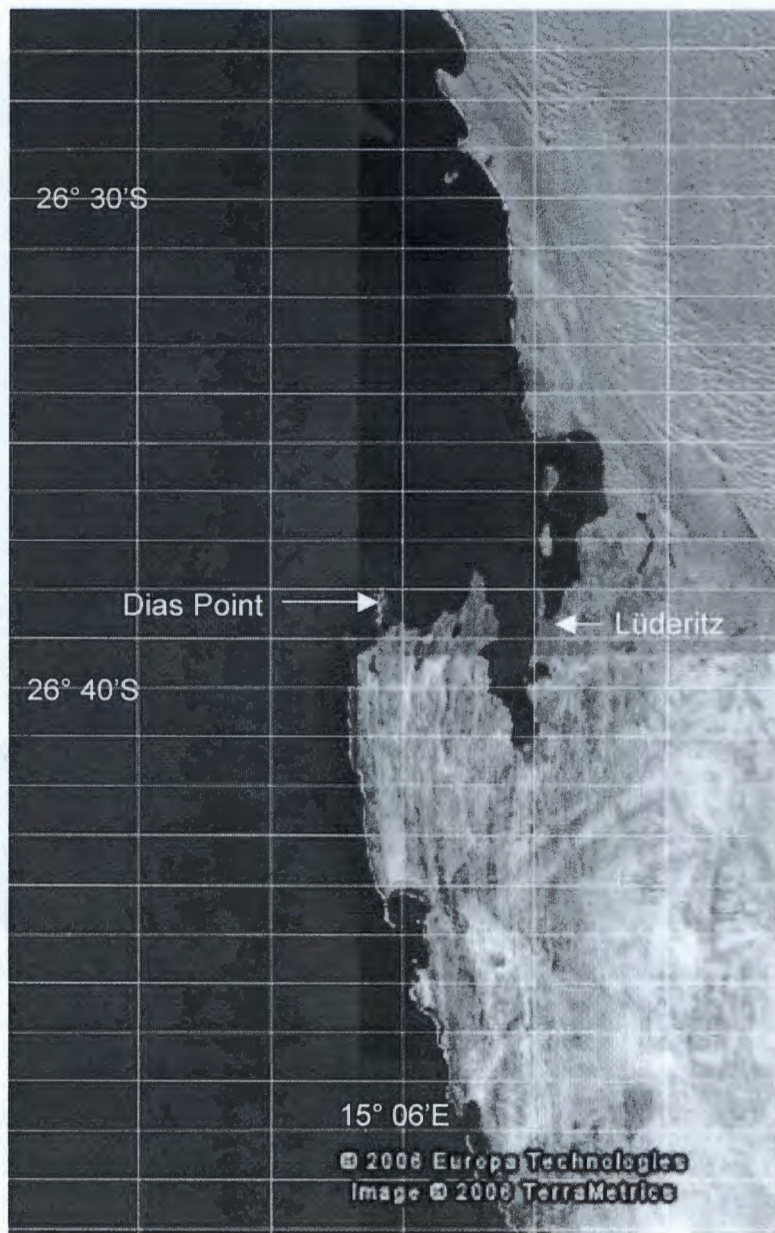


**Figure 2.5.** Map of the coastline in the region of Lüderitz showing the general orientation of the coastline to true north as indicated by the lines of longitude (Image from Google Earth <http://earth.google.com>).

Diurnal variability in the wind regime at Lüderitz

1.1 Introduction

## Chapter Three

### Diurnal variability in the wind regime at Lüderitz



R. Jones

## Diurnal variability in the wind regime at Lüderitz

### 3.1. Introduction

The Lüderitz upwelling cell is the principal centre of upwelling in the Benguela (Shannon 1985) and is possibly the strongest coastal upwelling centre in the world (Bakun 1996). At Lüderitz, and other eastern boundary upwelling cells, longshore, equatorward winds cause offshore surface Ekman transport resulting in upwelling of cold, nutrient-rich bottom waters along the coast.

The geostrophic wind field off Lüderitz is maintained by the South Atlantic Anticyclone (SAA) and driven by the pressure gradient between this high pressure cell over the southeast Atlantic ocean and the continental atmospheric low pressure (Bailey 1979). However, the continental pressure system is dynamic on both a diurnal and seasonal scale. In addition, the interface between the cold water of the Benguela current and the arid coastal plain along the Namibian coast constitutes a thermal discontinuity which results in local baroclinic pressure fields developing by day and night (Tyson and Preston-Whyte 2000). Along the west coast of South Africa and the Namibian coast where the horizontal pressure gradient between cold sea and arid interior is strongest, one expects that the coastal wind field would have a diurnal pattern of variability, which would change seasonally and could be of importance in modulating coastal upwelling dynamics on a diurnal scale.

Since the activity of the Lüderitz upwelling cell is critical for sustaining biological productivity in the Northern Benguela, an understanding of all processes that potentially modulate wind-driven coastal upwelling is necessary. The objective of this chapter is to determine whether there is a diurnal variability in wind speed and direction at Lüderitz that could influence the upwelling dynamics there, and if so whether such variability is subject to seasonal change.

### 3.2. Methods

Wind speed, direction and air pressure measurements for the period of investigation (November 1999 to November 2004) were recorded by an automatic weather station at Dias Point (26° 38.094'S 15° 05.612'E). The *M C Systems* station was equipped with an *MCS 157* barometer, *MCS 176-2* wind direction sensor and *MCS 177-3* cup anemometer. Details of the instrumentation and locality are given in Chapter Two.

Hourly readings from November 1998 to November 2004 were used to calculate the average wind direction ( $^{\circ}$ ), wind speed ( $\text{m}\cdot\text{s}^{-1}$ ) and air pressure (hpa) per hour (01h00 to 24h00) for each season. The number of data points ( $n$ ) per hourly average varied between 524 and 552 depending on the season. Frequency of occurrence of wind directions in eight main sectors was also calculated per hour per season. Seasons were determined by the data rather than by the conventional seasons, due to the strongest upwelling-favourable winds occurring from November to January, and weakest winds from May to July (Chapter Four). Seasons were therefore categorized as summer 15 Nov to 14 Feb, autumn 15 Feb to 14 May, winter 15 May to 14 August and spring 15 Aug to 14 Nov. Wind sectors comprised an arc of 45 degrees centered on each of the eight main wind directions. Thus South wind comprised readings between and including  $157.5^{\circ}$  to  $202.49^{\circ}$ , centered on 180 degrees. Winds  $< 1.5 \text{ m}\cdot\text{s}^{-1}$  were categorized as calm, regardless of direction.

### 3.3. Results

The diurnal changes in hourly sea level pressure showed the same bimodal pattern irrespective of season (Figure 3.1). Two peaks in pressure occurred within a 24-hour period, one around midnight (between 23h00 and 01h00) and another in the late morning (between 09h00 and 12h00). Two pressure minima occurred per day, at 05h00 to 06h00 and at 17h00 to 18h00. The pressure difference (average 2.9 hpa) between the late morning maximum and late afternoon minimum was larger than between the daily midnight peak and early morning pressure minimum (1 hpa). The seasonal increase in pressure from summer through autumn to a maximum in winter,

and decrease again in spring is also apparent, with sea level pressure being about 7 hpa higher in winter compared with summer (Figure 3.1).

The diurnal pattern in wind speed at Dias Point was also consistent throughout the seasons. Wind speeds increased from around 10h00 to an afternoon maximum between 15h00 (winter and autumn) and 17h00 (summer), dropping again to the initial level by midnight (Figure 3.2). The variability in wind speed as indicated by the standard deviation bars in Figure 3.2 was highest during the period of maximum wind speeds. The diurnal change in wind speed was least obvious in winter, the season during which the lowest wind speeds are experienced at Lüderitz. The maximum increase of  $5 \text{ m.s}^{-1}$  occurred in summer, with an increase of  $4 \text{ m.s}^{-1}$  on average during autumn and spring.

A negative relationship between hourly sea level pressure and hourly wind speed (15 November 1998 to 14 November 2004,  $n = 51965$ ) was apparent from correlation analysis ( $r = -0.049$ ,  $p < 0.001$ ). Thus high wind speeds occurred in conjunction with low air pressure, low wind speeds with high air pressure. The significance of this relationship is explained by the large sample size.

Southerly and southwesterly winds predominated throughout the day in all seasons (Figure 3.3). Wind direction changed from southerly ( $157.5^\circ - 202.49^\circ$ ) to southwesterly ( $202.5^\circ - 247.49^\circ$ ) between 08h00 and 12h00. The change occurred earlier in the day in summer than in winter. It coincided with the morning maximum in air pressure and at this time of day the wind speeds start to increase at Lüderitz. In summer and spring the average wind direction remained southwesterly for the rest of the day, but in autumn and winter the direction reverted to southerly at 20h00.

From standard deviations of the hourly average it is apparent that in summer wind direction was most variable in the morning (08h00 to 10h00), becoming markedly more consistent as wind speed increased in the afternoon. Highest variability in wind direction throughout the day occurred in winter (Figure 3.3). From an analysis of the hourly frequency and seasonal changes in occurrence of the eight main wind directions during the years 2000 to 2001 and 2003 to 2004 (Figure 3.4) the high

winter variability can be attributed to a higher frequency of calm observed throughout the day, and more frequent occurrence of winds from an easterly and southeasterly direction compared with other seasons.

The diurnal change in the predominant wind direction from southerly in the early morning to southwesterly in the afternoon is apparent in all seasons of both years analysed (Figure 3.4). There is also a diurnal pattern of occurrence of the "minor" wind directions with southeast and east winds and calm weather occurring mainly from 22h00 to 11h00, west and northwest winds are more frequent from 11h00 to 22h00. The main interannual differences apparent in Figure 3.4 are in the frequency of these "minor" directions (excluding north winds) rather than in the frequency of southerly or southwesterly winds.

### **3.4. Discussion**

Hart and Currie (1960) described a diurnal intensification of wind speeds at Lüderitz in conjunction with a change in wind direction from south to southwest. This has also been documented from Pelican Point wind records (Walvis Bay) where the maximum wind speed is also attained in the late afternoon. However more frequent northerly and calm conditions occur there in the morning and at night and wind speeds are lower than at Lüderitz (Stander 1964, Boyd 1987). Diurnal variation at these two stations is due to air pressure changes during the daytime heating and night-time cooling of the land. During the day, warm air rising over the land strengthens the low pressure thus intensifying the gradient between the SAA and the continental low causing coastal wind speeds to increase. Wind speeds are at a minimum at night and early morning when cooling of the land reduces the pressure gradient (Bailey 1979). The significant negative relationship between sea level pressure and wind speed at Lüderitz can be attributed to this thermal forcing of the horizontal pressure gradient.

Wind direction changes from south to southwest are also associated with thermal uplift of air over the land as it heats up, drawing colder more dense air overlying the sea towards the land, introducing an onshore component known as a sea breeze

(Hart and Currie 1960). This relaxes at night when the pressure systems become stable as the land cools.

Seasonal changes in the diurnal wind speed and direction regime were apparent at Lüderitz. The SAA is maintained throughout the year but its position changes seasonally, moving about 6° northwesterly and 13° offshore in the austral winter compared with its summer position (Tyson and Preston-Whyte 2000). As the Inter Tropical Convergence Zone (ITCZ) migrates northward in winter, the pressure over the continent changes from a well-developed low pressure in summer to a weak high pressure (Shannon and Nelson 1996). This seasonality was observed in the sea level pressure at Lüderitz. The combined effect of the northward migration of the SAA, weakening the control of the SAA on winds in Lüderitz, combined with a diminished gradient in winter between the SAA and the atmospheric pressure over the continent, is responsible for the lower wind speeds at Lüderitz in winter and for seasonal changes in wind directions observed in the diurnal wind field.

A well-known coastal weather phenomenon in winter at Lüderitz and along the central Namib coast is the higher frequency of hot easterly winds. These occur when high pressure cells form over the continent, often in conjunction with coastal lows (Tyson and Preston-Whyte 2000). Anticyclonic, subsiding air contracts and is adiabatically warmed as it descends from the interior escarpment, traversing the coastal plain and moving offshore with a velocity of typically  $15 \text{ m}\cdot\text{s}^{-1}$  (Shannon and Nelson 1996). In Lüderitz the easterly winds have a predictable diurnal cycle, commencing at night, strengthening during the morning and usually cease blowing during the afternoon. The relationship between east wind events and upwelling is uncertain, there might be no effect at all on the water column (Hart and Currie 1960), or upwelling could be totally suppressed, or locally enhanced close to the coast (Shannon 1985).

Northerly and westerly winds are associated with cyclonic air flow around coastal lows that form off Lüderitz. Coastal lows are significant in that they are associated with the relaxation of upwelling, bringing warmer surface water with higher oxygen content into the inshore benthic region (Peard and Roux 2002). Like east wind,

coastal low formation is associated with high pressure over the African sub-continent, usually preceded by the SAA ridging around the Cape. This modulation of the southerly wind regime at Lüderitz is under atmospheric control and occurs at a synoptic scale of 3 to 10 days (Shannon and Nelson 1996). Since the low pressure cells travel fairly rapidly southwards (4 to 5 degrees of latitude per day) in the manner of a Kelvin wave, their effect in Lüderitz is relatively short lived and within 3 days the SAA has re-established its position offshore and the upwelling favourable southerly winds are reinstated (Bailey 1979, Reason and Jury 1990).

### **3.5. Conclusion**

A daytime intensification and night-time modulation of wind speed at Lüderitz was found during all seasons, although the signal was weakest in winter. Diurnal changes in wind speed were statistically related to air pressure. In addition, a diurnal change in wind direction occurred at Lüderitz, with winds generally veering from south in the morning to southwest during the day, these wind directions predominated throughout the year. While the diurnal cycle in air pressure over the continent exerts an influence on the dynamics of the Lüderitz upwelling cell by modulating wind speed, the diurnal direction changes would have little effect on upwelling since the coastline orientation at Lüderitz is northwest to north (Boyd 1987). Thus both southerly and southwesterly winds favour coastal upwelling. A diurnal pattern in the frequency of calms and winds from the east, southeast, northwest and west was apparent, with seasonal differences in occurrence. Northerly winds occurred throughout the day in all seasons, indicating that they are under the control of atmospheric processes on a synoptic rather than a diurnal scale, being associated with the development of coastal low pressure cells which cause downwelling at Lüderitz.

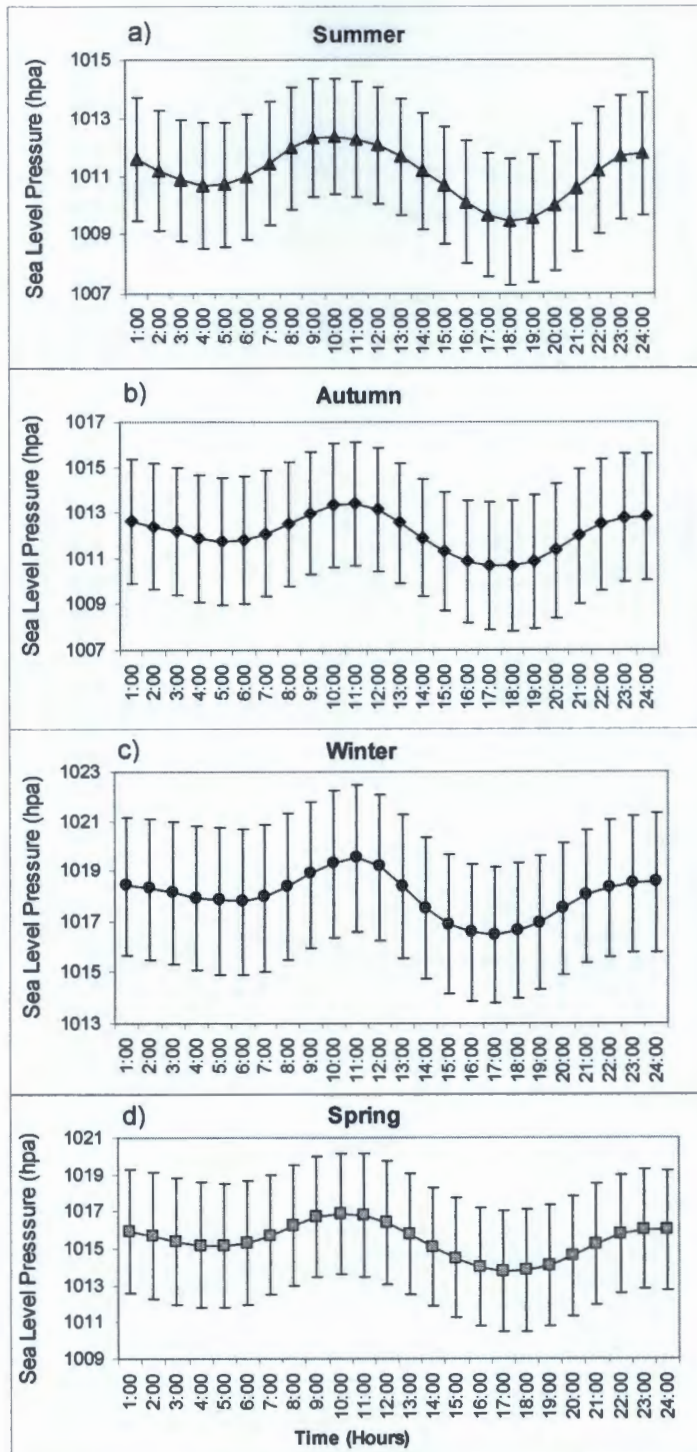


**Figure 3.1.** Seasonal changes in diurnal sea level pressure (hpa) at Dias Point. Hourly averages (bars indicate standard deviations) for November 1998 to November 2004. a) Summer: 15 November to 14 February, b) Autumn: 15 February to 14 May, c) Winter: 15 May to 14 August and d) Spring: 15 August to 14 November. Note axis scales differ.

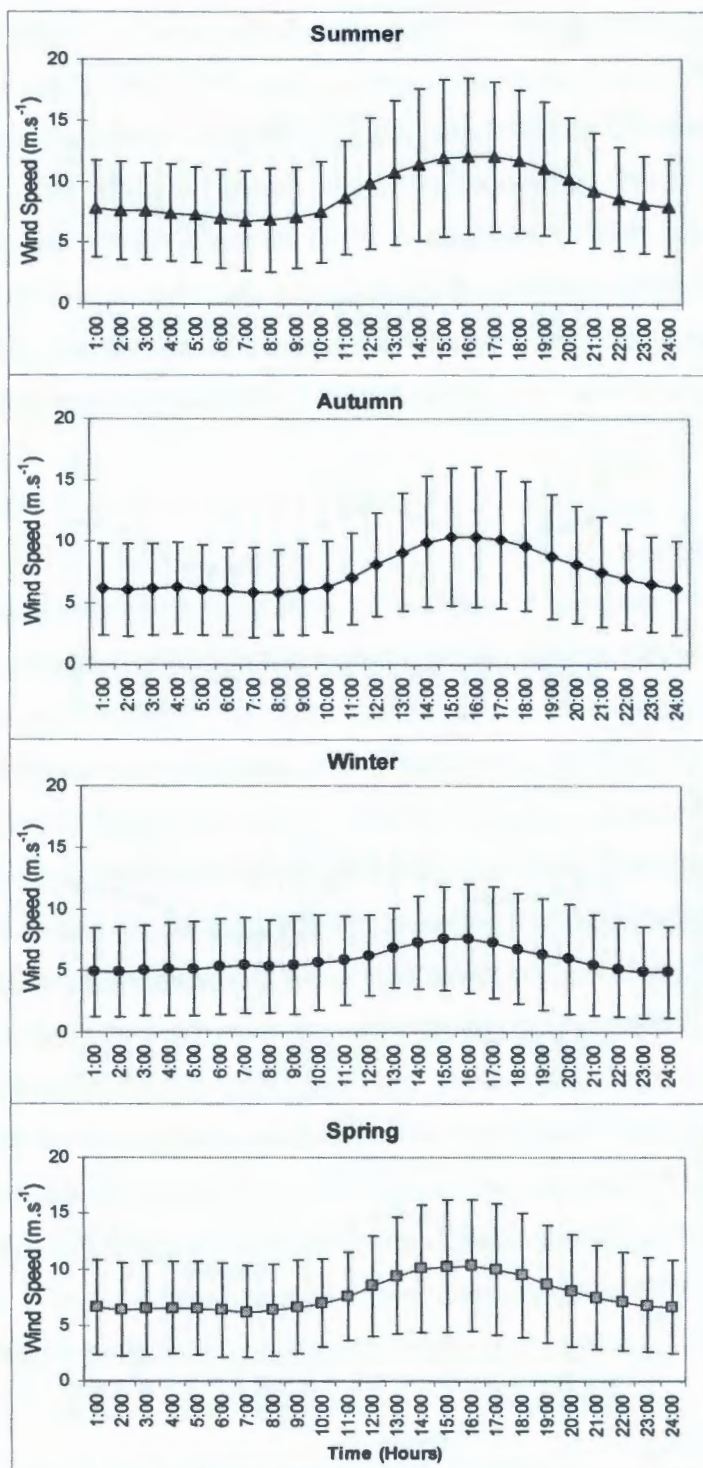


**Figure 3.2.** Diurnal cycle in wind speed ( $\text{m.s}^{-1}$ ) at Lüderitz showing afternoon intensification of wind velocity in all seasons. Hourly averages (bars indicate standard deviations) over the period November 1999 to November 2004 with seasons categorized as in Figure 3.1.

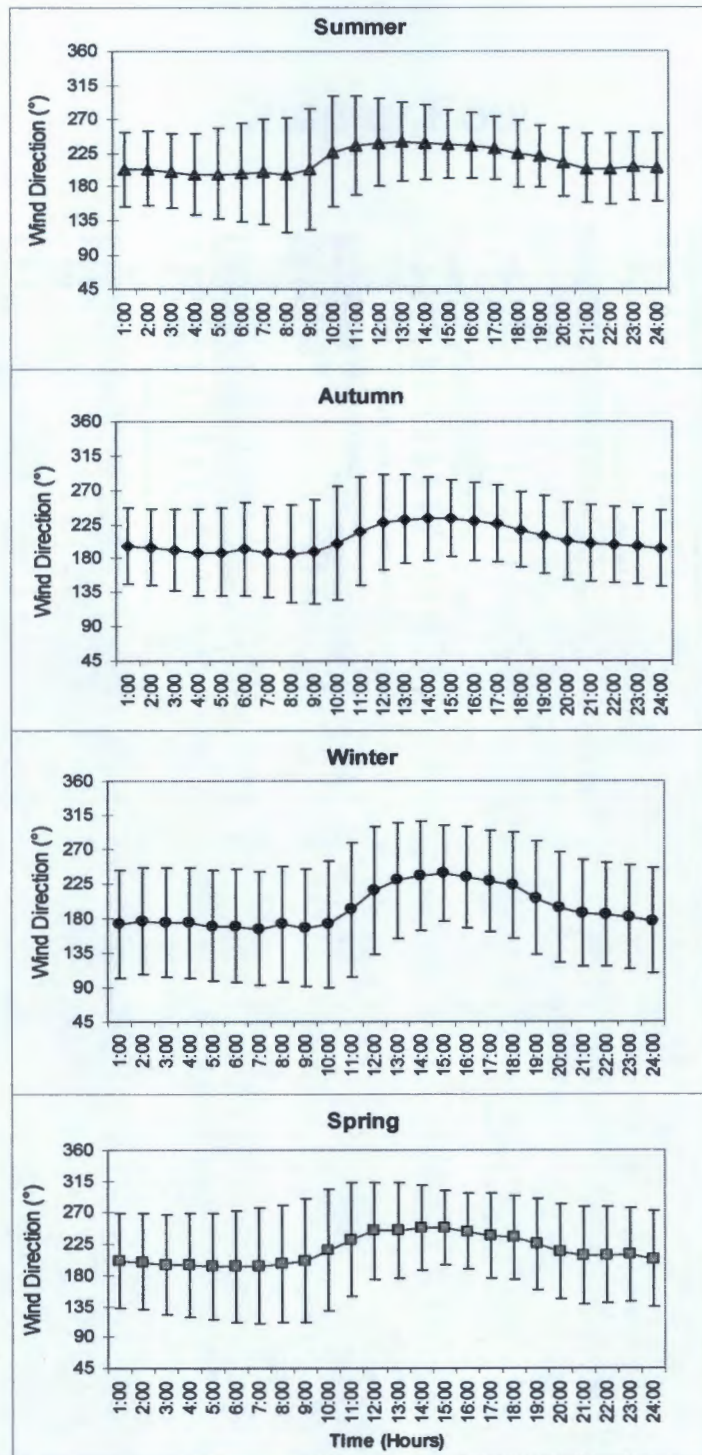


**Figure 3.3.** Diurnal change in wind direction (°) at Lüderitz. Hourly averages calculated per season (see Figure 3.1) from November 1999 to November 2004. Bars indicate the standard deviation of the hourly averages.

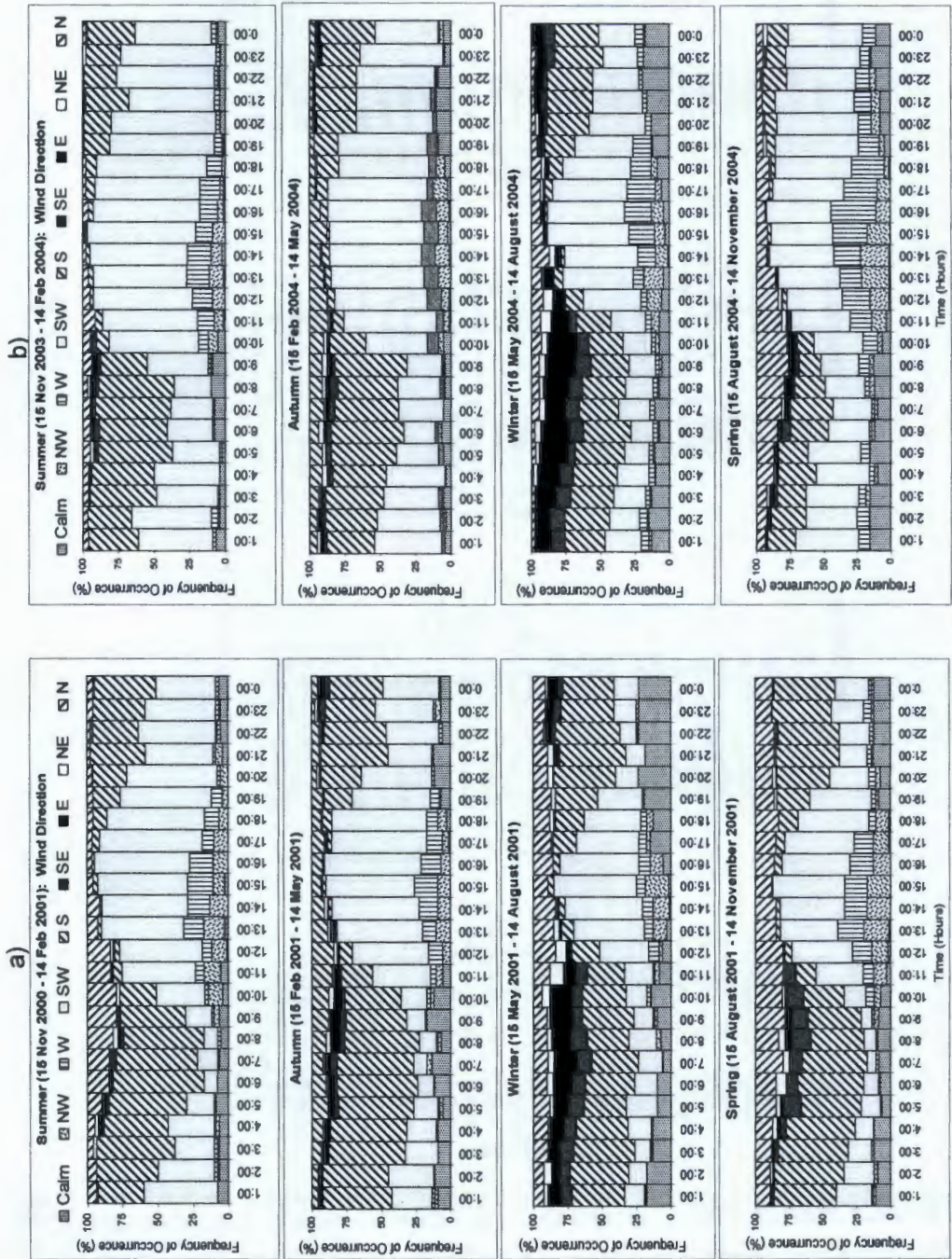


**Figure 3.4.** Diurnal frequency of occurrence (%) of wind directions at Lüderitz during a) November 2000 to November 2001 and b) November 2003 to November 2004. Seasons categorized as per Figure 3.1.

## Chapter Four

### Seasonal variability in wind-driven upwelling at Lüderitz



R. Jones

## Seasonal variability in wind-driven upwelling at Lüderitz

### 4.1. Introduction

The eastern boundary of the South Atlantic subtropical gyre between latitudes 15°S and 34°S and extending some 200 km offshore from the coastline is known as the Benguela Current system (Shannon 1970, Nelson and Hutchings 1983, Shillington *et al.* 2006). The oceanography of this highly dynamic current, flowing parallel to the coast in a north to northwestward direction is dominated by coastal upwelling initiated by an equatorward, longshore wind regime (Shannon 1985). Ekman transport set up by the wind stress on the ocean causes offshore flow of the nearshore surface water, locally lowering pressure at the sea surface. This is compensated by replacement from below, thus entraining a flow of cooler, nutrient-rich deep water flowing coastward along the sea floor, to the surface (Bakun 1996). Eastern boundary current systems, including the Benguela, Humboldt, California and Canary Currents sustain among the most important fisheries in the world due to enhanced primary productivity of their waters as a result of the input of nutrients required for phytoplankton growth, during upwelling (Carr and Kearns 2003).

Downstream of the upwelling cell the more stable euphotic zone is enriched with upwelled nutrients. However the intense, perennial upwelling and associated turbulence within the Lüderitz cell has implications for the population dynamics and distribution of pelagic fish species and some invertebrates in the Benguela system. It is thought that populations to the south and north of this upwelling centre are separated by an area of strong wind mixing that negatively affects primary productivity, creating a barrier to pelagic fish migration and invertebrates such as euphausiids (Agenbag and Shannon 1988, Barange *et al.* 1992). Years of anomalously low southerly winds in the Lüderitz area would presumably allow exchange of fish populations to the south and north (Agenbag and Shannon 1988).

A seasonal relaxation of upwelling in phase with high primary productivity could also facilitate such movement through the quiescent cell. While upwelling is considered

perennial at Lüderitz (Bailey 1979, Boyd 1987), a seasonal signal in the intensity of upwelling in the area has been described from shipboard measurements, coastal wind records and satellite-derived wind measurements (Hart and Currie 1960, Stander 1964, Bailey 1979, Hagen *et al.* 2001, Hardman-Mountford *et al.* 2003), although discrepancies exist in the literature as to the time of the year when minimum / maximum wind stress occurs in this region. The aim of this chapter is to describe the seasonal variability in wind direction and speed (and associated upwelling intensity) at Lüderitz from 44 years of wind measurements at Dias Point Lighthouse.

## **4.2. Methods**

Dias Point Lighthouse is situated south of Lüderitz at 26° 38.094'S, 15° 05.612'E. Wind speed and direction readings were measured by means of a deflection (pressure) plate and wind vane situated on a rising slope south of the watch office from 1960 to 1990. From 1990 onwards wind speed was measured by means of a cup anemometer with an associated wind vane for direction measurements. Details of the locality and instrumentation are given in Chapter Two.

### **4.2.1. Wind Stress**

Wind speed and direction readings were recorded at GMT 06h00, 12h00 and 18h00. From this data the South, West, North and East components were determined per reading and daily average wind speeds calculated for the South-North and West-East components. The South-North wind component is parallel to the coast at Lüderitz (Chapter Two). Positive values indicate southerly (upwelling favourable winds), negative values equate with northerly winds that result in downwelling. An index of upwelling was calculated from the square of the daily average speed of the South-North equatorward wind ( $m^2.s^{-2}$ ). A negative sign was applied to the index where the daily average value was negative. Wind stress is a component of the equation for Ekman transport ( $M_E$ ) (Chapter Two) (Mann and Lazier 1991, Johnson and Nelson 1999).

#### **4.2.2 Wind Mixing Index**

Wind speed cubed ( $W^3$ ) is a measure of the turbulent energy input from the wind to the ocean (Boyd 1987). The total hourly wind speed  $W$  (regardless of direction i.e. not decomposed into South-North or West-East components) at GMT 06h00, 12h00 and 18h00, was cubed, the sum determined and divided by 3 to calculate the daily average wind mixing index (see Chapter Two section 2.4.4).

#### **4.2.3 Curve Fitting to Daily Average Values**

The average South-North and West-East components were determined per day across 44 years (1960 - 2004), with 366 data points per year (including 29 February). In order to determine the long term average a sine curve was fitted across these daily averages: The Julian days 1 - 366 were converted to angles (theta) and the sine/cosine of theta was calculated for each Julian day. Multiple regression of the daily average (predictor) against corresponding days (sine/cosine theta) was used to plot a sine curve. The adjusted  $r$  value of the regression was noted. The first harmonic of the curve was computed by including sine /cosine  $2*\theta$  and for both wind components it was found to be the best fit from a combination of the adjusted  $r$  value and visual inspection of the fitted curve.

#### **4.2.4 Monthly Average and Coefficient of Variation**

The daily average wind speed / wind stress / wind mixing index (e.g.) of each January in the time series (1960 to 2004) was used to calculate the January monthly average ( $\bar{x}$ ) and standard deviation ( $sd$ ). The coefficient of variation (CV) was calculated per month as:

$$CV = sd/\bar{x} \quad (\text{Zar 1996}).$$

### 4.3. Results

Southwesterly winds predominate at Dias Point throughout the year as is apparent from the monthly average South-North and West-East components (Figure 4.1a and b). The southerly component dominates over the westerly component as can be seen in monthly average (Figure 4.1a, b), and daily average wind speeds (Figure 4.2a, b). A winter minimum in the southwesterly wind speed occurs at Dias Point during June and July. Southerly wind speeds increase through spring to a maximum in November to January, decreasing in strength in autumn to the winter minimum (Figure 4.1a, Figure 4.2a).

The westerly wind component shows a similar pattern with strongest westerly winds blowing in December and January, and weakest in June and July (Figure 4.1b and 4.2b). During winter, winds with an easterly component occur more frequently than at any other time of the year. The high coefficient of variation values of the West-East component from May to August (Figure 4.1b) indicates a high degree of variability in wind speed. This is due to strong easterly winds in winter that alternate with periods of southwesterly winds (Figure 4.2b). Variability in the South-North component is also highest during this period (Figure 4.1a). The lowest variability from November to January is due to this being the period of strongest and most consistent southerly winds (Figure 4.1a).

Wind stress, a proxy for upwelling intensity proportional to the square of the equatorward wind speed parallel to the coast, is at a maximum in summer (November to January) but reduced in intensity during winter, with a minimum in June and July (Figure 4.3a). There is approximately a fourfold difference between the winter minimum and summer maximum wind stress.

The wind mixing index ( $W^3$ ) shows the predominance of the southerly wind component in that its seasonal pattern is the same as that of the southerly wind (Figure 4.3b). The summer maximum  $W^3$  occurs in November ( $2300 \text{ m}^3 \cdot \text{s}^{-3}$ ), but wind mixing is high throughout spring and summer, causing both vertical motion in the

water column and surface mixing (Agenbag and Shannon 1988). The winter minimum value at Lüderitz (June,  $550 \text{ m}^3 \cdot \text{s}^{-3}$ ) (Figure 4.3b) is of the same order as the October maximum  $W^3$  in Walvis Bay ( $580 \text{ m}^3 \cdot \text{s}^{-3}$ ) (Figure 4.4c).

The seasonal cycle of wind speed differs from south to north along the Namibian coast. Although southerly winds also predominate at Walvis Bay, wind speeds are far lower throughout the year with maximum speeds (monthly average of  $3 - 4 \text{ m} \cdot \text{s}^{-1}$ ) falling within the range of the winter minimum southerly wind at Lüderitz, and the seasonality is clearly different (Figure 4.4a & b). Minimum southerly wind speeds occur there in summer (December to February) and maximum speeds in April and October. The range in wind speeds is far smaller than in Lüderitz. The westerly wind strength and seasonality at Walvis Bay is similar to that of Lüderitz. The wind speed cubed or mixing index ( $W^3$ ) in Walvis Bay also reflects the predominance of southerly winds, with a spring maximum (September to October) and a summer minimum (December to March) (Figure 4.4c).

#### 4.4. Discussion

Seasonality in the wind regime off Lüderitz as illustrated by the Dias Point wind time series, is caused by a seasonal change in the latitudinal position of the South Atlantic Anticyclone (SAA) which shifts about  $6^\circ$  northwesterly and  $13^\circ$  offshore in the austral winter compared with its summer position (Tyson and Preston-Whyte 2000). The effect on the wind field and thus on the upwelling regime of the entire Benguela system was described by Hart and Currie (1960). Using data from a 1944 Royal Meteorological Service publication they describe the resulting minimum in upwelling favourable southerly wind speeds during winter (June to August) in Lüderitz compared with austral summer (December to February) when the anticyclone is in its most southerly position. The 44-year time series of wind data from Lüderitz presented here confirms that although southerly winds are predominant throughout the year, a winter minimum in frequency and strength of southerly winds does occur. In the Southern Benguela the frequency of westerly winds, particularly strong northwesterlies, increases in winter due to the change in

position of the SAA, these onshore winds suppress upwelling which is therefore also at a minimum in winter. On the northern coast of Namibia the latitudinal shift in the SAA during winter results in a winter / spring maximum in longshore winds as illustrated by wind data from Walvis Bay (Boyd 1987).

A seasonal change also occurs in the pressure field over the African continent associated with the northerly shift of the Inter Tropical Convergence Zone (ITCZ) in winter. The prevailing continental low pressure in summer increases to a weak high in winter (Shannon and Nelson 1996), with associated changes in the gradient between oceanic and continental pressure fields. As a result there is higher variability in the wind regime at Lüderitz in winter. Strong easterly winds characteristically occur along the Namibian coast during winter. These adiabatically heated winds transport sand from the coastal desert up to 150 km offshore (Shannon 1985).

Thus general statements that "July (mid-winter) undoubtedly marks the onset of the upwelling along the South West African coast, attain(ing) its maximum in spring" (Stander 1964) better fits the pattern of southerly wind speeds at Walvis Bay. Hagen *et al.* (2001) describes seasonality in intense Benguela upwelling based on the areal coverage of SST  $\leq 13^{\circ}\text{C}$  (between the coast and the  $13^{\circ}\text{C}$  isotherm offshore) from satellite sea surface temperature (SST) imagery between  $9^{\circ}\text{S}$  and  $34^{\circ}\text{S}$ . This study found that the maximum area of upwelled water occurred during the austral winter/spring and the minimum during the austral summer within this region, with the Lüderitz and Namaqua cells dominating the region from May/June until October/November. This is not in agreement with the findings of this study, which are supported by the widely quoted monthly distribution per latitude ( $9^{\circ}\text{S}$  to  $34^{\circ}\text{S}$ ) of upwelling favourable wind stress described by Boyd (1987). Boyd showed winter/spring upwelling maxima for the Northern Benguela north of  $24^{\circ}\text{S}$ , and a winter minimum in the Southern Benguela as described earlier. Lüderitz and Cape Frio were identified as cells of perennial upwelling, with maximum wind stress from August through to March in Lüderitz (Boyd 1987).

A fundamental reason for the winter SST distribution described by Hagen *et al.* (2001) is related to the seasonality of SST due to the effect of the insolation cycle in winter, rather than due to increased upwelling. The insolation cycle plays a role in determining the mixed layer depth in areas of lower wind stress such as central Namibia (inverse relationship between mixed layer depth and solar radiation) (Boyd 1987). The longshore gradients of  $W^3$  that exist in the Benguela from spring to autumn largely break down in winter. Boyd (1987) describes the relatively homogenous thermal conditions in the Benguela system in winter from personal observation of steaming from Cape Town to the Kunene River in winter with the SST not differing much more than a degree variation around 14°C over the more than 1000 nautical mile distance. Boyd considered that this thermal homogeneity could facilitate winter migration of fish within the Benguela system. However, Agenbag and Shannon (1988) stated that wind-induced turbulent mixing coupled with offshore transport within the Lüderitz upwelling cell creates environmental conditions that may be unfavourable for spawning and perhaps habitation by pelagic fish. The mixing index ( $W^3$ ) is a measure of the rate of input of turbulent kinetic energy from wind to ocean (Bakun 1996) and is an index of the stability of the upper water column. High values of  $W^3$  cause both vertical motion within the water column and vertical mixing which destroys vertical stability, negatively affecting primary and secondary production (Agenbag and Shannon 1988). Despite the winter minimum in  $W^3$  described here for Dias Point, both this study and the investigation of Agenbag and Shannon found that the wind-mixing index in the Lüderitz region is around 500  $\text{m}^3 \cdot \text{s}^{-3}$  from April to June. At this time  $W^3$  is at its maximum of 300 - 500  $\text{m}^3 \cdot \text{s}^{-3}$  at Walvis Bay. Compared to Lüderitz, far lower levels of wind-induced turbulence are measured throughout the year in the Walvis Bay region with  $W^3$  around 250  $\text{m}^3 \cdot \text{s}^{-3}$  from December to April (Boyd 1987). Wind-induced turbulent mixing is not a function of latitude (Bakun 1996).

The average  $W^3$  value does not exceed 250  $\text{m}^3 \cdot \text{s}^{-3}$  in preferred pelagic spawning habitats (Cury and Roy 1989). The negative effect of turbulence on potential pelagic spawning habitat is both excessive offshore loss of pelagic larvae and dispersion of concentrated food patches for pelagic fish larvae. Patchiness in primary and

secondary production is a characteristic feature of upwelling ecosystems due to the pulsed nature of upwelling (under atmospheric control), creating parcels of newly upwelled, nutrient rich water in which phytoplankton blooms may develop if the necessary stability in the water column is achieved for the required length of time. These critical calm periods of sufficient duration to allow growth and concentration of micro-organisms have been termed Lasker windows (Bakun 1996). In the Lüderitz region, high phytoplankton biomass can be attained in quiescent periods, but generally chlorophyll concentrations are low ( $< 3\text{mg.m}^{-3}$ ) off Lüderitz due to turbulent mixing and Ekman transport during active upwelling conditions (Shannon and Pillar 1986, Carr and Kearns 2003). Low food availability to phyto- and zooplankters during active upwelling would enhance the biological barrier effect of the turbulent Lüderitz upwelling cell (Agenbag and Shannon 1988). Monthly mean composites of Sea Viewing Wide Field-of-view Sensor (SeaWiFS) chlorophyll *a* data between  $26^{\circ}\text{S}$  and  $28^{\circ}\text{S}$  show a minimum in chlorophyll *a* ( $< 1 - 2 \text{mg.m}^{-3}$ ) from May to August during which time the minimum in southerly winds occurs and sea surface temperatures are at a minimum (Hardman-Mountford *et al.* 2003).

#### 4.5. Conclusion

Seasonality in wind speed and direction along the Benguela coast is caused by a seasonal latitudinal shift in the position of the SAA and continental atmospheric pressure changes due to the northward migration of the ITCZ in winter. Thus although southerly winds predominate throughout the year maintaining a perennial upwelling cell off Lüderitz, there is a winter relaxation of the southerly wind in comparison with spring and summer. However wind mixing ( $W^3$ ) is nevertheless high throughout the year compared with the Northern Benguela, and phytoplankton biomass is generally low despite the enhanced nutrient concentrations. The nutrients exported downstream from the Lüderitz cell to the Walvis Bay area are utilised within an area of concentration and retention with a wind regime more closely approximating that of the optimal environmental window. The productive pelagic fisheries of the northern Benguela are thus supported by the high primary production north of the Lüderitz upwelling cell.

The Lüderitz southerly wind is thus a critical “engine” within the Northern Benguela ecosystem. Variability of the wind regime at different time scales therefore warrants further investigation in view of the potential consequences of diminished or enhanced upwelling at Lüderitz in initiating altered productivity of the Northern Benguela ecosystem through “bottom-up” control (Cury and Shannon 2004).



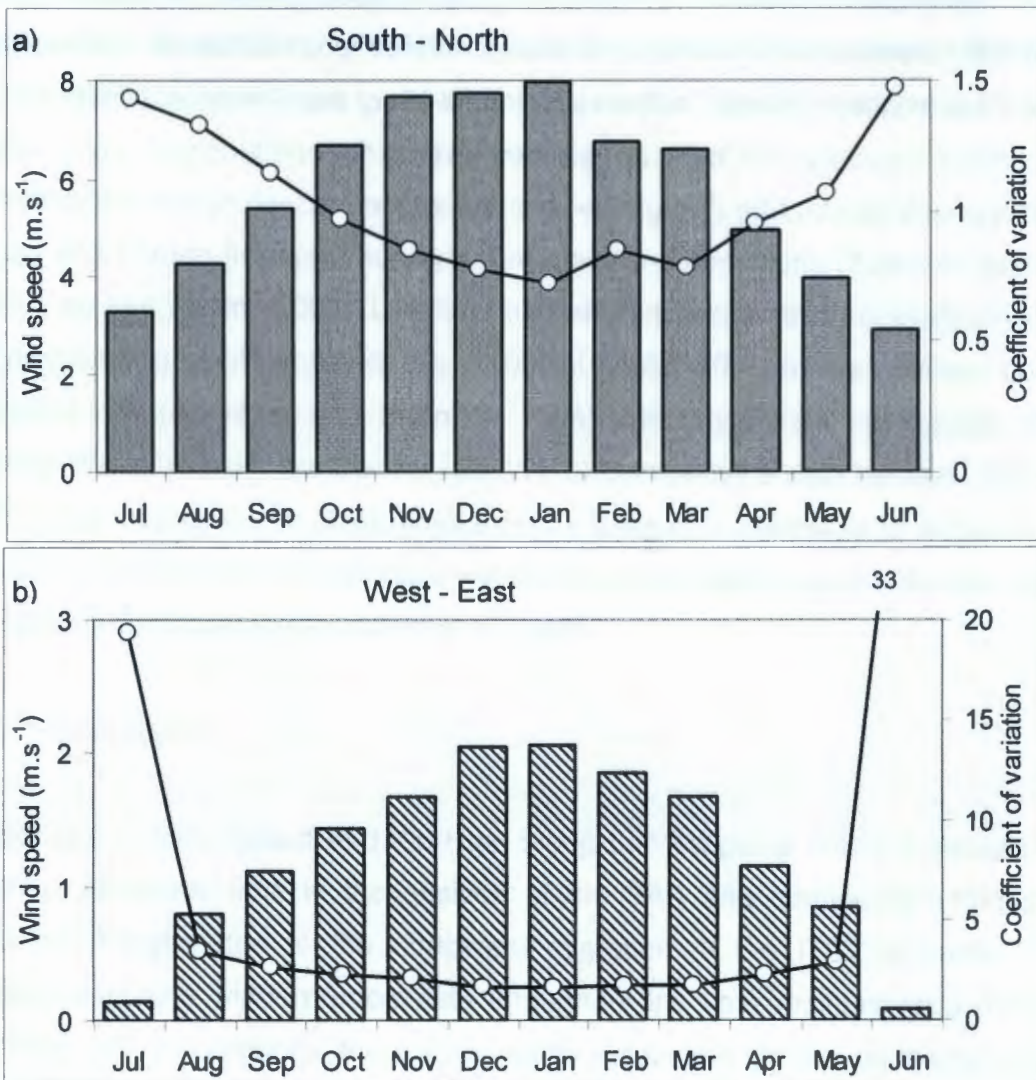


**Figure 4.1.** Monthly average a) South-North (m.s<sup>-1</sup>), b) West-East (m.s<sup>-1</sup>) wind components at Dias Point Lighthouse (bars) based on a 44-year time series. Southerly and westerly winds are positive, northerly and easterly winds are negative values. Higher variability in the wind regime occurs during winter months as shown by the coefficient of variation (lines). The year is depicted from July – June in order to keep the spring - summer upwelling season as an entity.

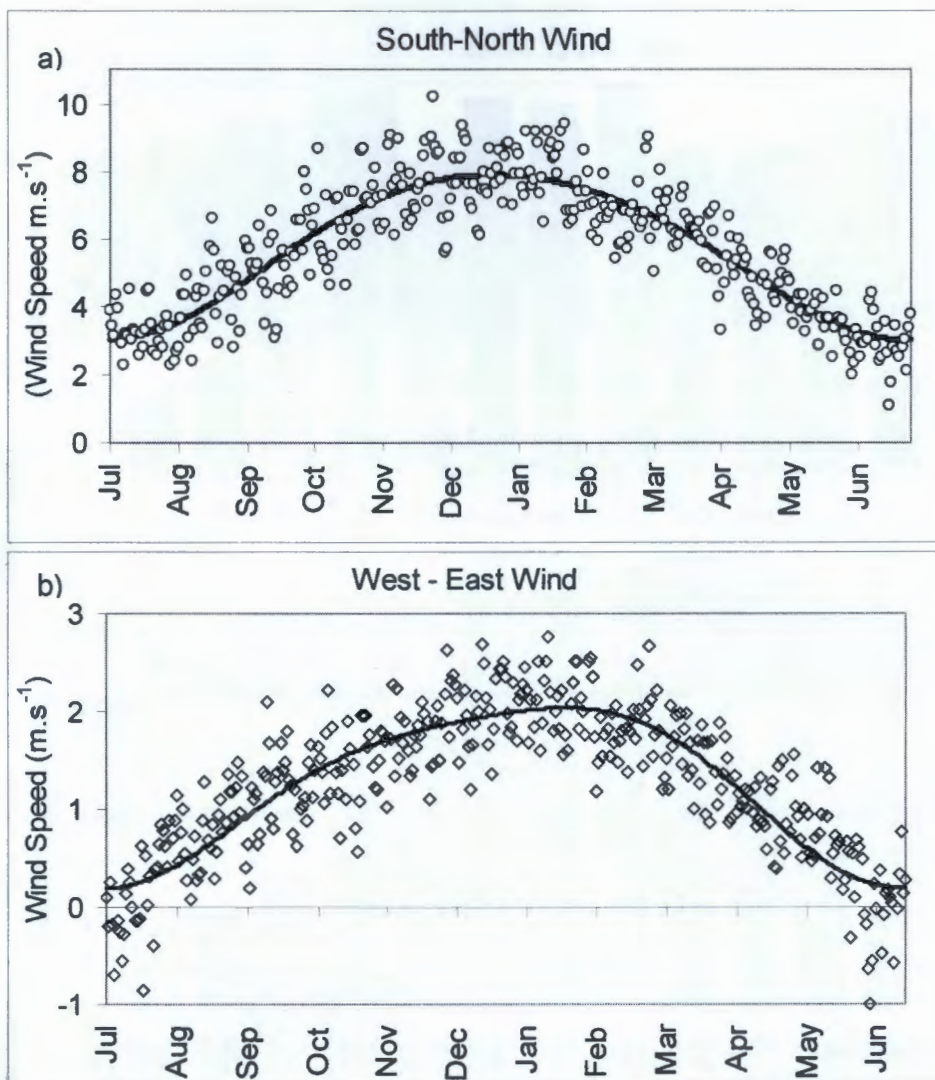


**Figure 4.2.** Seasonality in a) South-North and b) the West-East wind components measured at Dias Point Lighthouse, Lüderitz. The daily average wind speed (markers) was calculated over 44 years from 1960 to 2004 and a first harmonic curve (line) fitted to these values. Southerly and westerly winds are positive values, northerly and easterly winds negative values. Note that axis scales differ.

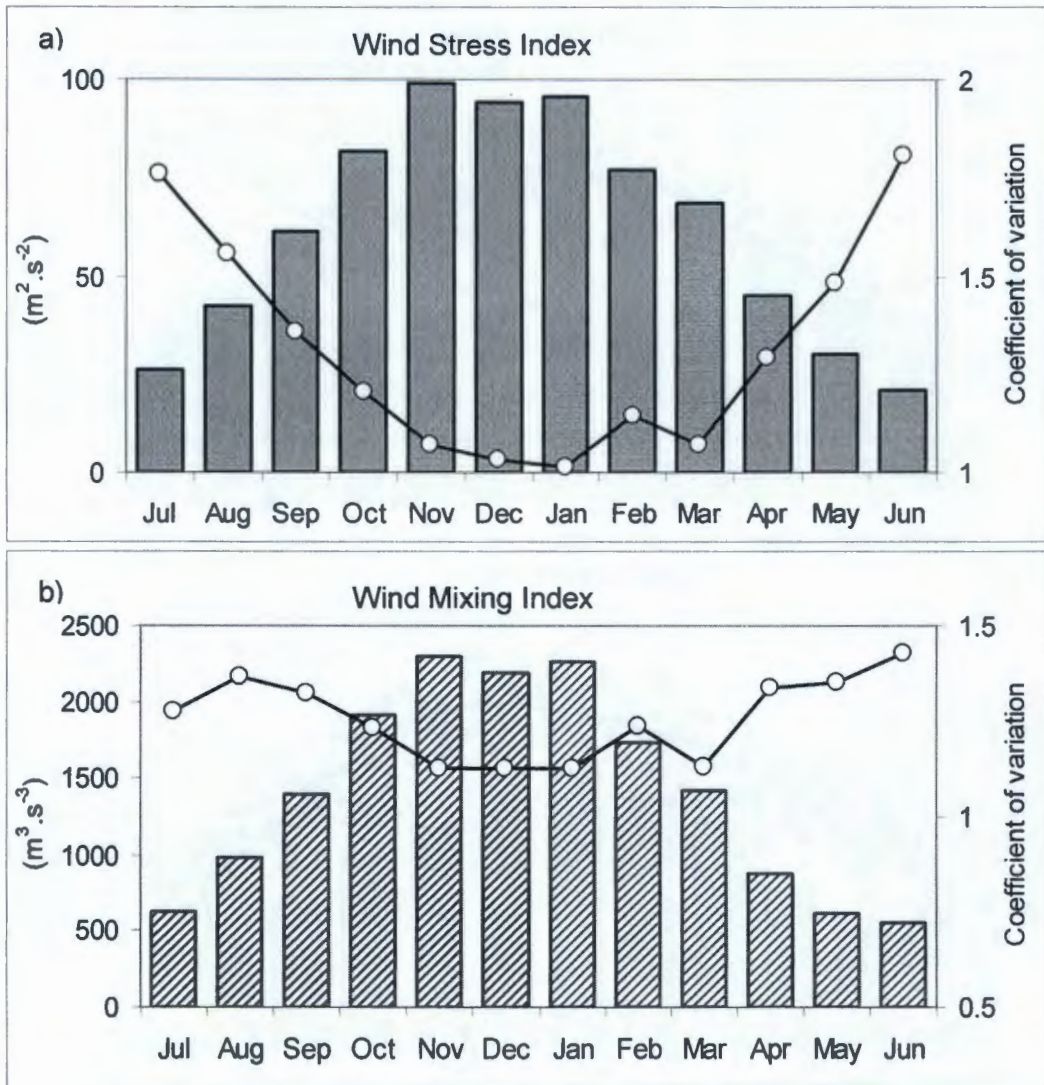


**Figure 4.3.** Monthly average a) wind stress as an index of wind-driven upwelling intensity and b)  $W^3$  an index of wind-induced turbulent mixing, at Dias Point Lighthouse (bars) based on a 44-year time series. The coefficient of variation (lines) is lowest in summer at the peak of the upwelling season.

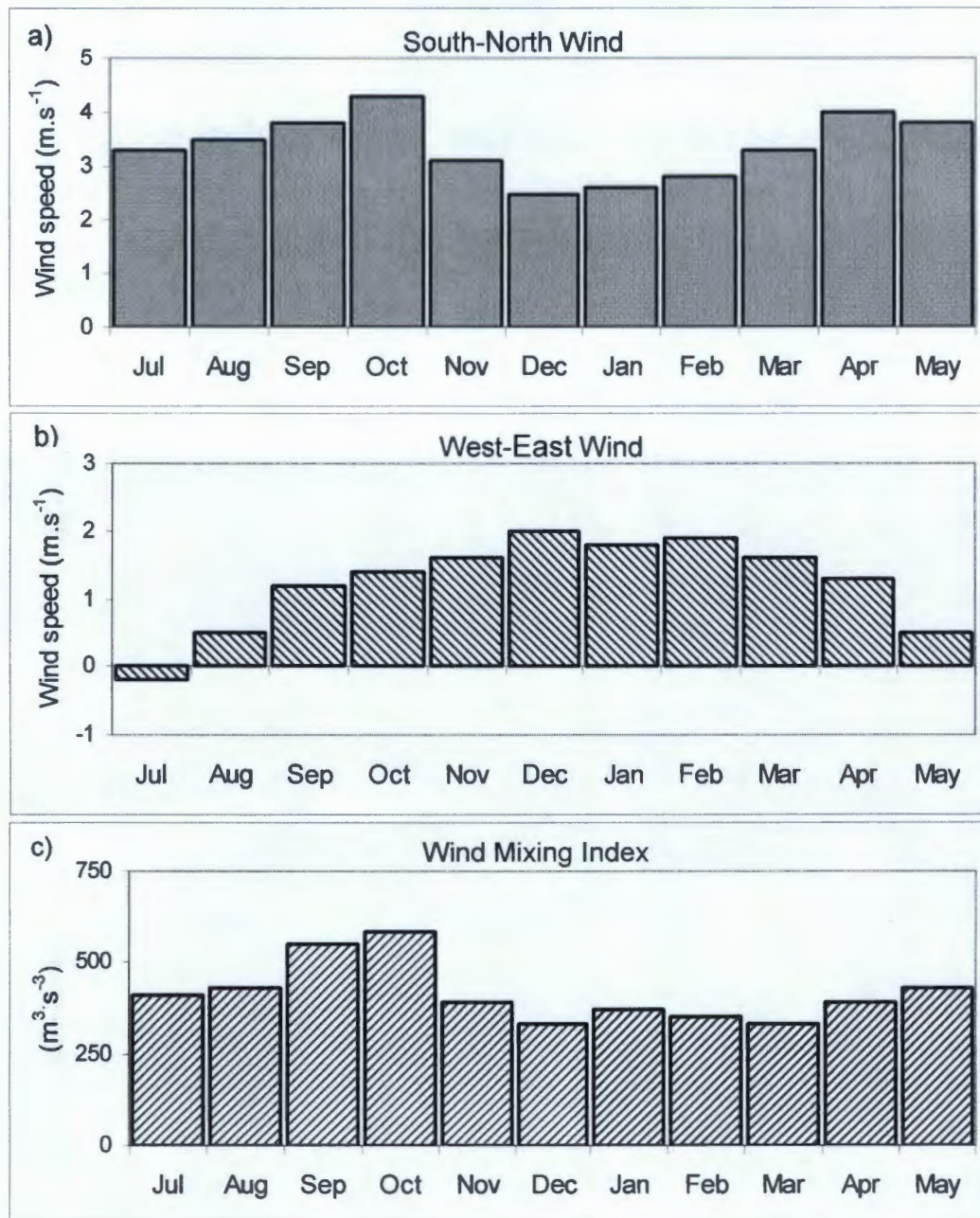


**Figure 4.4.** Seasonal cycle of a) South-North (m.s<sup>-1</sup>) b) West-East (m.s<sup>-1</sup>) winds and c) wind mixing Index  $W^3$  (m<sup>3</sup>s<sup>-3</sup>) measured at Pelican Point Lighthouse (Walvis Bay). Monthly average wind speeds calculated from 1978 to 1984, redrawn from Boyd (1987).



Figure 4.4. Seasonal cycle of wind mixing index  $W$  for (a) West-East, (b) West-South, (c) West-North, and (d) combined for West-East, West-South, and West-North directions. The data shows a seasonal cycle with higher values in winter and lower values in summer.

## Chapter Five

The influence of wind stress on sea surface temperature and on the temperature dynamics in the water column at Lüderitz



# The influence of wind stress on sea surface temperature and on the temperature dynamics in the water column at Lüderitz

## 5.1. Introduction

Historical oceanographic cruises that surveyed the entire Namibian coast such as the two "William Scoresby" cruises in 1950 (Hart and Currie 1960), and the work published by Stander (1964) based on nine cruises between 1959 and 1961, identified the southern Namibian coast and particularly the region between 28°S and Lüderitz (26° 38'S) as being a centre of upwelling. Another area of recurrent upwelling was noted between Cape Frio and the Kunene River (Hart and Currie 1960). Parrish *et al.* (1983) describe Lüderitz as an upwelling centre with intense offshore Ekman transport. Based on the work of these and other authors, Shannon (1985) singled out the Lüderitz region as the principal upwelling cell of the Benguela Current system.

The prevailing southerly winds driving coastal upwelling near Lüderitz originate in the South Atlantic Anticyclonic (SAA) circulation, one of a discontinuous band of mid-latitude high pressure cells which predominate over the climate of the southern Hemisphere (Tyson and Preston-Whyte 2000). The strength and persistence of upwelling in the Lüderitz cell is attributed to the protrusion of the southern Namibian coastline seaward of the mean west coast alignment (thus in close proximity to the SAA), the South-North orientation of the coast between Orange River and Lüderitz and the aridity of the coastal plain which acts as a thermal barrier to cross-flow, thus steering the equatorward winds alongshore (Nelson and Hutchings 1983, Boyd 1987). In addition, the relatively narrow shelf off Lüderitz is conducive to rapid upwelling due to the proximity of deep water to the inshore upwelling area and the influence of bottom topography on the vorticity of the flow (Nelson and Hutchings 1983). In the Lüderitz area water is upwelled from a depth of 250 to 350 m (Boyd 1987) resulting in an intense cold coastal temperature anomaly throughout the year (Parrish *et al.* 1983).

The variability of upwelling intensity at Lüderitz at diurnal, synoptic and seasonal scales is due to the pressure gradients between the SAA and the continental low pressure, migration of the SAA pressure locus seasonally and the effects of eastward moving cold fronts (cyclonic low pressure cells) south of the African subcontinent which are associated with coastal low development at Lüderitz (Shannon 1985, Tyson and Preston-Whyte 2000, Shillington *et al.* 2006).

The coupling between atmosphere and ocean suggests that meteorological data is valuable in understanding the role of wind-driven shelf circulation and the associated transport of water masses (Duncombe Rae 2005), thermocline formation / breakdown, nutrient fluxes and primary productivity (Anon 1998). The Lighthouse records of wind speed and direction from 1960 to 2006 at Lüderitz are a unique record of the coastal wind field on the shoreline of one of the most intense wind-driven upwelling cells in the world. However, Lighthouse data have been considered unsuitable for consideration in conjunction with hydrographic data (Stander 1964). The primary goal of this chapter is to show that the wind field measured at Dias Point Lighthouse, situated close to the shore on an exposed peninsula, correlates well with both inshore and nearshore upwelling dynamics in the Lüderitz cell. To this end inshore sea surface temperature (SST) at Dias Point is related to the longshore wind stress and the response time to wind forcing determined. The formation and breakdown of the thermocline in response to changes in intensity of the longshore winds is examined using temperature profiles through the water column within 20 km offshore of the Lighthouse.

## 5.2. Methods

Wind speed and direction data from an anemometer / wind direction vane were recorded at Dias Point Lighthouse at 08h00, 14h00 and 20h00 local time (06h00, 12h00 and 18h00 GMT) daily from 1 March 1990 to 20 June 1998. The weather station was located at 26° 38.094'S, 15° 05.612'E. The component parallel to the coastline (aligned South to North in the Lüderitz area) was derived and a daily average wind speed determined. A proxy for upwelling intensity was calculated from

the wind stress component ( $\tau = r \cdot C_d \cdot V^2$ ) of Ekman transport (Johnson and Nelson 1999, Mann and Lazier 1991) and is referred to as wind stress. In calculating the daily average wind stress the square of negative daily average values (North wind) was multiplied by  $-1$  (Chapter Two).

Seawater for sea surface temperature (SST) measurements was sampled with a bucket within 0.5 meter of the water surface. Readings were taken with a mercury thermometer of  $0.1^\circ\text{C}$  accuracy. The SST measurement site was located in a wave-inundated bay approximately 20 m away from the Dias Point weather station. SST readings were taken daily at 08h00 (06h00 GMT) from 1 March 1990 to 20 June 1998.

CTD profiles were made from RV Kuiseb, using a SEA-BIRD ELECTRONICS SBE 19 SEACAT profiler. The CTD was deployed for 2 – 5 minutes at the surface to allow sensors to equilibrate before being lowered at approximately 1 m per second through the water column. Temperature profiles from CTD casts are presented from the five deepest stations (8 to 12) on the CTD line off Dias Point from August 1993 to February 2001. Station positions are given in Table 5.1. Certified calibrations of the SBE 19 SEACAT temperature sensor used in these measurements were carried out by SEA-BIRD in March 1993, June 1994, November 1995, July 1998 and August 1999.

### **5.3. Results**

#### **5.3.1. Response of Inshore SST to Local Wind Stress**

In order to determine whether the SST measurements at Dias Point were related to the longshore wind regime, the daily wind stress was used as the independent variable in a correlation analysis with SST. Correlation of all daily wind stress values against SST during the period 1 March 1990 to 20 June 1998 showed a significant relationship ( $r = -0.021$ ,  $p < 0.001$ ,  $n = 3003$ ). Introducing a time lag and thus comparing SST with the previous day's wind stress (one-day lag) improved the fit

( $r = -0.051$ ,  $p < 0.001$ ,  $n = 3001$ ). Comparing SST with the wind stress of two-days previously (a two-day lag) was also significant ( $r = -0.034$ ,  $p < 0.001$ ,  $n = 3000$ ).

During the summer (here defined as 15 November to 14 February), the relationship between wind stress and SST was stronger than in winter (15 May to 14 August) although highly significant in both seasons. In both cases the best fit was with a one-day time lag as described above (Figure 5.1). Table 5.2 gives the correlation statistics of the fits at different time lags.

Comparing the winter - summer wind stress / SST at the best fit relationship of a one-day lag of SST behind wind stress it is apparent that surface temperatures warmer than  $15^{\circ}\text{C}$  occurred only in summer and then mainly during calm wind conditions (wind stress close to zero) (Figure 5.1). The SST range in summer was  $10^{\circ}$  to  $17.4^{\circ}\text{C}$ . Temperatures  $> 15^{\circ}\text{C}$  correspond to a narrow wind stress range of  $-11$  to  $3 \text{ m}^2.\text{s}^{-2}$  with the exception of one outlier in Figure 5.1a. SST of  $15.2^{\circ}\text{C}$  on 9 January 1994 was measured after wind stress of  $165 \text{ m}^2.\text{s}^{-2}$  on 8 January 1994 as a strong southerly wind started to blow after a 4-day period of light northerly winds (4 - 7 January). SST at the Dias Point shoreline had increased from  $12$  to  $16.2^{\circ}\text{C}$  during this period of wind reversal (Figure 5.2a). Warming of the surface water was also apparent in the water column off Dias Point to a depth of 20 - 25 m at CTD stations within 11 nautical miles from the shore (Figure 5.3a). Consistent southerly winds on 8 and 9 January resulted in this surface layer being replaced by cooler water ( $13^{\circ}\text{C}$ ) on 10 January 1994, when the SST inshore decreased to  $13^{\circ}\text{C}$  (Figure 5.2a), the average January SST being  $12.6^{\circ}\text{C}$  ( $n = 248$ ) at Dias Point. The stratified surface waters inshore of the station at  $15^{\circ}\text{E}$  were replaced with water  $< 12^{\circ}\text{C}$  by 14 January 1994 (Figure 5.3b).

In winter the SST range was narrow ( $9.5^{\circ}$  to  $14.1^{\circ}\text{C}$ ) and the warmest surface temperatures ( $> 13.5^{\circ}\text{C}$ ) occurred at a comparatively wide range of wind stress ( $-22$  to  $65 \text{ m}^2.\text{s}^{-2}$ ) compared with summer (Figure 5.1b).

Southerly winds can blow uninterrupted at Lüderitz for a period of two weeks (Bailey 1979), and the effect of such extended periods of south wind can be seen in SST of December 1995 (Figure 5.2c). During the first ten days of the month wind stress (proportional to the longshore wind speed squared which is the South-North component at Lüderitz) with a daily average value of up to 250 occurred at Dias Point. SST within a narrow range of 0.5°C (11.5 – 12.0°C) was recorded during this period. With the reversal of wind direction to north on 11 December, SST began to increase over the following nine days to a maximum of 17°C. Even a short pulse of wind stress (e.g. 20 - 21 December 1995) caused SST to decrease by 5°C. Towards the end of the month wind stress was more consistent and SST again decreased to 11.6°C by the end of December (Figure 5.2c).

During the winter months, illustrated by June 1990, July 1991 and August 1996, wind stress was reduced and winds less consistent than in summer, while inshore SST at Dias Point had a far smaller range (10 to 13.5°C) than in summer (Figure 5.2d - f). The increase in sea temperature following cessation of a pulse of upwelling-favourable wind was not more than 2°C during periods of calm or northerly wind in winter. For example during a nine-day calm period in July 1991, SST rose from 11.4° to 12.5°C (Figure 5.2e) in comparison with a 6°C increase during nine days of calm weather in December 1995 (Figure 5.2c). A decrease in SST in response to the onset of wind stress was also evident in winter for example from 13 - 18 August 1996 (Figure 5.2f).

### **5.3.2. Response of the Water Column to Local Wind Stress**

The effect of the wind regime measured at Dias Point on the vertical temperature structure of the water column up to 11 nautical miles offshore of Dias Point was also investigated. At each station the near-surface temperature at 4 m was subtracted from the temperature at a depth consistently below the thermocline when present. After visual inspection of the temperature profiles the temperature at 40 m was considered to be representative of the lower water column. The temperature difference ( $\Delta t$ ) between 40 m and 4 m was therefore used to indicate the degree of mixing in the water column. The  $\Delta t$  value would be highest in the presence of

stratification and warming of the surface layer. When the water column was well mixed, thus having a nearly uniform temperature structure throughout, the  $\Delta t$  value would be small. Figure 5.4a and 5.4b illustrate these two scenarios using vertical temperature sections off Dias Point sampled on the 14<sup>th</sup> and 25<sup>th</sup> February 1994. This figure also shows temperature profiles and the calculated  $\Delta t$  values at selected stations on the Dias Point CTD line. The daily average wind stress for February 2004 is given in Figure 5.2b showing strong wind stress prior to sampling on 14<sup>th</sup> February, thus  $\Delta t$  values are low (Figure 5.4c - e) compared with those on 25<sup>th</sup> February (Figure 5.4f - h) when the water column was well stratified after four days of calm weather.

To determine whether the wind measured onshore at Dias Point could be related to changes in the vertical temperature structure in the water column up to 11 nautical miles (20.4 km) offshore, the wind stress at the time lags used previously was compared with the  $\Delta t$  values from the time series (1993 to 2001) of profiles sampled at the five deepest stations (8 to 12) on the Dias Point line (Table 5.1). At all five stations wind stress prevailing two days prior to the temperature profile was significantly related to the  $\Delta t$  values as was the wind stress averaged over the two previous days. Regression statistics are given in Table 5.3. The wind one day prior to the CTD cast sampling was not significant at all stations while the wind stress on the same day as the profile and 3 days prior to sampling were not significant at any of the stations analysed (Table 5.3).

Vertical temperature profiles from CTD casts at Station 8 (26° 38'S, 14° 58'E) were categorized according to the wind stress two days prior to sampling in order to determine the effect of wind stress of different intensities on the shape of the temperature profile and on the thermocline depth. Wind stress categories were determined as follows: < 16 (northerly / light southerly < 7.8 knots),  $\geq 16$  to < 100 (moderate southerly  $\geq 7.8$  to < 19.4 knots),  $\geq 100$  (strong southerly  $\geq 19.4$  knots). Summer profiles ( $n = 15$ ) were compared with winter profiles ( $n = 11$ ) within these wind categories (Figures 5.5 and 5.6).

In summer, profiles sampled after northerly / light winds had highest  $\Delta t$  values ( $1^{\circ}\text{C}$  to  $2.8^{\circ}\text{C}$  difference between near surface and sub-thermocline) due to warming of the surface water to  $13^{\circ}$  to  $15^{\circ}\text{C}$ . The thermocline (calculated as a  $> 0.6^{\circ}\text{C}$  change per 10 m, after Boyd 1987) in these profiles was at 8 – 20m depth, on average 14 m (Figure 5.5a). Following moderate southerly winds in summer, the temperature of surface water was lower and only  $0.5^{\circ}$  to  $1^{\circ}\text{C}$  higher than at 40 m. The thermocline depth when present was shallower, 4 m (29 January 1996) to 16 m (3 February 1998), average 6 m (Figure 5.5b). Following strong southerly winds the temperature profiles were near vertical throughout the water column with small to no difference in  $\Delta t$  ( $0.07^{\circ}\text{C}$  –  $0.6^{\circ}\text{C}$ ) (Figure 5.5c).

In winter the vertical profiles after wind stress  $< 16$  (light / northerly winds) and  $< 100$  (moderate southerly winds) could not be distinguished from each other in shape or on the basis of the  $\Delta t$  values (Figure 5.6a,b). There were no instances of high wind stress ( $\geq 100$ ) prior to sampling in winter.

### 5.3.3. Temperature - Salinity (T-S) Relationships

The temperature and corresponding salinity data per meter from CTD profiles with strong ( $\Delta t > 0.9$ ) and weak ( $\Delta t < 0.9$ ) stratification are investigated using summer and winter profiles (1993 to 2001) from Station 8 of the Dias Point monitoring line (Figure 5.7).

The data depicted by open and filled circles in Figure 5.7a are the summer profiles with  $\Delta t > 0.9^{\circ}\text{C}$ , sampled two days after light to moderate wind stress ( $< 100 \text{ m}^2 \cdot \text{s}^{-2}$ ). The open circles denote water from surface to 40 m and filled circles the deeper water ( $> 40\text{m}$ ). Profiles with  $\Delta t < 0.9$  are depicted by filled squares. The T-S of the latter ( $10.2^{\circ}\text{C}$  to  $12.7^{\circ}\text{C}$ ; 34.77 to 35.06 psu), overlaps in range with the sub-thermocline water (filled circles) of the  $\Delta t > 0.9^{\circ}\text{C}$  profiles. Above the thermocline (open circles) these profiles had a wide T-S range ( $10.5^{\circ}$  to  $15.3^{\circ}\text{C}$ , 34.77 to 35.08 psu) (Figure 5.7a).

The winter T-S range generally overlapped with the water mass depicted by filled squares in the summer T-S diagram ( $\Delta t < 0.9$ ), but with a slightly colder temperature range due to temperatures  $< 10^{\circ}\text{C}$  (34.74 to 35.06 psu), while the warmest water ( $12^{\circ}\text{C} - 13^{\circ}\text{C}$ ) had a higher salinity than in summer (Figure 5.7b).

## 5.4. Discussion

### 5.4.1. Response of Inshore SST to Local Wind Stress

Boyd (1987) from an analysis of ship's wind observations between  $10^{\circ}\text{S}$  and  $34^{\circ}\text{S}$  has shown that within these latitudes the strongest continuous wind stress occurs within the Lüderitz region ( $26^{\circ}\text{S} - 27^{\circ}\text{S}$ ). The smaller range in positive wind stress in winter compared with summer is due to minimum southerly wind speeds during June (Chapter Four). This seasonal minimum in wind stress in Lüderitz in June - July coincides with the seasonal minimum in SST and solar insolation. Maximum wind stress and offshore Ekman transport occurs in summer (November to February) (Chapter Four). Although this is the season of maximal solar heating of surface waters in the austral summer, Parrish *et al.* (1983) showed a strong negative SST anomaly in January - February at Lüderitz associated with a maximum of offshore Ekman transport. This low SST / high wind stress relationship has been established at Dias Point to be highly significant ( $p < 0.001$ ) throughout the year with the strongest relationship in summer.

Since wind-driven upwelling at Dias Point suppresses the inshore SST, the periodicity of the wind regime is one of the main sources of variability in SST. The pulsed nature of wind stress is evident in summer and in winter at Dias Point, with relaxation of upwelling-favourable wind causing an increase in sea surface temperature as long as calm or northerly weather persists. Inshore SST decreases on resumption of wind stress as cold water from a depth of 200 – 300 m in the Lüderitz region is brought to the surface and displaces warmer water seaward (Bailey 1979, Smith 1995). The increase in SST during periods of calm or northerly winds is relatively small during winter compared with summer, thus the seasonal

change in insolation is the underlying reason for the stronger relationship between the summer wind stress and SST fit compared with that in winter.

Wind reversals occur at 3 to 10 day intervals (Shannon and Nelson 1996) although longer upwelling events of two weeks or more can occur at Lüderitz particularly in spring and summer Bailey (1979). The development of coastal lows in association with the ridging of the South Atlantic Anticyclone south of the subcontinent as described in Chapter One results in northerly winds due to cyclonic circulation around the coastal low pressure cell which develops north of Lüderitz and travels southwards along the coastline towards the Cape (Reason and Jury 1990). For the duration of the north wind spells, warmer offshore surface water is advected inshore and downwells against the coast (Peard and Roux 2002). Productivity is enhanced during the quiescent phase with new nitrogen having been introduced in the previously upwelled waters (Jury and Brundrit 1992, Hutchings *et al.* 1994).

The best response time of SST to wind stress at Dias Point was with a one-day lag, although the response of SST to wind stress two to four days previously was also significant where tested in summer and in winter. The response of SST to the onset of upwelling-favourable winds following a period of relaxation of upwelling is initially negatively correlated but under continuous upwelling over a period of days there is no further temperature response at the sea surface as near constant source water is upwelled (Andrews and Hutchings 1980). As a result, the correlations between wind stress and SST given in Table 5.2, although significant, explain only a small percentage of the variance. An analysis of isotherm depth in response to wind stress would be preferable given a more suitable time series of oceanographic data.

Response time of SST is probably dependent on the depth of the thermocline, which develops due to warming of surface water in calm conditions, and on the inertial period at that latitude. This is the time a current of water will take to gain or lose momentum at the onset or cessation of the wind driving it (Open University 1989). At Lüderitz the inertial period is 26.9 hours. If a shallow thermocline only a few meters below the surface (e.g. Figure 5.5b) develops during a short period of calm or moderate winds, the warmed surface layer will be rapidly displaced at the onset of

strong wind stress. However if a stable deep thermocline is present with onshore flow under downwelling conditions, the resumption of southerly winds cannot have an immediate response in reversing the flow, due to inertial effects. This was probably the reason for the two day response time of the inshore SST to wind stress on 10 January 1994 after a four day period of northerly / calm conditions described in 5.3.1 (Figure 5.2a). Looking at the cross section of temperature within 11 nautical miles of the coast on 6 January 1994 (Figure 5.3a), discussed in the next section, and the vertical temperature profile at Station 8 on 6 January 1994 (Figure 5.5a), the stability of the water column is evident with a lens of warm surface water overlying colder, denser water below.

#### **5.4.2. Response of the Water Column to Local Wind Stress**

To show that the wind regime measured at Dias Point can be related not only to inshore SST but also to the vertical structure of temperature profiles from deeper water, temperature sections of the Dias Point CTD line sampled under contrasting wind conditions were illustrated in January and February 1994. Downwelling is evident from isotherms dipping down towards the coast at 15° 04'E on 6<sup>th</sup> January 1994 during light northerly winds (Figure 5.3a). The station was sampled again the following week under strong southerly winds on 14<sup>th</sup> January 1994. The uplift of the 12°C isotherm to the surface at the 15°E station and the presence of cold water throughout the water column inshore of this station indicates active upwelling (Figure 5.3b).

The vertical temperature section off Dias Point sampled on 14<sup>th</sup> February shows the initiation of surface stratification on the second day of calm after a pulse of southerly wind (Figure 5.4a,c,d,e). Later in the month the surface warming and stratification had intensified (Figure 5.4b), due to calm weather recorded at Dias Point (Figure 5.2b). Only remnants of 11°C – 12°C water were present in the lowermost and offshore depths while the thermocline had deepened to 20 – 40m (Figure 5.4b,f,g,h).

### 5.4.3. Temperature - Salinity (T-S) relationships

The analyses in this chapter relate the wind regime at Dias Point to upwelling events in the inshore and nearshore coastal region. It is expected that the T-S properties of the water column would also differ in relation to the intensity of wind stress, used as a proxy for coastal upwelling. The temperature and salinity properties of the water masses present a) in the lower water column during quiescent conditions, b) after and during active upwelling and c) during winter presented in this chapter overlap each other within the T-S bounds of 9.5° to 13.2°C; 34.74 to 35.06 psu. These T-S properties conform to those of Central Water, described by Shannon (1985) as the linear portion of the curve connecting the approximate points 6°C, 34.5 psu and 16°C, 35.5 psu and as being upwelled on the coast from Cape Point to Cape Frio. Shannon states that in the temperature range 10°C – 12°C it is difficult to distinguish between the Central Waters, which are described in more detail in terms of salinity and potential temperature in Duncombe-Rae (2005). The intention of the T-S analyses in this chapter was to not to identify the water mass origin but to categorize it as having the properties of Benguela coastal upwelled water (Shannon and Nelson 1996, Shillington *et al.* 2006). Modifications of this water mass due to warming and contact with the atmosphere were evident from the different T-S properties of the upper water column sampled after calm conditions and with a high  $\Delta t$  due to stratification (open circles in Figure 5.7a).

### 5.5. Conclusion

The significant negative relationship between wind stress and SST at Lüderitz is evidence of classic wind-driven coastal upwelling as described for the four major eastern boundary upwelling systems (Bakun and Nelson 1991) In this study a strong relationship is apparent between low SST at Dias Point and equatorward wind stress (a proxy for coastal upwelling) at Lüderitz throughout the year. The two main influences on SST were found to be the seasonal change in solar insolation and the periodicity of wind stress at a synoptic scale. Upwelling pulses under strong wind stress of differing duration alternated with periods of calm or northerly winds at Dias Point. The cessation of upwelling in summer coupled with high solar heating of the

surface water enabled a stable stratified water column to develop. The duration of these calm periods in summer determined the thickness of the surface warm layer and the thermocline depth, while in winter surface stratification was minimal. Solar radiation in turn influences primary productivity as variations in light intensity affect photosynthesis on a seasonal basis (Shannon and O'Toole 1999). Intense upwelling, although supplying nutrients to surface waters, can also limit primary production due to turbulent mixing during which phytoplankton cells are constantly removed from the euphotic zone. This is one of the main reasons that Lüderitz has a low chlorophyll biomass despite high nutrient input due to perennial upwelling (Carr 2002, Hardman-Mountford *et al.* 2003). The combination of a year-round negative temperature anomaly in this region, high turbulent mixing and low chlorophyll biomass are thought to present a biological barrier to the longshore movement of pelagic species through the Lüderitz upwelling cell (Agenbag and Shannon 1988).

CTD profiles from a station 7 nautical miles offshore sampled over eight years show a) that the T-S properties of the water mass present during and after upwelling-favourable wind stress corresponds to Central Water which constitutes the water mass upwelled onto the shelf in the Benguela system (Duncombe-Rae 2005) and b) that the dynamics of the water column in terms of the development and breakdown of stratification can be related to the wind regime measured at Dias Point Lighthouse. The time series of wind at this coastal station can therefore be considered highly relevant and useful to investigations of the hydrography of the Lüderitz upwelling cell.

**Table 5.1.** Location of Dias Point Line CTD stations.

<b>Station</b>	<b>Latitude:</b>	<b>Longitude:</b>	<b>Distance from Shore (nautical miles)*</b>
1	26°38'S	15° 05'E	0.2
2	26°38'S	15° 04'E	1
3	26°38'S	15° 03'E	2
4	26°38'S	15° 02'E	3
5	26°38'S	15° 01'E	4
6	26°38'S	15° 00'E	5
7	26°38'S	14° 59'E	6
8	26°38'S	14°58'E	7
9	26°38'S	14°57'E	8
10	26°38'S	14°56'E	9
11	26°38'S	14°55'E	10
12	26°38'S	14°54'E	11

\* 1 nautical mile = 1.852 km

**Table 5.2.** Significance of the trend between wind stress and SST at Dias Point during summer (15 November to 14 February) and winter (15 May to 14 August) with different time lags.

<b>Season</b>	<b>Time lag*</b>	<b><i>r</i></b>	<b><i>p</i>-value</b>	<b><i>n</i></b>
Summer	None	-0.0838	< 0.001	828
Winter	None	-0.030	< 0.001	769
Summer	1 day	-0.147	< 0.001	828
Winter	1 day	-0.097	< 0.001	768
Summer	2 day	-0.100	< 0.001	828
Winter	2 day	-0.093	< 0.001	767
Summer	3 day	-0.044	< 0.001	826
Winter	3 day	-0.060	< 0.001	765
Summer	4 day	-0.014	< 0.001	827
Winter	4 day	-0.031	< 0.001	765

\* SST (dependent variable) was compared with the previous days wind stress (1 day lag) and with the wind stress of two to four days prior to the SST measurement.

**Table 5.3.** Significance statistics for relationship between Dias Point Lighthouse wind stress and  $\Delta t$  ( $^{\circ}\text{C}$ ) at four stations between 7 and 11 nautical miles off Dias Point ( $26^{\circ} 38'S$ ). CTD casts from 1993 to 2001 were used to derive  $\Delta t$  values from each temperature profile by subtracting the temperature at 4 m from that at 40 m.

Station No (Longitude $^{\circ}\text{E}$ )	Time lag*	$r$	$p$ -value	$n$
8 ( $14^{\circ} 58$ )	None	-0.008	0.488	64
8	1 day	-0.035	0.074	64
8	2 day	-0.177	< 0.001	64
8	3 day	-0.044	0.052	64
8	2 day mean	-0.142	< 0.01	64
9 ( $14^{\circ} 57$ )	None	0.027	0.799	37
9	1 day	-0.146	< 0.05	37
9	2 day	-0.267	< 0.001	37
9	3 day	-0.078	0.052	37
9	2 day mean	0.263	< 0.001	37
10 ( $14^{\circ} 56$ )	None	-0.016	0.932	64
10	1 day	-0.105	< 0.01	64
10	2 day	-0.200	< 0.001	64
10	3 day	-0.043	0.054	64
10	2 day mean	-0.203	< 0.001	64
11 ( $14^{\circ} 55$ )	None	0.023	0.64	35
11	1 day	-0.074	0.06	35
11	2 day	-0.300	< 0.001	35
11	3 day	-0.046	0.113	35
11	2 day mean	-0.242	< 0.01	35
12 ( $14^{\circ} 54$ )	None	0.020	0.973	50
12	1 day	-0.087	< 0.05	50
12	2 day	-0.149	< 0.01	50
12	3 day	-0.041	0.084	50
12	2 day mean	-0.151	< 0.01	50

\*  $\Delta t$  (dependent variable) was compared with the previous days wind stress (1 day lag), with the wind stress of two and three days prior to the CTD cast and with the average wind stress over 2 days prior to sampling (2 day mean).

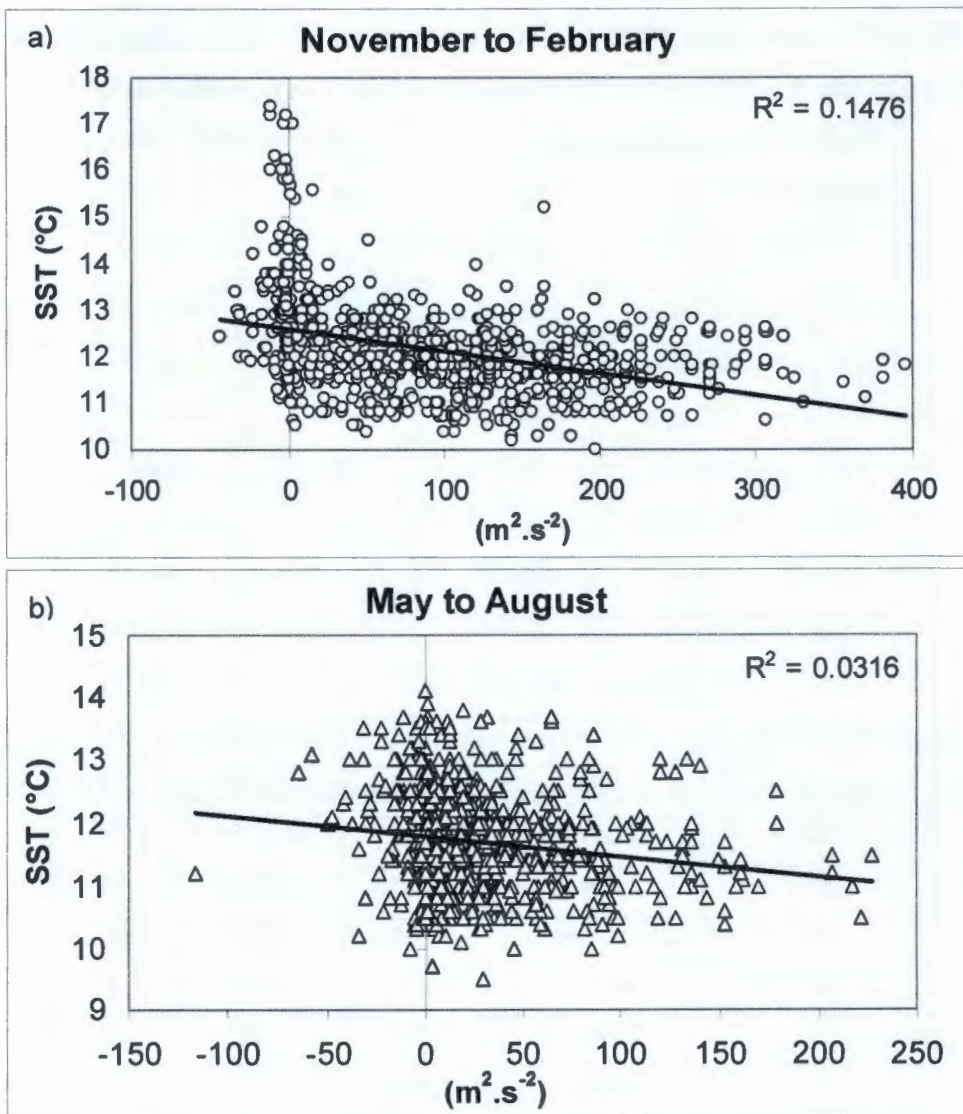


**Figure 5.1.** Daily wind stress and SST measurements at Dias Point from March 1990 to June 1998. The significant negative relationship between wind stress and sea surface temperature (SST) was improved by introducing a time lag of one day in both (a) summer (15-Nov to 14-Feb) and (b) winter (15-May to 14-Aug), thus comparing SST with wind stress of the previous day.

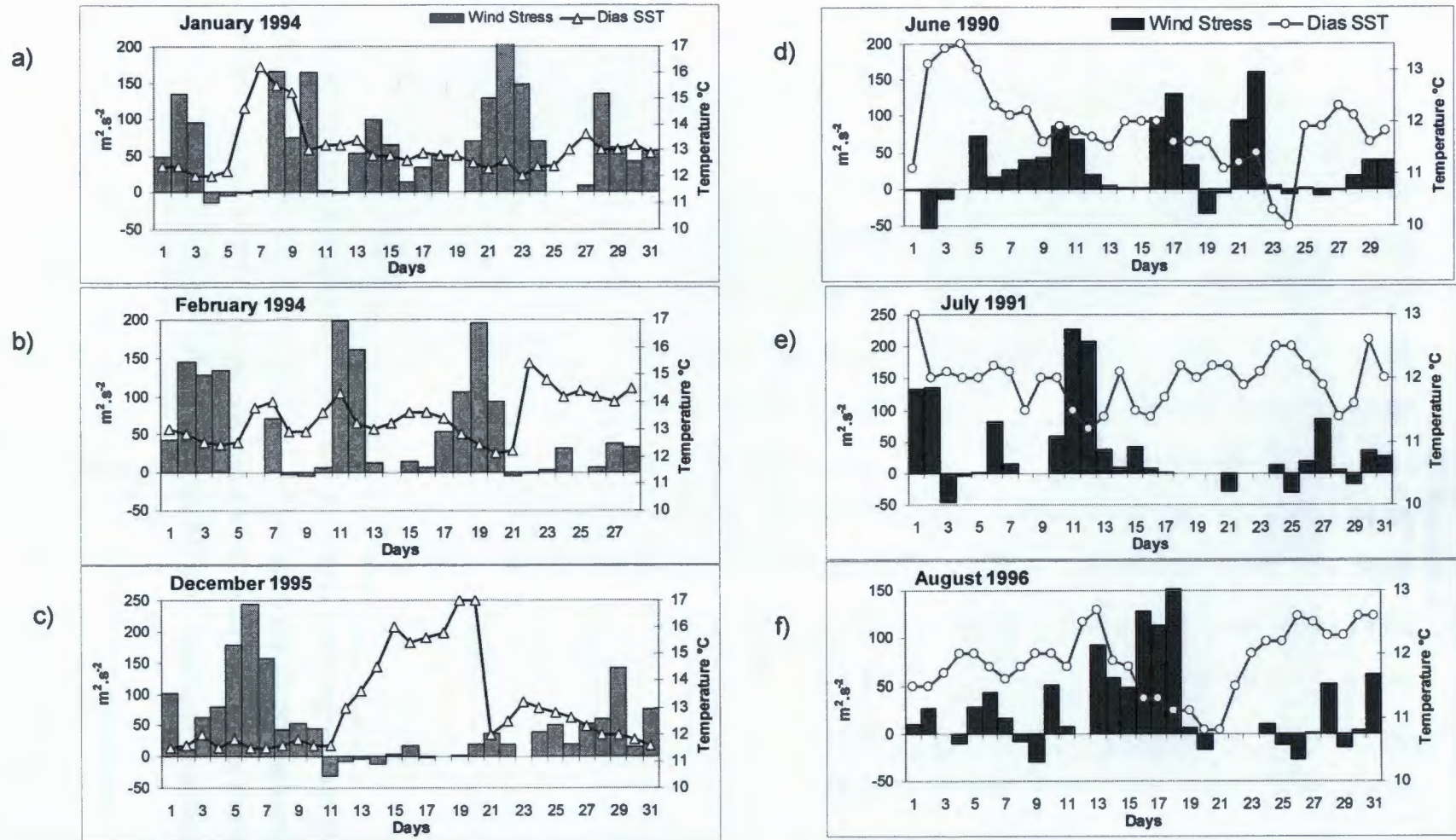


**Figure 5.2.** Daily average wind stress ( $m^2 \cdot s^{-2}$ ) showing the effect of southerly wind, calm and north wind on Sea Surface Temperature during summer months (a-c) compared with winter months (d-f). Note that axis scales differ. Positive values indicate upwelling-favourable southerly winds, negative values correspond to downwelling due to northerly winds.

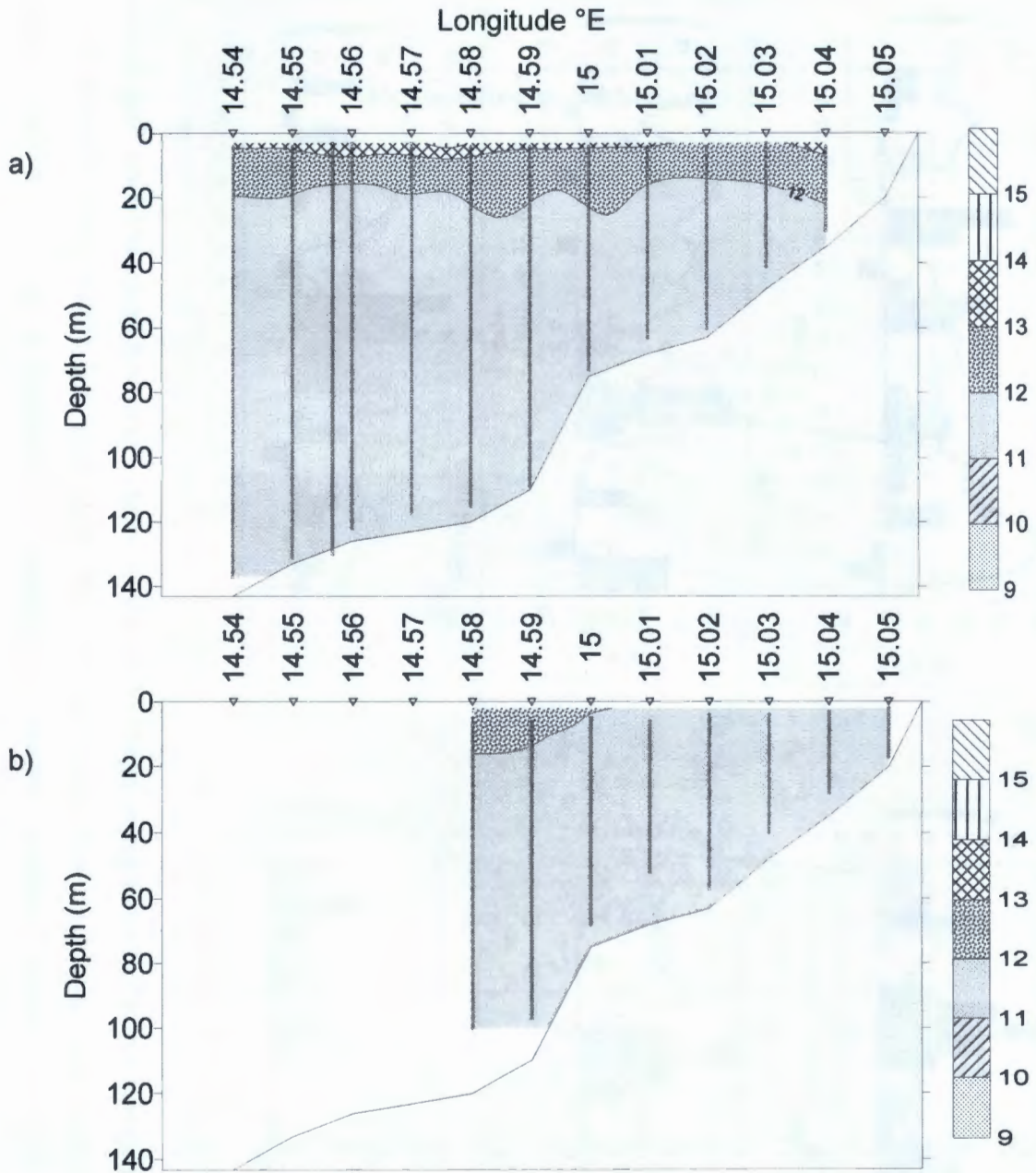


**Figure 5.3.** Vertical temperature profile off Dias Point showing surface stratification and inshore downwelling during a period of light northerly winds (a) sampled on 6 January 1994 and (b) breakdown of the thermocline within 10 km of the shore during southerly upwelling-favourable winds (14 January 1994).

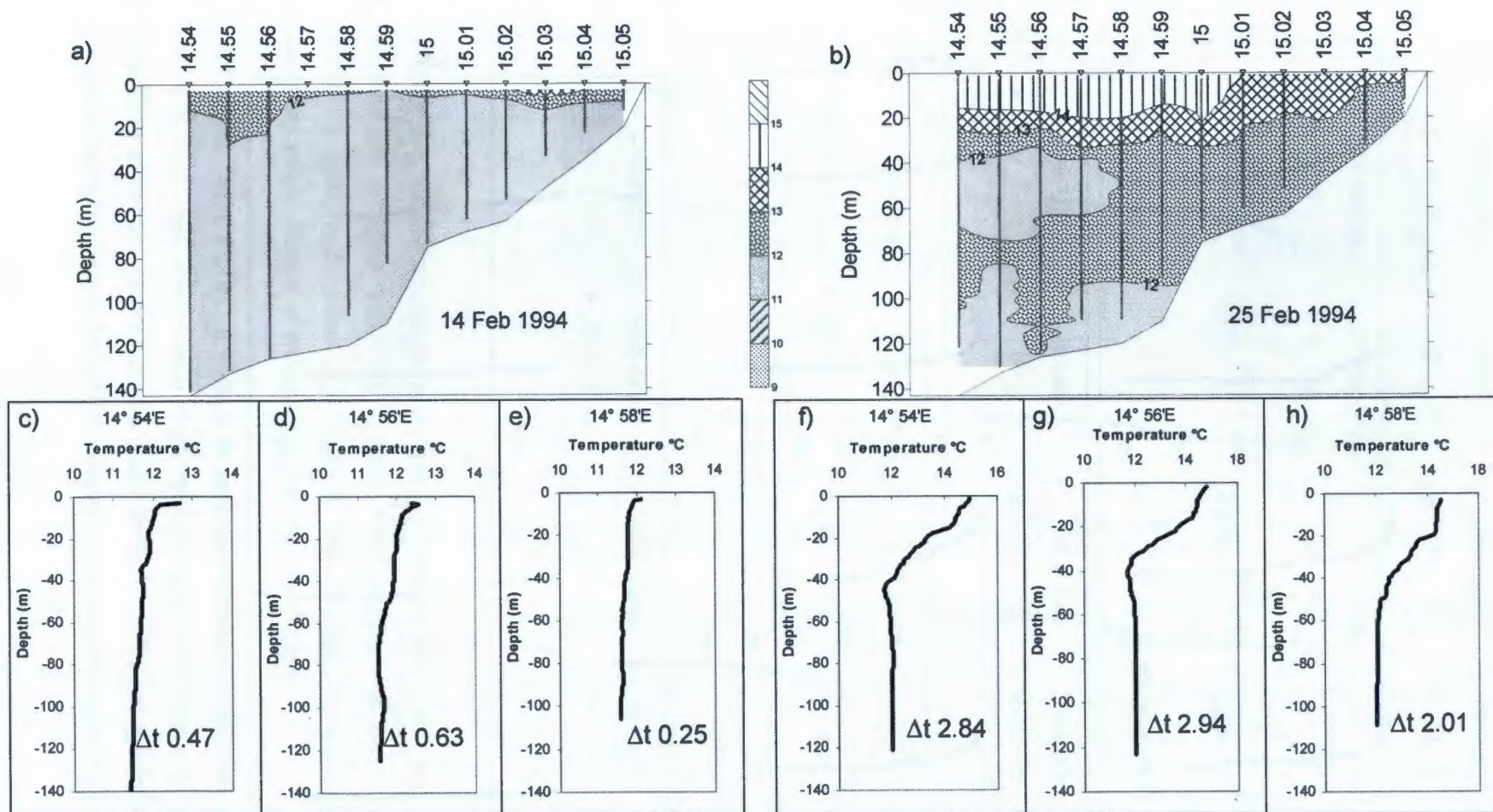


**Figure 5.4.** Vertical temperature section off Dias Point, 26° 38'S on 14 February 1994 (a) and 25 February 1994 (b). Contour intervals are 1°C. Vertical sections at stations 14° 54'E, 14° 56'E and 14° 58'E are illustrated for 14 February (c-e) and 25 February (f-h). The  $\Delta t$  value given at bottom right of graphs c to h is the difference in temperature (°C) between 4 m and 40 m.

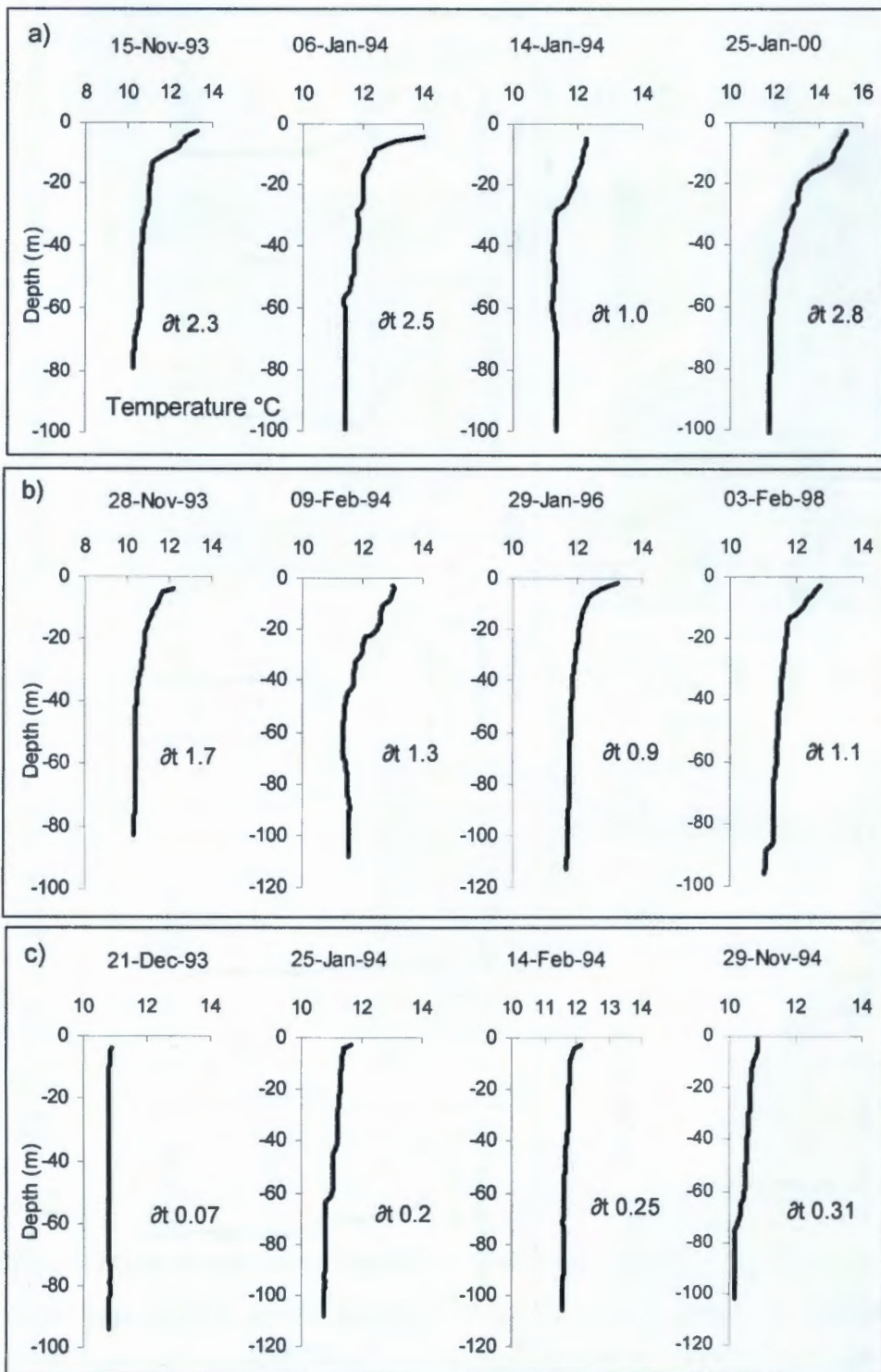


**Figure 5.5.** Summer temperature profiles at Station 8 (26° 38'S 14° 58'E). The profiles are grouped according to Dias Point wind stress two days prior to sampling, showing the effect of a) northerly / light wind b) moderate southerly winds and c) strong southerly winds. Details of wind categories are given in text.

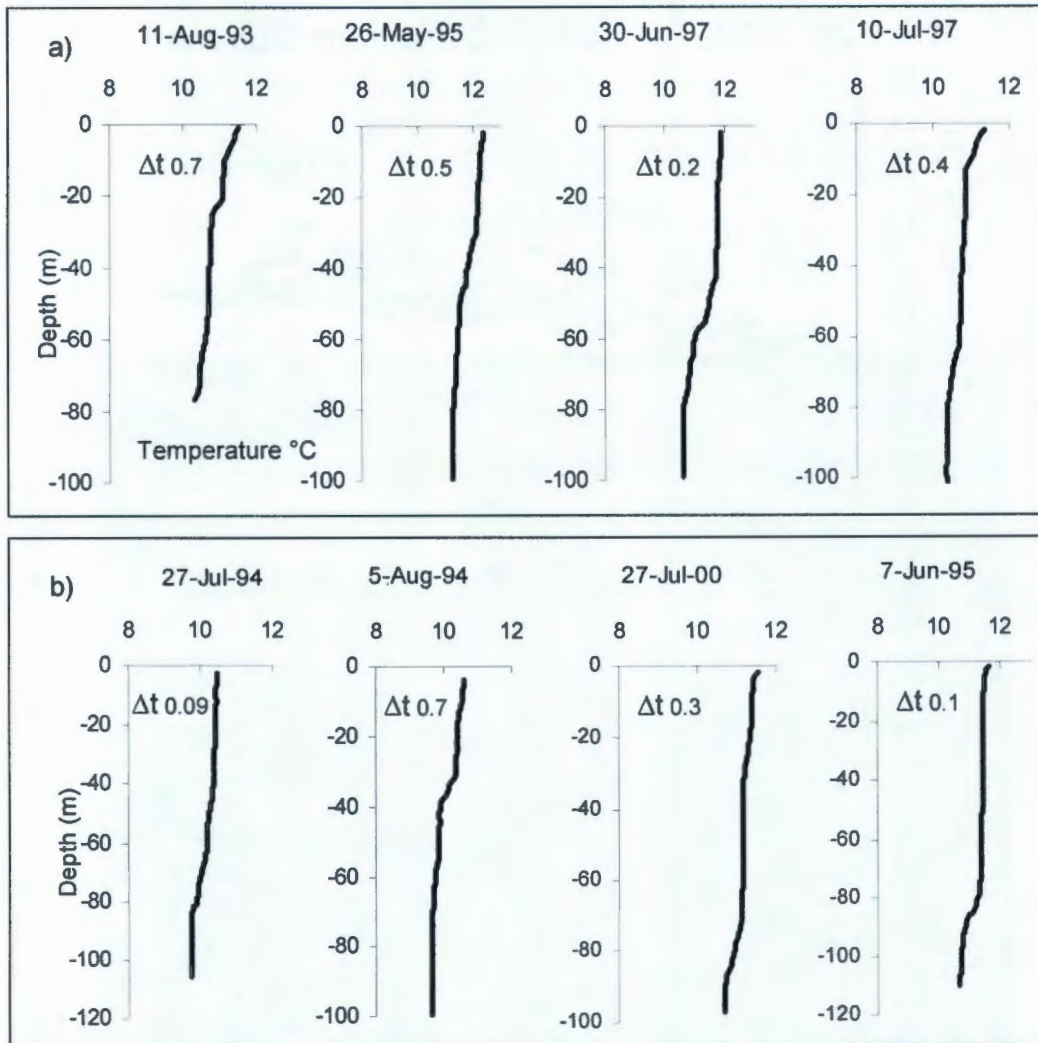


**Figure 5.6.** Winter temperature profiles at Station 8 (26° 38'S 14° 58'E). The profiles are grouped according to Dias Point wind stress two days prior to sampling, showing the effect of a) northerly / light southerly wind and b) moderate southerly winds. Details of wind categories are given in text.

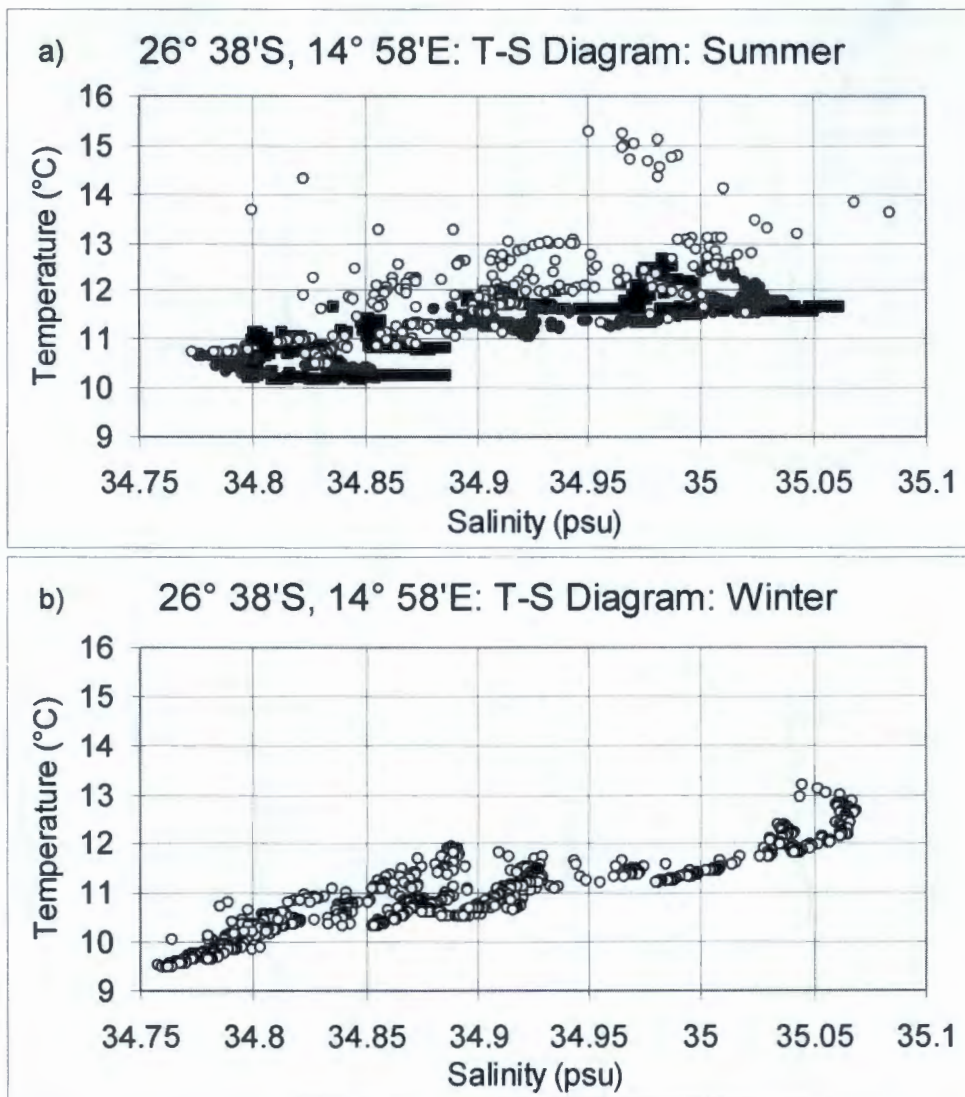


**Figure 5.7.** Temperature - Salinity (T-S) diagrams of profiles sampled in a) summer, defined as 15-November to 14-February, and b) winter, 15-May to 14-August. In the summer diagram (a) open circles indicate upper water column T-S of profiles with warm surface layers ( $\Delta t$  values  $> 0.9$ ), the T-S 40 m and deeper of these profiles are depicted by closed circles. Profiles with  $\Delta t \leq 0.9$  are closed squares. CTD profiles were sampled at Station 8 (26° 38'S, 14° 58'E) during the period 1993 to 2001.

## Chapter Six

### Long-term variability in the wind regime at Lüderitz



Rock erosion caused by wind-blown sand

## Long-term variability in the wind regime at Lüderitz

### 6.1. Introduction

The Lüderitz upwelling cell, the main centre of coastal upwelling in the Benguela, is driven by one of the strongest coastal upwelling-favourable wind regimes in the world (Bakun 1996). Intense offshore Ekman transport results from the perennial equatorward wind stress and causes year-round negative coastal water temperature anomalies due to upwelling of cold bottom water (Parrish *et al.* 1983). Wind-driven turbulent mixing at Lüderitz suppresses primary production locally as phytoplankton cells are not being retained in the photic zone (Agenbag and Shannon 1988). However the high biological productivity of the northern Benguela is sustained by nutrient-rich upwelled water exported downstream of the Lüderitz cell (Shannon 1985).

Longshore equatorward winds in the Lüderitz region are maintained by a strong pressure gradient between a permanent high pressure cell over the ocean, the South Atlantic Anticyclone (SAA), and a thermal low over the hot, arid continental land mass (Shannon 1985). Atmospheric low pressure fronts passing the southernmost tip of the African subcontinent from west to east cause intensification and modulation of the wind regime off Lüderitz, by entraining the SAA closer to the African landmass, thus increasing local wind stress. Depending on the intensity and position of the frontal low system it can cause the SAA to be entrained past the continent (ridging high pressure), causing coastal lows to be generated to the north of Lüderitz, wind speed to decrease and wind direction to reverse to north (Nelson and Hutchings 1983). The seasonal pattern in upwelling intensity in the Lüderitz region, controlled by macroscale features such as the position and intensity of the SAA, is disrupted in some years by anomalous atmospheric conditions in the equatorial Western Atlantic (Florenchie *et al.* 2003). Four major warm events in the northern Benguela, characterized by large-scale advection of tropical and equatorial water, triggered by processes in the equatorial Atlantic, (Shannon *et al.* 1990) and termed Benguela

Niños, occurred in 1934, 1963, 1984 (Shannon *et al.* 1986) and most recently in 1995 (Gammelsrød *et al.* 1998).

Due to the important role of the Lüderitz upwelling cell in the Northern Benguela ecosystem, any perturbation of wind-forcing of coastal upwelling at Lüderitz whether on the medium term (e.g. Benguela Niños, warm and cool events) or on the longer term (such as a long-term decrease or increase in upwelling intensity), would have multiple effects on the ecosystem. The aim of this chapter is to present long-term changes in the wind regime measured at Dias Point Lighthouse in terms of wind speed, wind direction and related atmospheric pressure changes both locally and in relation to the El Niño Southern Oscillation mode of variability, and to discuss the impacts of wind regime changes on the marine biota of the Northern Benguela ecosystem.

## **6.2. Materials and Methods**

### **6.2.1. Instruments and Data Quality**

The meteorological instruments were situated at the Lighthouse Keeper's watch office at Dias Point, 26° 38.094'S 15° 05.612'E, on a narrow, exposed rocky peninsula. Details of the instruments, instrumentation changes and validation of wind speed, direction and air pressure data are given in Chapter Two.

### **6.2.2. Data Analysis**

#### **6.2.2.1. Wind Stress**

The calculation of wind stress, a proxy for upwelling intensity, using the wind component parallel to the coast (the South-North component) measured at Dias Point, is described in Chapter Two. Monthly average wind stress was determined for the period January 1960 to July 2006.

Standardised anomalies of monthly average wind stress were calculated as follows, using January 1960 as an example:

$$\text{January 1960 Anomaly} = [(\text{Jan AVG} - \text{Jan LTAVG}) / \text{Jan LTSTDEV}]$$

where:

Jan AVG = Average wind stress for January 1960

Jan LTAVG = long-term average January wind stress 1960 – 2004 ( $n = 1388$ )\*.

Jan LTSTDEV = standard deviation of Jan LTAVG.

Units of the monthly anomalies are standard deviations.

\* Using daily average wind stress values across all January months.

Dias Point monthly standardised Sea Level Pressure (SLP) anomalies were calculated in the same way. The long-term average per month was calculated over the period 1978 - 2004 ( $n = 798$  for the January LTAVG).

Annual mean wind stress was determined across two calendar years, from 1 July to 30 June, from 1996 to 2006. The long-term annual average wind stress was calculated for the whole time series (1 July 1960 to 30 June 2004,  $n = 16020$ ) and the standard deviation of that average. Standardised annual anomalies were calculated as for monthly wind stress by subtracting the long-term annual average from the average of years, and dividing by the standard deviation. Units of the anomalies are standard deviations. The period 1 July to 30 June was used to keep the main summer upwelling season (November to February) within one year rather than splitting it over two calendar years, in keeping with the rationale of depicting seasonal cycles of wind speed and wind stress at Lüderitz from July to June (Chapter 4).

#### **6.2.2.2. Sea Level Pressure (SLP)**

SLP data was only available from Dias Point Lighthouse from 1978 onwards. In order to compare SLP over the same time period as the Dias Point wind data, i.e. from 1960, recourse was made to the National Center for Environmental Prediction /

National Center for Atmospheric Research (NCEP/NCAR) Reanalysis monthly SLP database in a block off Lüderitz for the period 1960 to June 2006 (Kalnay *et al.* 1996). Monthly average Sea Level Pressure (hpa) were obtained from the NCEP / NCAR SLP Reanalysis (<http://www.cdc.noaa/timeseries/>) for the block 25°S - 27°S, 7.5°E - 12.5°E. The long-term monthly average SLP and standard deviation were calculated per month from 1960 to 2004. Standardised monthly anomalies were calculated as for monthly wind stress (see section 6.2.2.1) by subtracting the long-term monthly average SLP from the average of individual months, and dividing by the standard deviation. Since the NCEP data were extracted as monthly averages, these values were used to calculate the long-term averages, thus  $n = 45$  for each LTAVG.

### 6.2.2.3. Wind Direction

Prior to determining the percent frequency of winds from the South-North and West-East sectors it was necessary to transform the automatic weather station data from January 1999 to December 2004 in order to make it comparable to the manually recorded Lighthouse data. According to the technical manual that was used for first order weather stations such as Dias Point Lighthouse, wind speeds  $< 1.543 \text{ m.s}^{-1}$  ( $< 3$  knots) were recorded in the Lighthouse weather books as calm, thus calculated as zero direction and zero speed. Thus automatic weather station data wind speeds  $< 1.543 \text{ m.s}^{-1}$  recorded at 06h00, 12h00 or 18h00 GMT were changed to zero, and the daily average wind speed calculated from the transformed data. The percent frequency of calm (wind speed  $< 1.543 \text{ m.s}^{-1}$  equals zero wind) and wind speeds  $\geq 1.543 \text{ m.s}^{-1}$  were then calculated for the South-North and West-East direction sectors per month from 1960 - 2004 taking into account missing daily average data. The frequencies per annum were also calculated. In order to keep the upwelling season intact within one year, annual frequencies were calculated for a 12-month period - 1 July to 30 June.

#### 6.2.2.4. Southern Oscillation Index (SOI)

Standardised monthly anomalies of the Mean Sea Level Pressure difference between Tahiti and Darwin (this SLP difference is known as the Southern Oscillation Index) were obtained from the Australian Bureau of Meteorology (<http://www.bom.gov.au/>) and had been calculated as:

$$\text{SOI} = 10x [ (\text{Pdiff} - \text{Pdiffav}) / \text{SD}(\text{Pdiff}) ]$$

where:

Pdiff = (average Tahiti MSLP for the month) – (average Darwin MSLP for the month),

Pdiffav = long-term average of Pdiff for the month in question, and

SD(Pdiff) = long-term standard deviation of Pdiff for the month in question.

### 6.3. Results

#### 6.3.1. Wind Stress

Annual average wind stress (Figure 6.1a) was calculated per year from July to June, thus incorporating an entire upwelling season (Chapter Four). Throughout most of the 1960s wind stress was below average, reflected in negative annual anomalies (Figure 6.1b). Strong negative wind stress anomalies occurred particularly in winter and spring of 1963 (Figure 6.2c, d). The decade ended in a cool event, reflected in the Dias Point wind record as positive annual wind anomalies in 1970 - 1971 (Figure 6.1b). The strongest winter wind-driven upwelling in the time series was recorded in 1970 (Figure 6.2c).

A period of reduced wind-driven upwelling began early in 1972 and lasted in the Lüderitz region until 1974 - 1975 (Figure 6.1a). As in 1963, reduced equatorward wind forcing was measured at Dias Point, with a strong negative annual wind stress anomaly in 1973 - 1974 (Figure 6.1b). The lowest summer wind stress anomalies in the first four decades of the time series were recorded between November 1973 and February 1974 (Figure 6.2a). The Lüderitz record changes markedly in 1975 - 1976 to a period of positive wind anomalies indicating enhanced upwelling off Lüderitz.

The switch to positive wind anomalies began in winter 1975 (Figure 6.2c). Maxima in positive wind stress anomalies per season were recorded in 1977 (spring), 1979 (autumn) and summer of 1982 - 1983 (Figure 6.2). The maximum annual average wind anomaly in the time series occurred in 1979 - 1980 (Figure 6.1b).

The pattern of generally positive annual wind anomalies prevailed from mid-1975 until the late 1980s. Due to above average wind stress for the last six months of 1987, the 1987 - 1988 annual wind stress average was one of the highest in the time series. In early 1988 upwelling was below average in autumn (February to May). Winter and spring 1988 wind anomalies were above average, but the wind stress switched again to negative anomalies in the summer (November 1988 to February 1989) (Figure 6.2).

Reduced wind stress prevailed at Lüderitz with increasingly negative annual anomalies from 1989 until 1995 - 1996. During autumn and spring of 1994 upwelling was low (Figure 6.2b,d). The lowest annual wind stress anomaly within this early 1990s period of reduced upwelling was the year 1994 - 1995 (Figure 6.1b).

In 1996 - 1997 and 1997 - 1998 annual average wind stress was the highest in the past decade and the only positive wind stress anomalies since 1987 - 1988 occurred during these years (Figure 6.1a,b).

From 1999 - 2000 onwards the decline in upwelling-favourable wind stress at Lüderitz persisted, with anomalously low wind stress recorded in all seasons from 2000 to autumn 2006 (Figures 6.1 and 6.2). The lowest annual average wind stress in the entire time series was measured in 2005 - 2006 (Figure 6.1a).

### **6.3.2. Sea Level Pressure (SLP)**

The offshore NCEP/NCAR block SLP and Dias Point SLP monthly anomalies show similar trends during the period March 1978 to June 2006 when simultaneous data are available, although the NCEP SLP series is more variable (Figure 6.3). There

was no marked negative or positive shift in the anomalies coinciding with the instrument change, described in Chapter Two, at Dias Point in August 1998.

From monthly SLP anomalies three periods could be identified in the time series (Figure 6.3): i) pre mid-1975, generally negative to average anomalies in the NCEP/NCAR SLP, with intermittent, short-lived positive anomalies. ii) a transition in mid-1975 to generally positive anomalies from 1976 to 1992 - 1993. Dias Point SLP anomalies were all positive during this period. iii) Mainly negative monthly anomalies at Dias Point from 1993 to 2006, but with some positive anomalies while the NCEP/NCAR SLP anomalies were generally positive during this period. In the NCEP SLP time series the strongest negative anomalies were recorded in 1963 and 1974 while the highest SLP anomalies were recorded in 1978, 1987 and 1997. Periods of sustained decreases in the NCEP/NCAR anomalies occurred during 1984 - 1986, 1988 - 1989, 1995 - 1996 and 1999 - 2000 (Figure 6.3). These trends in the SLP anomalies can also be seen in the data for NCEP/NCAR Reanalysis blocks between 25°S and 30°S, 7.5°E to 15°E (not shown).

### 6.3.3. Wind Direction

In order to determine long-term trends, the percentage occurrence of wind speeds  $\geq 1.543 \text{ m.s}^{-1}$  and speeds  $< 1.543 \text{ m.s}^{-1}$  (calms) in the South-North (longshore) sector from 1960 to 2004 was determined (section 6.2.2.3). Similarly the annual frequency of winds  $<$  and  $\geq 1.543 \text{ m.s}^{-1}$  in the West-East (onshore-offshore) sector was calculated per year. Changes in the frequency of occurrence (%) were determined from 1960 - 1961 (July to June) to 2003 - 2004 ( $n = 44$  years).

In the South–North Sector, southerly winds predominated in terms of frequency of occurrence and there was no change in frequency of South winds at Dias Point during the time series ( $r = 0.005$ ,  $p = 0.374$ ). The frequency of North winds increased ( $r = 0.207$ ,  $p < 0.01$ ). The percentage of calms decreased ( $r = -0.152$ ,  $p < 0.01$ ) in this sector (Figure 6.4).

The years with the lowest frequency of South winds per decade were 1963 - 1964, 1973 - 1974, 1988 - 1989, 1995 - 1996 and 2001 - 2002 (Figure 6.4a). 2001 - 2002 also stands out in the time series as the year in which northerly winds were most frequent (Figure 6.4b). The highest percentage occurrence of calms in the time series was during 1973 - 1974 (Figure 6.4c).

In the West-East sector, the frequency of west winds increased ( $r = 0.525$ ,  $p < 0.001$ ). East winds decreased in frequency during the 44-year period ( $r = -0.138$ ,  $p < 0.01$ ). The frequency of calms decreased ( $r = -0.434$ ,  $p < 0.001$ ) (Figure 6.5). In the last decade of the time series, the years 1996 - 1997 and 1997 - 1998 stand out as outliers in the trends described above, with low occurrence of westerly winds and a high frequency of easterly winds and calms. There was a high frequency of East winds in 1969 - 1970, 1970 - 1971 and 1971 - 1972 (Figure 6.5b).

#### **6.3.4. Southern Oscillation Index (SOI)**

From visual inspection of the monthly SOI anomalies a trend to more negative anomalies begins in 1975 - 1976 (Figure 6.6a). SOI and Lüderitz wind stress anomalies are in opposite phases from 1976 to 1987 (Figure 6.6a,b). SOI monthly anomalies are mainly negative in the 1990s and from 2002 to 2005 (Figure 6.6a), similar to the mainly negative anomaly trends in Lüderitz wind stress during the same time period (Figure 6.6b). The SOI and Lüderitz wind time series have few values lying close to the long-term average (zero anomaly baseline). The monthly anomalies are either strongly positive or strongly negative. During the period of strong positive wind stress anomalies in Lüderitz (1975 to 1987), SOI was mainly negative, including an extremely negative SOI anomaly from spring 1981 to summer 1983. Another strongly negative SOI period in 1997 also corresponded with positive wind stress anomalies in Lüderitz.

## 6.4. Discussion

### 6.4.1. Wind Stress

The time series at Lüderitz shows interdecadal change in wind stress, a proxy for upwelling intensity derived from the Ekman model (Chapter Two section 2.4.3). The strongest and most persistent upwelling cell of the Benguela is located at Lüderitz. Here nutrients are brought into the surface waters by Ekman transport, but high wind speeds cause advective losses as well as turbulent mixing which is detrimental to phytoplankton if mixing removes cells from the photic zone (Hardman-Mountford 2003). The maximum annual primary production in the Benguela current, calculated from satellite-measured data, is the highest of all the Eastern Boundary currents (Carr 2002). The least productive area in the Benguela is that between 25°S and 28°S, approximately the area of the Lüderitz cell, and the most productive area lies between 18°S and 24°S, to the north of it (Carr 2002). North of 24° 30'S, downstream of the Lüderitz upwelling cell, there is a marked reduction in turbulent wind mixing (Agenbag and Shannon 1988). More stable conditions combined with the input of upwelled nutrients enhances the suitability for phytoplankton growth north of the Lüderitz cell. The intense upwelling in Lüderitz is considered a biological barrier to movement of certain fish species between the northern and southern Benguela due to food limitation. Migration through the area is only possible for these species in years of much reduced upwelling (Agenbag and Shannon 1988).

Over the past 46 years, three periods of differing wind stress intensity at Lüderitz can be identified, namely a) moderately below average wind stress from the beginning of the time series to 1975 (15 years), b) strong wind stress for 13 years until 1988, c) below average to low wind stress from 1989 for the following 18 years until the end of the analysis in June 2006 (Figure 6.1). Each of these periods lasted longer than 10 years. In view of the key role of the Lüderitz upwelling cell in the Northern Benguela, these different wind-driven upwelling scenarios, resulting from large-scale atmospheric changes being transferred to the marine ecosystem, could have initiated ecosystem regime shifts as defined by Cury and Shannon (2004).

The wind stress time series also indicates the occurrence of warm (and cold) events including extreme warm and persistent events termed Benguela Niños (Shannon *et al.* 1986). Wind stress at Lüderitz was reduced during warm events, for example during the 1963 Benguela Niño, which affected the entire Benguela (Shannon *et al.* 1986), strong negative wind stress anomalies occurred at Lüderitz, particularly in winter and spring of 1963.

A regional warm period began early in 1972 and lasted in the Lüderitz region until 1974 - 1975 (Walker 1987). As in 1963, this warm period was characterised by reduced equatorward wind forcing, with a strong negative annual wind stress anomaly in 1973 - 1974 at Lüderitz.

The Benguela Niño of 1984 (Shannon *et al.* 1986, Shannon and Agenbag 1990) was apparent from strong positive sea surface temperature (SST) anomalies in the Walvis Bay coastal region, but there was little evidence of warming from Voluntary Observing Ship's data near Lüderitz (Walker 1987). Positive SST anomalies occurred during April 1984 in Lüderitz Harbour, the standardised monthly SST anomaly for April (calculated from a LTAVG of 21 years) was 0.84 (Peard, unpublished data). The summer wind stress (November 1983 to February 1984) was close to the long-term average in Lüderitz, above the LTAVG during autumn and winter but negative in spring 1984.

In early 1988 upwelling was below average in autumn (Feb to May) when a significant warm event occurred in Lüderitz. The Lüderitz Harbour SST standardised monthly anomaly for March was 0.85 (Peard unpublished data). Winter and spring 1988 wind anomalies were above average, but the wind stress switched again to negative anomalies in the summer (November 1988 to February 1989). A Benguela Niño in 1995 (Gammelsrød *et al.* 1998) coincided with very low wind stress at Lüderitz, the annual average wind stress in 1994 - 1995 was the lowest in the first forty years of the time series.

As shown in Chapter Five, southerly wind relaxation events result in increased SST at the coast and if sustained cause warm events. Higher water temperatures occur due to stratification in calm weather (Chapter Five) and downwelling of warmer offshore water - if prolonged this can constitute a warm event, identified by positive sustained temperature anomalies only. Shannon *et al.* (1990) have pointed out that while local equatorward wind stress might be significantly lower during Benguela Niños, these events are not triggered by locally reduced upwelling but by relaxation in zonal wind stress off northern Brazil and resulting changes in geostrophic flow in the equatorial Atlantic (Bakun 1996, Florenchie *et al.* 2003). These equatorial waves and remote wind forcing (equatorial mode of variability) play a significant role in the generation of SST anomalies on an interannual time scale and are similar to the Pacific ENSO (Servain and Dessier 1999). The warm tropical water is propagated across the Atlantic ocean via eastward moving Kelvin waves which deflect at the African coast, causing anomalous poleward flow and intrusions of high salinity warm water from Angola into Namibia. These intrusions differ from the annual summer southward displacement of the Angola - Benguela front in the depth and latitudinal extent of the intrusion and duration of the warming (Shannon *et al.* 1990, Gammelsrød *et al.* 1998). The persistence of weak winds at the equator for several months seems to determine the intensity of warm events in the Northern Benguela (Hardman-Mountford 2003).

The warm event that resulted in anomalously high SST in Lüderitz and the northern Benguela during early 1988, and in March 1988 in particular, was not categorised by Shannon and Agenbag (1990) as a Benguela Niño as it differed in extent and duration from the 1984 Benguela Niño. Hardman-Mountford *et al.* (2003) show that the origin of this anomalous event was in the western central Atlantic. In Benguela Niño years the period of below average southerly winds at the equator persists for several months while in 1988 the equatorial wind anomaly was of much shorter duration. During 1999, however, strong temperature and sea level anomalies spreading from the equator to the Benguela coincided with an extended period of anomalous (weak) southerly winds at the equator, thus Hardman-Mountford *et al.* (2003) suggest that this may have been a Benguela Niño year.

Cold events due to sustained anomalously strong wind stress resulting in vigorous upwelling and therefore subsequently colder than average water temperatures, can also be identified in the time series. The 1960s decade ended with a cool event during which below average sea surface temperatures were measured at coastal and offshore sites throughout the Benguela region from 1969 to 1971 in association with higher equatorward wind speeds (Walker 1987), as were recorded at Dias Point in 1970 - 1971. Later in the decade the maximum annual average wind stress in the Dias Point time series was recorded in 1979 - 1980, during a period of stronger wind stress at Lüderitz. This preceded a prolonged cool anomaly from summer 1981 - 1982 to summer 1982 - 1983 described by Walker (1987) as being confined to the nearshore region, with its maximum expression near Lüderitz. Another strong cold event was observed in the Northern Benguela in 1997 (Hardman-Mountford *et al.* 2003, Reason *et al.* 2006) coinciding with anomalously high wind stress at Lüderitz during 1996 - 1997 and 1997 - 1998 as well as strongly negative SOI, the latter indicating Pacific El Niño warming. The two major cold events in the Northern Benguela (1982 and 1997) have been noted to precede the two strongest Pacific El Niños of 1982 - 1983 and 1997 - 1998 (Reason *et al.* 2006). Anomalously high wind stress at Lüderitz in 1983 (strong positive wind stress anomalies in summer 1982 - 1983 and in winter 1983) preceded the Benguela Niño of 1984.

#### **6.4.2. Sea Level Pressure**

The wind speed at Lüderitz is determined by the position and strength of the atmospheric high pressure cell situated over the South Atlantic (South Atlantic Anticyclone or SAA) and the intensity of the pressure gradient between the SAA and the juxtaposed continental low pressure system (Nelson and Hutchings 1983). Air pressure is the forcing factor of the Lüderitz wind regime at diurnal and seasonal time scales (Chapters Three and Four). Bailey (1979) showed a significant correlation between wind speed at Dias Point Lighthouse and the atmospheric pressure difference, as a proxy for the horizontal pressure gradient, between an oceanic reference point at 30°S 10'E, and three reference points on the continent - Lüderitz, Windhoek and Keetmanshoop, the latter two situated on the inland plateau (but with air pressure adjusted to SLP). Wind speed at Lüderitz was best correlated

with the pressure gradient between the oceanic point and Lüderitz ( $r = 0.71$ ) (Bailey 1979).

Crawford *et al.* (unpublished manuscript) identified 1975 as a turning point in the GOSST (Global Operational Sea Surface Temperature) monthly SST / SLP and COADS (Comprehensive Ocean-Atmosphere Data Set) SLP time series for the block 24°S to 26°S, 9° to 11°E. 1975 and 1992 are turning points in the NCEP and Dias Point SLP anomaly time series and these coincide with the changes observed in the wind stress anomalies at Dias Point. Negative SLP trends and minima in monthly SLP anomalies occurred at Lüderitz in 1963, 1973 - 1974, 1984, 1988, 1995 and 1999, coinciding with the warm events described in section 6.4.1. Peaks in SLP due to positive anomalies coincided with cold events in 1987 and 1997. Using Voluntary Observing Ship's data, Walker (1987) reported minima in SLP anomalies corresponding to reduced equatorward wind forcing particularly between 20°S and 28°S during the warm events of 1963 and 1972/74.

#### **6.4.3. Wind Direction**

Anticyclonic air flow around the SAA is guided by the northeast coastline orientation and arid nature of the south-west African interior, which enhances longshore flow by setting up a thermal cross-flow barrier (Nelson and Hutchings 1983, Shannon and Nelson 1996). Winds from a southerly direction prevail throughout the year in Lüderitz with a minimum in winter due to a northerly-westerly shift in the position of the SAA (Tyson and Preston-Whyte 2000, Chapter Four of this thesis). The frequency of occurrence of southerly winds has not changed significantly over the 46-year time series, although the intensity of the longshore wind stress has varied on an interannual / interdecadal scale as described in section 6.3.1. The atmosphere-ocean changes, albeit basin-wide or local, which caused anomalously low wind stress and warming at Lüderitz in the years 1963 - 1964, 1973 - 1974, 1988 - 1989, 1995 - 1996 and 2001 - 2002 also resulted in a reduced frequency of occurrence of south winds in these years. This indicates modulated intensity of the SAA / continental low pressure gradient which could also be brought about by a shift in the

position of the SAA akin to that causing the winter minimum in winds at Lüderitz (Chapter Four).

Southerly winds at Lüderitz are periodically modulated by the development of coastal low pressure cells off 25°S (north of Lüderitz), resulting in wind direction changing from South to North (Reason and Jury 1990). The modulation of the southerly wind regime at Lüderitz occurs at a synoptic scale of three to ten days (Shannon and Nelson 1996). It is preceded by ridging of the SAA to the south of the southern African landmass, resulting in the establishment of a high pressure over the south-eastern part of the African continent and offshore easterly flow over the Namib prior to the formation of the coastal low pressure cell (Chapter One). Northerly winds predominate during the southward passage of the coastal low (Reason and Jury 1990, Tyson and Preston-Whyte 2000). The increased frequency of occurrence of northerly winds could therefore indicate a higher frequency of ridging of the SAA between 1960 and 2006.

#### **6.4.4. Southern Oscillation Index**

The Southern Oscillation Index (SOI) refers to a fluctuation in inter-tropical pressure, between the southeast Pacific subtropical high and the Indonesian equatorial low. Positive SOI anomalies occur during La Niña or non-ENSO (El Niño-Southern Oscillation). As an El Niño develops, the SOI index falls, pressure rises over Indonesia and the pressure gradient along the equator decreases or reverses (Tyson and Preston-Whyte 2000).

Dias Point wind stress and SOI anomalies appear to be in opposite phases at times. The shift to above average wind stress at Lüderitz in 1975 was accompanied by an increase in SLP at Lüderitz and preceded the change of SOI to a negative phase in 1976. During the period of generally negative SOI anomalies from 1976 to late in 1987, positive wind stress anomalies prevailed at Lüderitz. Lüderitz wind stress and the SOI anomalies were also in opposite phases during 1997, a cold event in the northern Benguela during which above average wind stress was recorded at Lüderitz. A Pacific ENSO event in 1997 coincident with stronger equatorward trade

winds in the Atlantic could be due to an atmospheric teleconnection between the Pacific and Atlantic oceans causing weaker northeasterly trade winds during ENSO years, resulting from a northward shift in the position of the ITCZ, intensifying southeasterly winds at the equator (Bakun 1996, Hardman-Mountford 2003). Conversely the relaxation and reversal of winds at the equator corresponds possibly to a southward shift in the ITCZ and reinforcement of the North-Atlantic trade winds (Servain and Dessier 1999). This causes a collapse of the sea slope elevation in the western equatorial area and propagation of warm water from above the deep thermocline eastward across the Atlantic and southward along the west African coast to Angola as described for the equatorial mode in section 6.4.1 (Bakun 1996, Servain and Dessier 1999). However, with the exception of the 1996 - 1997 cold event, the Lüderitz wind stress anomalies and SOI anomalies were in phase during the 1990s and 2000s, when Lüderitz wind stress anomalies became strongly negative. ENSO-like decadal modes have been shown to influence atmospheric circulation, SST and rainfall in the southern-African region (Reason *et al.* 2006). Interdecadal variability in wind-driven coastal upwelling intensity at Lüderitz is probably linked to such complex global ocean - atmospheric forcing but further understanding of the Pacific ENSO-induced variability on the south Atlantic wind field is required for cause-effect analyses and predictive capabilities for modes such as Benguela Niños and Benguela Niñas (Reason *et al.* 2006).

#### **6.4.5. Impacts of variability in wind-driven upwelling on marine biota in the Northern Benguela**

Warm events and perturbations in ocean-atmosphere circulation patterns which cause downwelling and offshore - inshore advection of warm water in the central and northern Benguela have negative impacts on the cold-adapted marine biota of the central and Northern Benguela (Crawford *et al.* 1990, Shannon *et al.* 1992, Jury 1996, Gammelsrød *et al.* 1998). The large-scale incursion of warm, nutrient-poor waters due to cessation of upwelling during Benguela Niños with resulting mortalities and reproductive failures of commercially important fish species have been well documented (Shannon *et al.* 1992). In the early 1960s the northern Benguela was in a sardine-dominant phase. Negative impacts of the Benguela Niño of 1963 on the

sardine (*Sardinops sagax*) population included decreased sardine egg production and gonad weight. Mean yields of oil per ton of fish decreased considerably in 1963, 1974 and 1984 and were ascribed to the warm perturbations in these years. Southward migration of the pilchard and other species occurred during the Benguela Niños of 1963 and 1995, bringing the stocks under intense fishing pressure close to Walvis Bay. In 1963 the pilchard stock was fished as far south as Lüderitz where a cannery was opened in 1964 (Crawford *et al.* 1990, Boyer and Hampton 2001). Sardine catches peaked (1.4 million tons) in 1968 but plummeted in 1971 during a protracted warm event in the northern Benguela to 300 000 tons and again in 1977. The adverse environmental conditions probably exacerbated a decline that was largely attributable to overfishing (Boyer and Hampton 2001). During the 1995 Benguela Niño, anomalously warm water (> 8°C warmer than average in March 1995) extended at least to 24°S and some 300 km offshore (Gammelsrød *et al.* 1998, Boyer and Hampton 2001). Mortalities of sardine; young horse mackerel (*Trachurus capensis*) and silver kob (*Argyrosomus inodorus*) occurred and recruitment and catches of other species was suppressed. The anchovy (*Engraulis capensis*) stock, already at a low level in the early 1990s, virtually disappeared after the 1995 event (Boyer and Hampton 2001).

Environmental effects on top predators in the northern Benguela appear to be mediated through prey availability (Roux 1998, Boyer and Hampton 2001). Long-term variability in the upwelling regime alters the entire marine food web, forcing top predators to switch to alternate prey species, and in severe circumstances (e.g. 1994 / 1995) to succumb to starvation (Roux 2003). In addition there are direct effects on these cold-adapted species during periods of anomalously low wind stress. Physiological stress leading to hyperthermia and death of young Cape Fur seal (*Arctocephalus pusillus pusillus*) pups and African Penguin (*Spheniscus demersus*) chicks has been described on breeding colonies near Lüderitz (de Villiers and Roux 1992, Kemper 2006).

## 6.5. Conclusion

Characteristic of upwelling centres, the shelf off Lüderitz is relatively narrow, placing cold South Atlantic Central Water close to the coast (Boyd 1987). The “normal” condition for the Lüderitz upwelling zone as described by this time series is that of upwelling favourable winds for at least eight months of the year, with modulation of the wind regime and upwelling minima in winter (Chapter Four). Sea level pressure is a key factor underlying the variability of wind regime at Lüderitz from diurnal to interdecadal time scales and probably also underlies the observed low frequency changes (longer than a decade) in wind speed and direction at Dias Point from 1960 to 2005. Turning points in the SLP and wind stress time series from negative to positive anomalies were seen to coincide in the two time series in 1975 with a return to negative SLP and wind stress in the early 1990s.

The atmospheric circulation over the Northern Benguela may be influenced on an interannual to interdecadal time scale by large-scale modes of variability such as ENSO (Shillington *et al.* 2006). The warm events in the Northern Benguela, including those events classified by Shannon *et al.* (1986) as Benguela Niños, were characterized by below average wind stress, coincident with negative SLP anomalies at Lüderitz while cold events corresponded to above average wind stress and SLP.

Reduced wind stress at Lüderitz is related to the intensity of the pressure gradient between SAA and continental low due to a change in the position of the SAA, or to modulation of the air pressure in the SAA. Interdecadal variability in the GOSST (Global Operational Sea Surface Temperature) SLP time series from 1900 to 1992 is apparent in a block 24°S - 26°S, 9 - 11°E off Lüderitz, including a significant turning point identified in 1975 (Crawford unpublished manuscript). Major atmospheric changes during the mid-1970s were reported by Walker (1987) and Marshall *et al.* (1985) as cited in Walker (1987). The higher SLP and stronger equatorward winds post-1975 were attributed to longitudinal movements of the SAA from 1970 to 1984. From seasonal average localities of the SAA published by the South African Weather Bureau, Walker (1987) found that when SLP was higher than average, the SAA was situated in a more westerly position while it was further eastwards from its average

position when SLP was low. Changes in the strength of the SAA at 14 to 16 year intervals was identified from an analysis of SLP and SST COADS data (1953 to 1992) in the South Atlantic between the equator and 40°S (Venegas *et al.* 1996). A low-frequency interannual mode of variability at six to seven year intervals was characterised by east-west displacements of the SAA causing strong SST fluctuations off the coast of Africa. A high frequency interannual mode, characterized by north-south displacements of the subtropical anticyclone at four-year intervals, is strongly related to ENSO (Venegas *et al.* 1996). Walker cell circulation and the Southern Oscillation Index substantially influence the air pressure, temperature and wind anomalies over southern Africa. The teleconnection is not thoroughly understood, with only two Atlantic warm events having occurred in the last two decades (1983 and 1995). The teleconnection between events in the Pacific and Atlantic oceans are complicated by ocean-atmosphere feedback loops, atmospheric circulation features such as the Quasi-Biennial Oscillation and the effect of Southern Oscillation in producing upper-air perturbations and affecting standing waves in the atmosphere (Tyson and Preston-Whyte 2000).

This preliminary analysis suggest links between anomalies of Lüderitz wind stress, Lüderitz sea level pressure and SOI which need to be further investigated by time series analysis techniques to establish the statistical properties of these time series in the time and frequency domains (Hewitt 1992). Prior to such analyses the time series need to be detrended and the autocorrelation within the series removed.

The Lüderitz wind time series is one of the few long-term, point monitoring series on the Namibian coast that can be used to analyse present and historical trends in the coastal environment at a main upwelling cell. The time series reflects interdecadal changes in wind stress, a proxy for upwelling intensity, macroscale anomalies such as Benguela Niños and localised warm and cool events. These short or long-term changes in the upwelling regime impact on water temperature, nutrient supply, mixing, primary productivity, oxygen dynamics and shelf circulation in the Benguela system (Shannon *et al.* 1990), and are significant to the biology, ecology and population dynamics of the marine ecosystem of the northern Benguela.

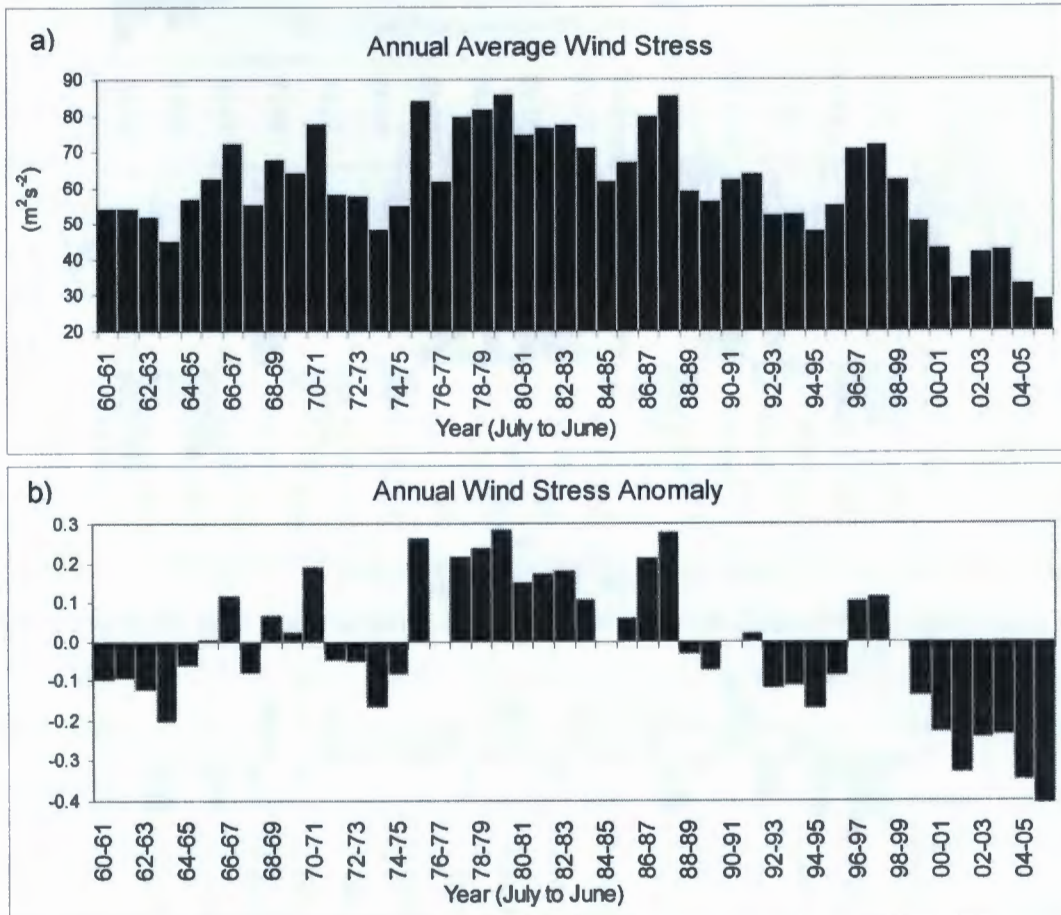


**Figure 6.1.** a) Annual average wind stress measured over 46 years at Dias Point from 1960 to 2006. b) Standardised wind stress anomalies calculated per annum from July to June; units are standard deviations. Positive (negative) anomalies indicate stronger (weaker) than average upwelling.

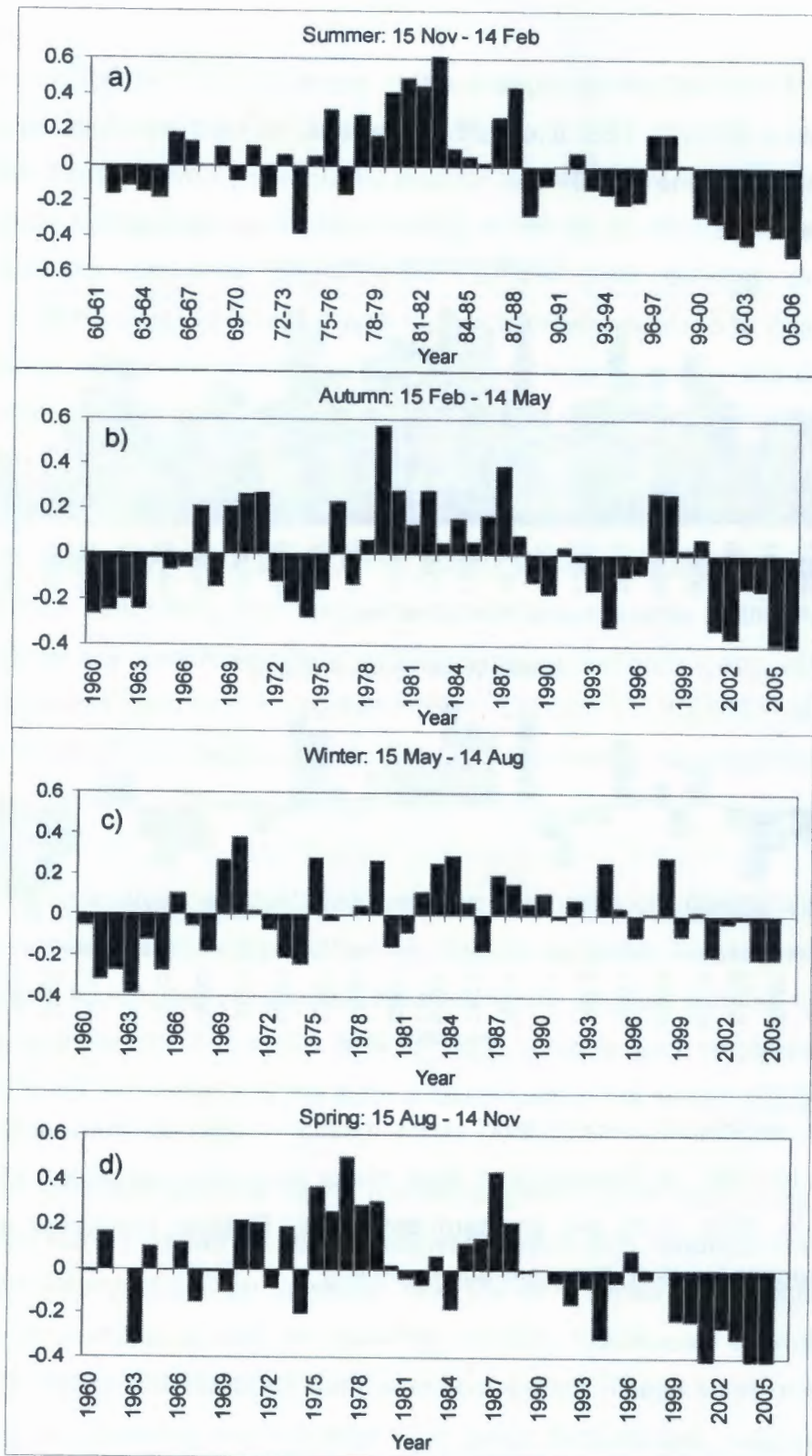


**Figure 6.2.** Interannual differences in upwelling intensity at Lüderitz between 1960 and 2006 in a) summer, b) autumn, c) winter and d) spring using wind stress as an upwelling proxy. Units are standard deviations. Positive (negative) anomalies indicate stronger (weaker) than average upwelling.

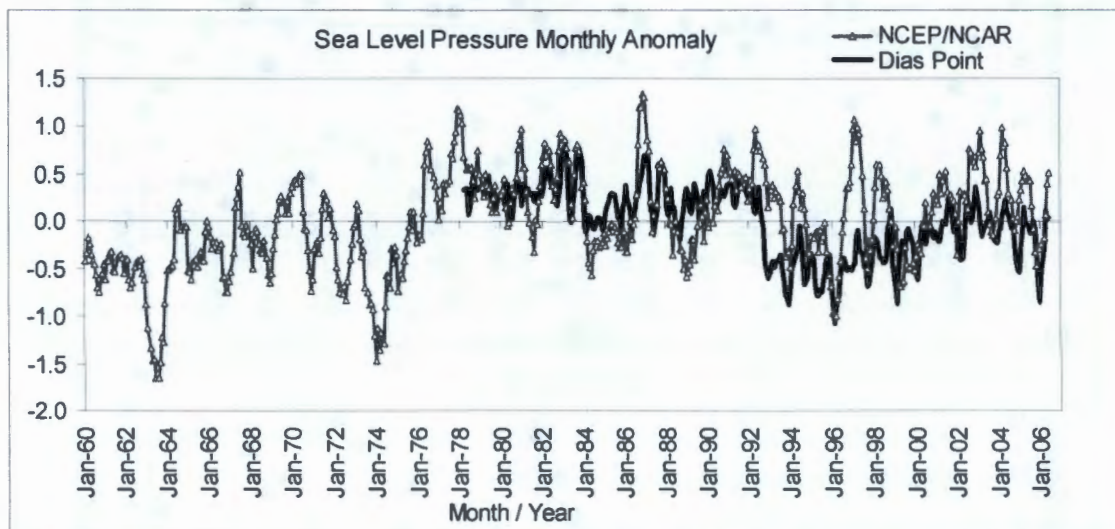


**Figure 6.3.** NCEP/NCAR Reanalysis monthly SLP anomalies from Jan 1960 to June 2006 compared with the monthly SLP anomalies from Dias Point Lighthouse time series (March 1978 to June 2006). The monthly anomalies are smoothed with a 3-month (Dias Point) and 7-month (NCEP/NCAR) running average. Units are standard deviations.

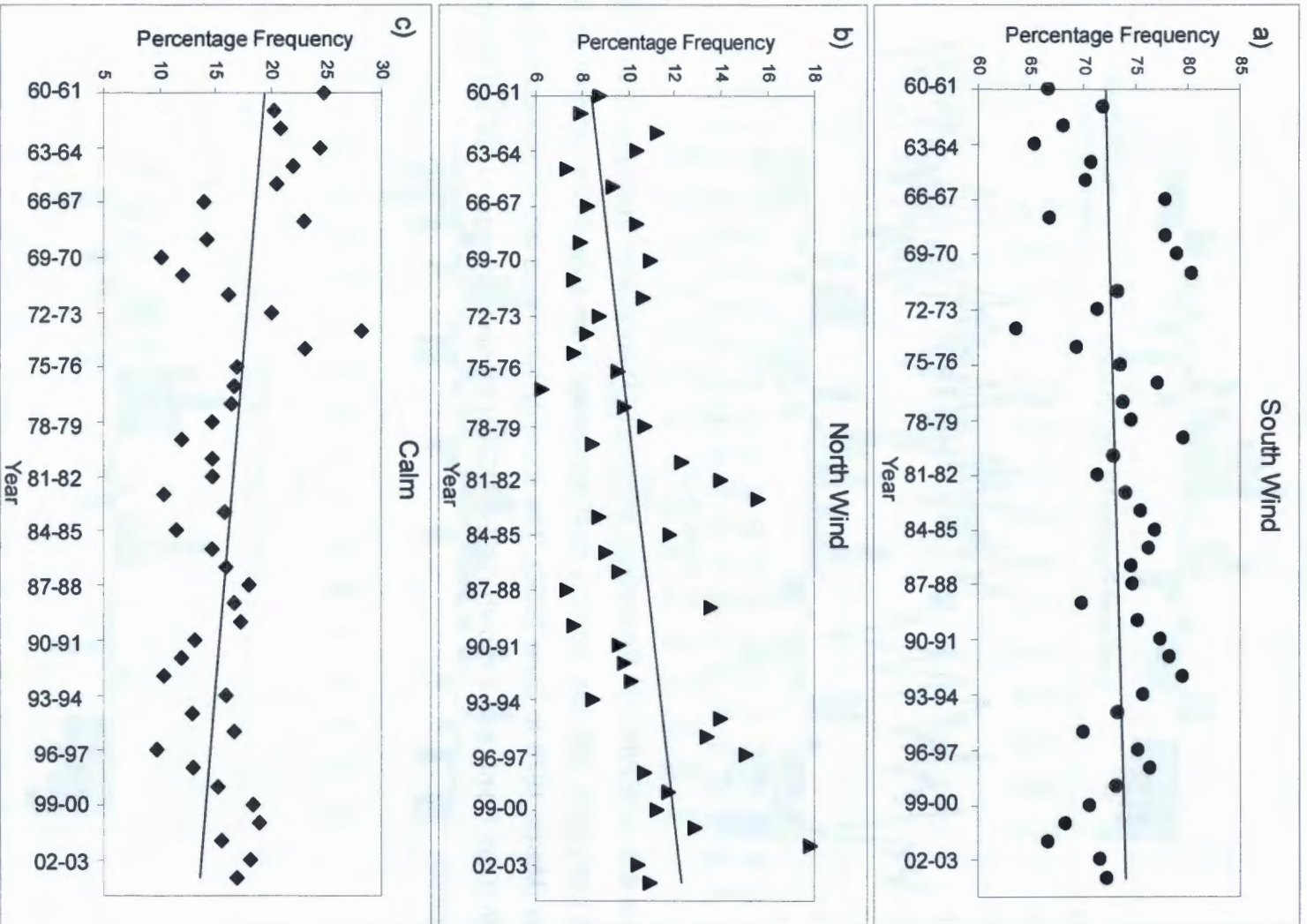


**Figure 6.4.** Percentage frequency of occurrence of (a) South and b) North winds at Dias Point from 1960 to 2004. The frequency of calms (winds  $< 1.543 \text{ m.s}^{-1}$ ) is given in c). Years calculated from July to June to keep the summer upwelling season intact.

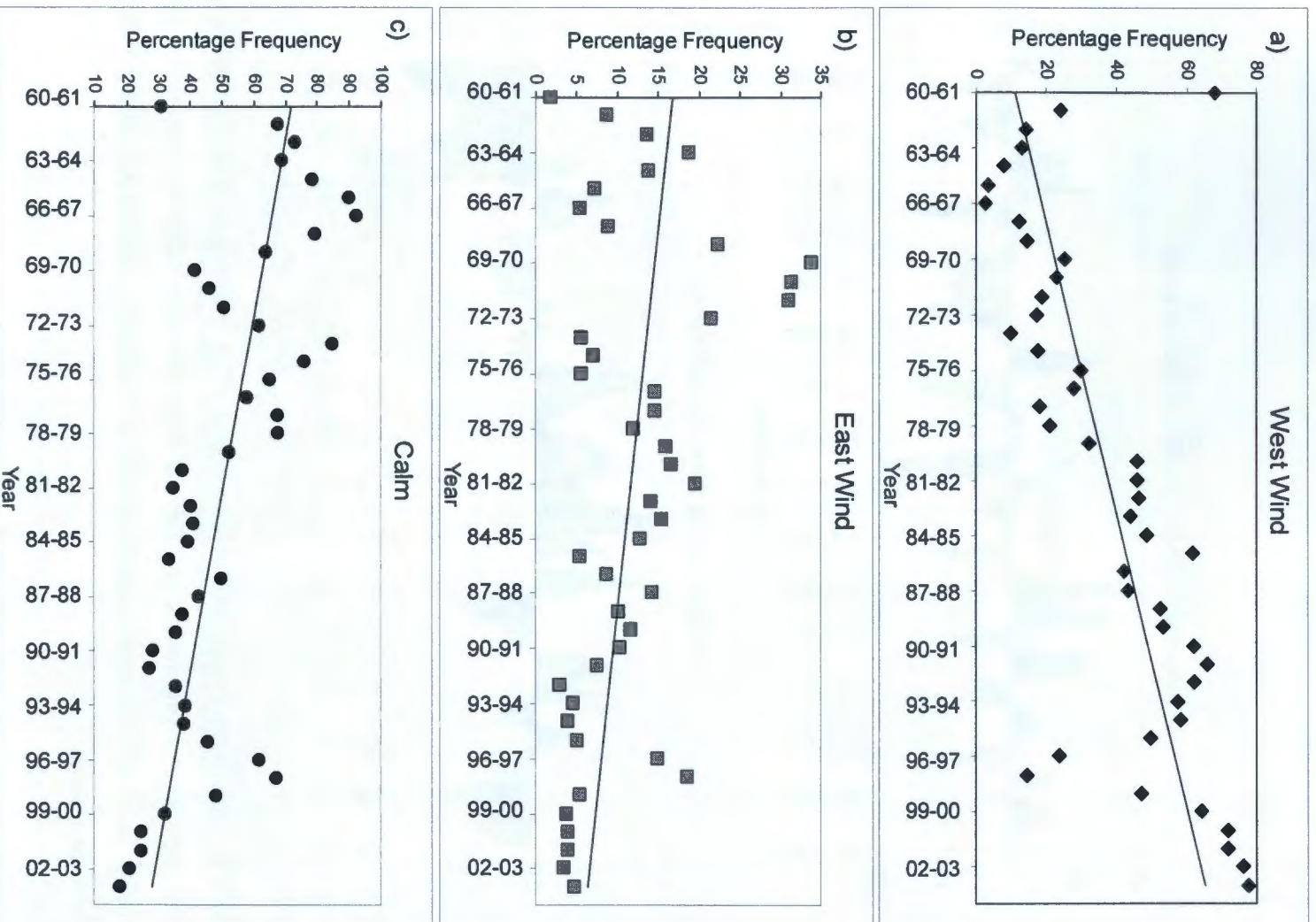


**Figure 6.5.** Percentage frequency of occurrence of (a) West and b) East winds at Dias Point from 1960 to 2004. The frequency of calms in this sector (winds  $< 1.543 \text{ m.s}^{-1}$ ) is given in c). Years calculated from July to June.

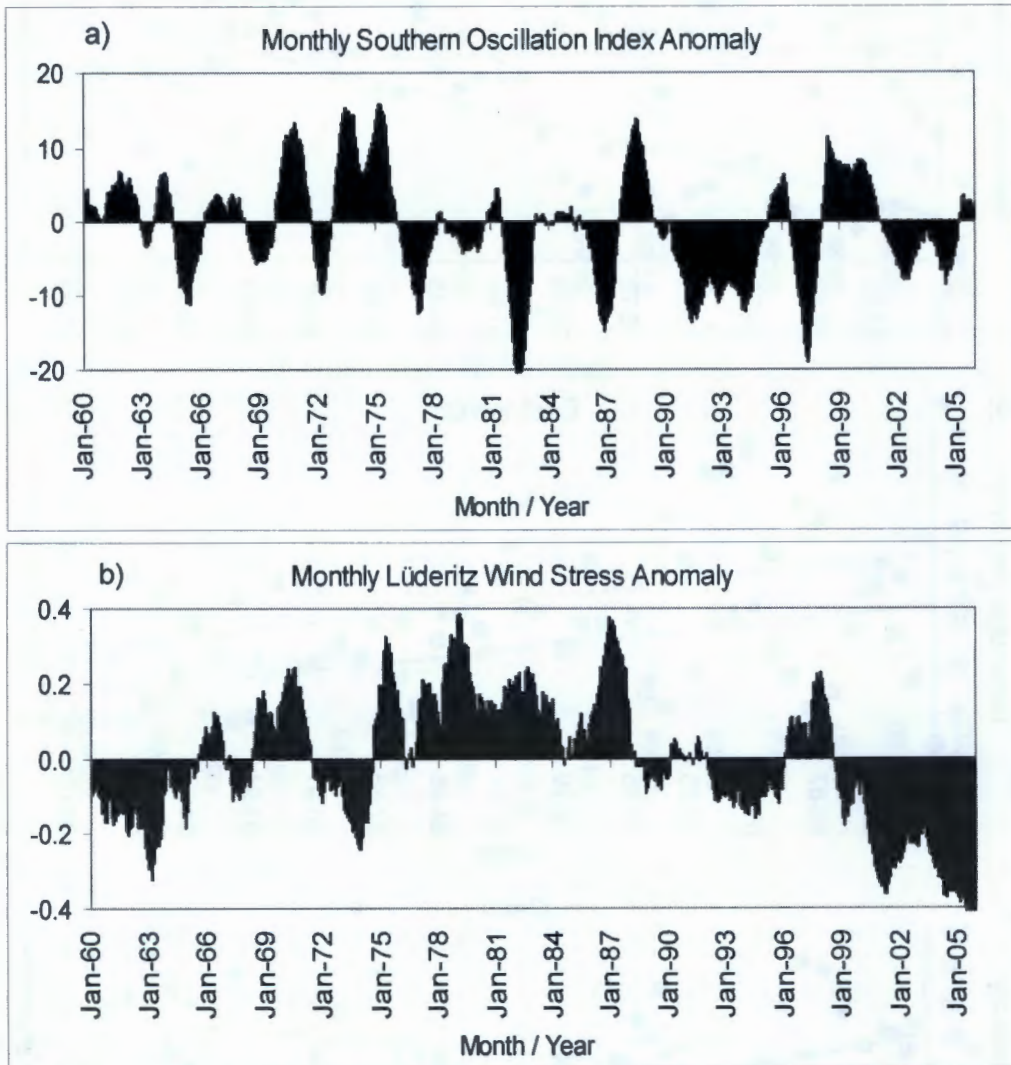


**Figure 6.6.** Long-term trends in the time series of a) monthly SOI anomalies and b) monthly wind stress anomalies at Lüderitz from January 1960 to December 2005. Anomalies in a) and b) were smoothed with a 12-month running average. Units are standard deviations.

# Chapter Seven

## Conclusion



## Conclusion

This thesis has examined the wind regime at Lüderitz, using wind stress as a proxy for upwelling intensity, from 46 years of data from Dias Point Lighthouse, a unique time series of coastal wind and SLP measurements on the Namibian coast. The location of the weather station on an exposed peninsula makes Dias Point an ideal land-based weather station for point measurement of the coastal wind regime. Frictional effects of the land on the measured wind should be at a minimum to the extent that a significant agreement was found between the Lighthouse wind speed and direction measurements and those made by research vessels within a 30 mile radius of the coast (Bailey 1979).

Instrumentation changes potentially introduce a source of error into a time series. In this thesis overlapping data sets have been used when available to compare the measurements of the two instrument types e.g. pressure plate and anemometer, mercury barometer and digital barometer (Chapter Two). No changes in trends (significant increase or decrease in anomalies), coincident with known instrument changes, were detected in the time series of wind speed, direction or sea level pressure anomalies.

Key questions relating to variability in the wind regime posed in Chapter One attempted to provide a perspective on wind-driven upwelling at Lüderitz beginning with an hourly time scale and in a local context (e.g. land/sea breeze) broadening to an interdecadal time frame and an Atlantic Basin-wide / global context (e.g. occurrence of warm events such as Benguela Niños). The main findings relating to each of the key questions are summarised in this chapter.

- 1) *What is the diurnal variation in the sea level pressure (SLP), wind speed and wind direction at Dias Point? Does the diurnal variation exhibit a seasonal modulation?*

Wind speed and wind direction at Lüderitz were found to vary diurnally at a similar time scale and both with a unimodal pattern due to the change in atmospheric pressure gradients during daytime heating and night-time cooling of the landmass (Chapter Three). The pressure gradient between the South Atlantic Anticyclone (SAA) and the continental low pressure increased during the day as rising warm air intensified the low pressure over land. Thus wind speed at Lüderitz increased from a morning minimum to a mid-afternoon maximum with a concomitant change in wind direction from south to southwest. Wind speed decreased again at night. Seasonal changes in this diurnal pattern were due to a northerly and offshore shift in the position of the SAA during the austral winter causing wind speeds to decrease at Lüderitz. However, southerly to southwesterly (upwelling favourable) winds prevailed throughout the year. A pattern of diurnal occurrence of "minor directions" (easterly, southeasterly, northwesterly and westerly winds), and calm ( $< 1.5 \text{ m.s}^{-1}$ ) was apparent, with seasonal differences.

*What is the seasonal pattern in wind speed at Lüderitz?*

The prevailing longshore (equatorward) winds at Lüderitz initiate and sustain coastal upwelling at one of the most intense eastern boundary upwelling cells in the world (Bakun 1996). Maximum wind speeds were measured from November to January in the austral summer, with a fourfold decrease in wind speed to a winter minimum in June / July (Chapter Four). The strength of the southerly winds predominated over that of the westerly component, easterly winds contributed to a higher degree of variability in wind speed during winter compared with the consistent summer winds.

The seasonal cycle of wind speed at Lüderitz is caused by the latitudinal movement of the SAA pressure centre during austral winter as well as by the winter northward migration of the Inter Tropical Convergence Zone causing higher pressure over the continent, thus a weakened geostrophic pressure gradient. The winter minimum in turbulent wind mixing ( $W^3$ ) off Lüderitz could facilitate fish migration through the upwelling cell. Turbulent mixing decreases the primary productivity in the Lüderitz region and it is consequently hypothesised that the upwelling cell forms a biological barrier due to low food availability for planktivorous fish, dividing the Benguela into a

northern and southern component with little exchange (by migration) of pelagic species (Agenbag and Shannon 1988). However, seasonally cold water temperatures in winter and minimal warming of the surface waters during periods of relaxation of upwelling-favourable winds in winter (Chapter Five) result in productivity remaining low in winter in Lüderitz despite the relatively low wind speeds from May to August (Chapter Four). Thus if the biological barrier is due to low chlorophyll biomass, the Lüderitz upwelling cell will remain a deterrent to migration during winter, despite reduced turbulent mixing in the water column.

*Can the wind regime at Dias Point be used as a proxy for upwelling events close inshore and within 20km of the coast?*

Coastal upwelling occurs in response to longshore equatorward winds, resulting in a divergence of surface water away from the coastal boundary. This causes upwelling of water from subsurface layers, thus significantly colder than surface water, at a rate directly proportional to the wind stress and inversely proportional to the sine of the latitude. Coastal upwelling areas are characterised by cooler than normal surface waters and the upward slope of isotherms towards the coast in active upwelling (Open University 1989).

It was apparent that southerly, longshore winds predominate, with a diurnal and seasonal pattern of intensity, throughout the year at Lüderitz (Chapter Three and Chapter Four). The following evidence linking high wind stress at Lüderitz to suppressed sea surface temperatures (SST) at the coast and to the breakdown of the thermocline in the water column (Chapter Five) was obtained from analysis of daily SST at Dias Point and from CTD profiles sampled within twenty kilometres of the coast:

- a significant relationship between daily wind stress (proportional to the square of the longshore, equatorward wind speed) and SST throughout the year was determined, the strongest relationship was found during highest wind stress in summer.

- SST warmer than 15°C was measured only during calm to northerly conditions in summer when relaxation of wind stress caused surface warming and stratification of the nearshore water column.
- resumption of southerly winds broke down the water column stratification and caused uplift of the isotherms at the coast one to two days after the wind started to blow.
- Temperature - Salinity (T-S) properties of water sampled during / after a southerly wind event conformed to those of Central Water masses, which are upwelled onto the shelf within the Benguela Current system near the coast due to equatorward wind forcing (Duncombe Rae 2005).

*What long-term changes in the wind regime have taken place on an interannual and interdecadal time scale of a) wind speed and b) wind direction?*

The analysis of changes in the wind regime at Lüderitz between 1960 and 2006, presented in Chapter Six, has shown interdecadal variation in wind-driven upwelling intensity that could underlie ecosystem-wide changes or regime shifts that have been documented for the Northern Benguela (Cury and Shannon 2004). A turning point in this time series was identified in 1975 when wind stress changed from below average to a 13-year period of intense upwelling-favourable winds, throughout most of the 1980s, ending in 1988. Subsequently, wind stress was below average for 18 years (1988 to 2006), with the exception of strong wind stress during a cold event in 1996 - 1998. While the frequency of occurrence of South winds did not change during the time series, there were significant changes in the frequency of North winds and the occurrence of calms (wind speed  $< 1.543 \text{ m.s}^{-1}$ ) in the South-North sector. Changes in the frequency of West and East winds also occurred during the time series.

Superimposed on the long term changes in the wind regime at Lüderitz are the occurrence of major environmental anomalies (Benguela Niños) which originate in the tropical Atlantic ocean and have severe biological effects at all levels of the food web (Roux 2003, Roux and Shannon 2004). These large scale, persistent warm

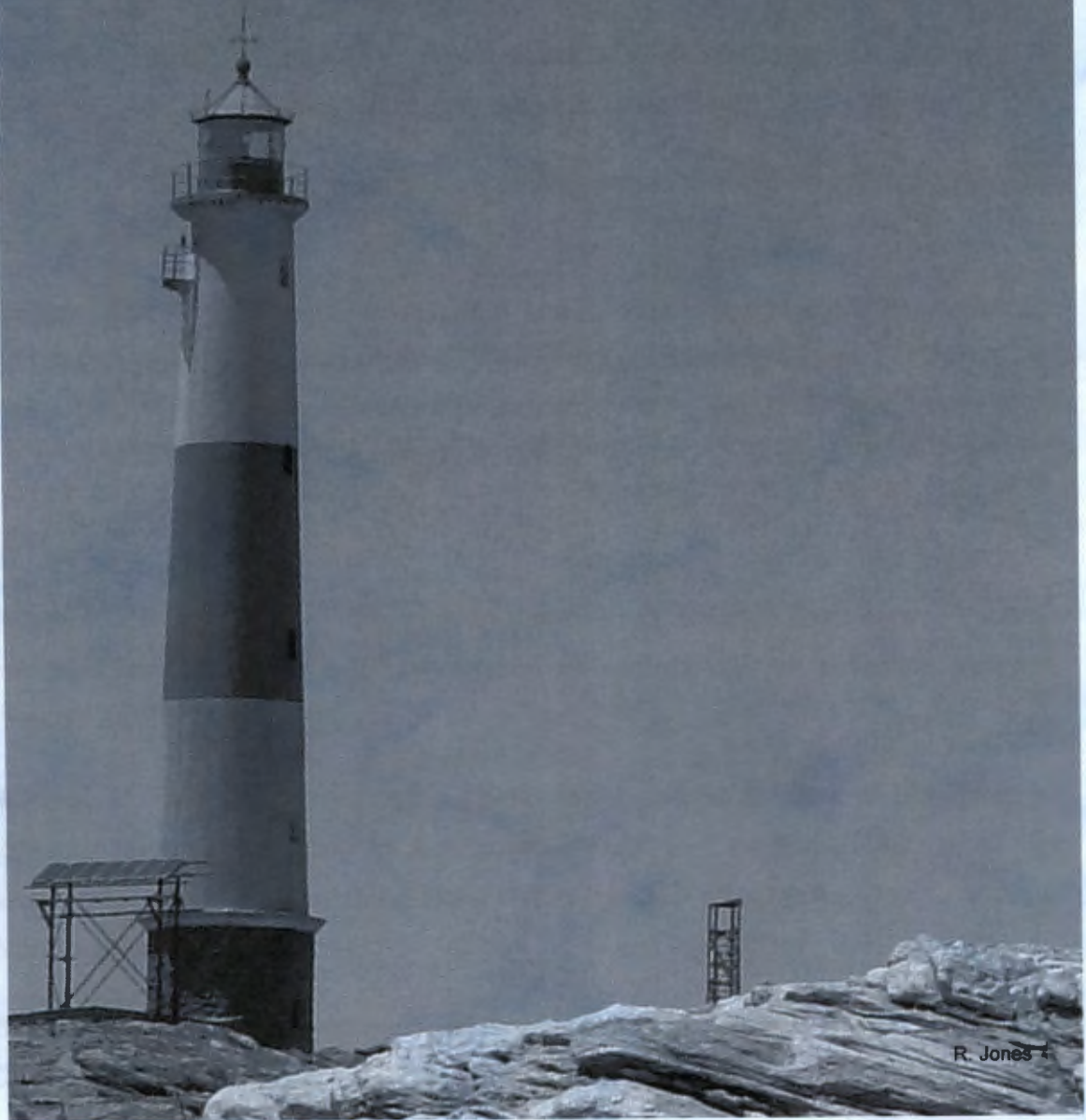
events occur during the seasonal cycle of the summer southward migration of the Angola-Benguela front, having their origin in the equatorial sub-surface SST anomalies which are manifested in salinity and SST anomalies in the Northern Benguela ecosystem (Gammelsrød *et al.* 1998). The link to the Pacific ENSO events is hypothesized but the relationships between the equatorial and Benguela events is not fully understood nor why equatorial wind anomalies do not always lead to significant SST anomalies off Angola (Bakun 1996). The interaction between the wind-driven upwelling cell at Lüderitz, at a seasonal maximum in summer when warm events and Benguela Niños historically occur in the Northern Benguela, has also not been determined. During the Benguela Niños of 1963, 1973 / 1974 and 1995, reduced wind stress and low frequency of south winds was recorded at Lüderitz. Wind stress was also below average during warm events in 1988 and 1999. It is likely that strong wind stress and active upwelling at Lüderitz could prevent the potential southward progression of anomalously warm water during relaxations of the Angola – Benguela front.

Recent regional scientific effort in the Benguela Current Large Marine Ecosystem (BCLME) has been focused on the assessment of environmental variability and its ecosystem impacts as a means of improving predictability in order to implement enhanced management strategies for the living marine resources within the BCLME (Shannon *et al.* 2006). Forecasting is based on an understanding of the variability of key environmental parameters, such as wind forcing, at time scales ranging from hours to months, years to decades (Shannon 2006). The identified key parameter must have been monitored at the correct locality and at the correct time scale and cause-effect linkages must have been established in order to develop a useful fisheries management tool. The time series of wind at Lüderitz is a potentially important predictive tool in combination with process and modelling studies. Of concern is the relative sparseness of *in situ* observations in the Benguela region which could hamper prediction efforts due to lack of data with which to validate model outputs (Reason *et al.* 2006). Currently, wind stress at Lüderitz is used to predict recruitment of top predators such as Cape Fur Seals (*Arctocephalus pusillus pusillus*) (MFMR unpublished data) and African Penguins (*Spheniscus demersus*) (Kemper 2006, Roux *et al.* 2007).

Ecological changes in the Northern Benguela ecosystem, namely the collapse of the small pelagic stocks such as sardine (*Sardinops sagax*) in the late 1960's, and the increase in the biomass of the bearded goby (*Sufflogobius bibartus*), horse mackerel (*Trachurus capensis*) and jellyfish, could not be ascribed to overfishing alone (Roux 2003). Climatic forcing can cause such regime shifts through bottom-up control of the food web via phyto- or zooplankton as a result of changes in circulation, intensity of upwelling and temperature (Cury and Shannon 2004). The observed major changes in upwelling intensity and pelagic resources have provided fuel for speculation on the effect of climate change such as global warming on the Benguela ecosystem (Bakun 1990, Roux 2003, Bakun and Weeks 2004). The two scenarios of increased (Bakun 1990) or decreased (Siegfried *et al.* 1990) upwelling intensity at Lüderitz would have extreme consequences for the biota of the Northern Benguela ecosystem (Roux 2003) indicating the importance of the Lüderitz upwelling cell. Changes in the wind regime at Lüderitz affect biological production through enhanced or reduced nutrient supply to the downstream marine environment.

The time series described in this thesis is the longest time series of coastal weather on the Namibian coast and is at a key locality at the main upwelling centre of the Benguela system. The measurements made at Lüderitz are crucial to the understanding of the dynamics and variability of the Northern Benguela and hence are of national interest to the Namibian Fisheries sector. The Ministry of Fisheries and Marine Resources should make every effort to secure the measurement site at Dias Point, (in cooperation with the landowner the Namibian Ports Authority, NAMPORT), and should ensure that accurate wind and air pressure measurements contribute to the long-term continuation of this time series.

# References



R. Jones

## References

- Agenbag JJ, Shannon LV (1988) A suggested physical explanation for the existence of a biological boundary at 24° 30'S in the Benguela system. *South African Journal of Marine Science* **6**: 119-132
- Andrews WRH, Hutchings L (1980). Upwelling in the southern Benguela current. *Progress in Oceanography* **9**: 1-81
- Anon (1998) Wind driven Transport Science Plan Technical Report *UMCES TS-170-98*. University of Maryland Center for Environmental Science, 18pp
- Bailey GW (1979) Physical and chemical aspects of the Benguela current in the Lüderitz region. MSc Thesis, University of Cape Town, South Africa, 225 pp
- Bakun A (1990) Global climate change and intensification of coastal upwelling. *Science* **247**:198-201
- Bakun A (1996) *Patterns in the Ocean: Ocean Processes and Marine Population Dynamics*. Sea Grant College System, University of California 323pp
- Bakun A, Nelson CS (1991) The seasonal cycle of wind-stress curl in subtropical eastern boundary current regions. *Journal of Physical Oceanography* **21 (12)**: 1815-1834
- Bakun A, Weeks S (2004) Greenhouse gas buildup, sardines, submarine eruptions and the possibility of abrupt degradation of intense marine upwelling systems. *Ecology Letters* **7**: 1015-1023
- Barange M, Pillar SC, Hutchings L (1992) Major pelagic borders of the Benguela upwelling system according to euphausiid distribution. In: Payne AIL, Brink KH, Mann KH, Hilborn R (eds) *Benguela Trophic Functioning*. *South African Journal of Marine Science* **12**: 3-17
- Boyd AJ (1987) The oceanography of the Namibian shelf. PhD Thesis, University of Cape Town, South Africa, 190pp

Boyer DC, Hampton I (2001) An overview of the living marine resources of Namibia. In: Payne AIL, Pillar SC, Crawford RJM (eds) A decade of Namibian Fisheries Science. *South African Journal of Marine Science* **23**: 5-35

Carr M-E (2002) Estimation of potential productivity in Eastern Boundary Currents using remote sensing. *Deep Sea Research II* **49**: 59-80

Carr M-E, Kearns EJ (2003) Production regimes in four Eastern Boundary Current systems. *Deep-Sea Research II* **50**: 3199-3221

Copenhagen WJ (1953) The periodic mortality of fish in the Walvis region. A Phenomenon within the Benguela Current. *Investigational Report Division of Fisheries South Africa* **14**: 1-35

Crawford RJM, Siegfried WR, Shannon LV, Villacastin-Herrero CA, Underhill LG (1990) Environmental influences on marine biota off Southern Africa. *South African Journal of Science* **86**: 330-339

Crawford RJM, Shannon LJ, Kreiner A, van der Lingen CD, Alheit J, Bakun A, Boyer D, Cury P, Dunne T, Durand M-H, Field JG, Fréon P, Griffiths M, Hagen E, Hutchings L, Klingelhoeffer E, Moloney CL, Mouton D, Roy C, Roux J-P, Shannon LV, Shillington FA, Underhill LG, Verheye HM (unpublished manuscript) Periods of major change in the structure and functioning of the pelagic component of the Benguela ecosystem, 1950 - 2000

Cury P, Roy C (1989) Optimal environmental window and pelagic fish recruitment success in upwelling areas. *Canadian Journal of Fisheries and Aquatic Science* **46(4)**: 670-680

Cury P, Shannon L (2004) Regime shifts in upwelling ecosystems: observed changes and possible mechanisms in the northern and southern Benguela. *Progress in Oceanography* **60**: 223-243

De Villiers DJ, Roux J-P (1992) Mortality of newborn pups of the South African Fur Seal *Arctocephalus pusillus pusillus* in Namibia. In: Payne AIL, Brink KH, Mann KH,

Hilborn R (eds). *Benguela Trophic Functioning*. *South African Journal of Marine Science* **12**:881-889

Duncombe Rae CM (2005) A demonstration of the hydrographic partition of the Benguela upwelling ecosystem at 26° 40'S. *African Journal of Marine Science* **27** (3): 617-628

Florenchie P, Lutjeharms JRE, Reason CJC, Masson, Rouault M (2003) The source of Benguela Niños in the South Atlantic Ocean. *Geophysical Research Letters* **30** (10): 12-1 - 12-4

Gammelsrød T, Bartholomae CH, Boyer DC, Filipe VLL, O' Toole MJ (1998) Intrusion of warm surface water along the Angolan-Namibian coast in February - March 1995: The 1995 Benguela Niño. *South African Journal of Marine Science* **19**: 41-56

Grobler CAF, Noli-Peard KR (1997) *Jasus lalandii* fishery in post-Independence Namibia: monitoring population trends and stock recovery in relation to a variable environment. *Marine and Freshwater Research* **48** (8): 1015-1022

Grobler CAF, Peard KR (2006) Ministry of Fisheries Internal Report to the Marine Advisory Council of Namibia. September 2006, pp29-45

Hagen E, Feistel R, Agenbag JJ, Ohde T (2001) Seasonal and Interannual changes in Intense Benguela Upwelling (1982-1999). *Oceanologica Acta* **24**: 557-568

Hardman-Mountford NJ, Richardson AJ, Agenbag JJ, Hagen E, Nykjaer L, Shillington FA, Villacastin C (2003) Ocean climate of the South East Atlantic observed from satellite data and wind models. *Progress in Oceanography* **59**: 181-221

Hart TJ, Currie RI (1960) The Benguela Current. *Discovery Report* **31**: 123-298

Hewitt CN (ed) (1992) *Methods of Environmental Data Analysis*. Elsevier, London, 309 pp

Hutchings L, Pitcher GC, Probyn TA, Bailey GW (1994) The chemical and biological consequences of coastal upwelling. In: Summerhayes CP, Emeis K-C, Angel MV, Smith RL, Zeitzschel B (eds) *Upwelling in the Ocean: Modern Processes and Ancient records*. Wiley, New York, pp 65-82

Jury MR (1996) South-east Atlantic warm events: composite evolution and consequences for southern African climate. *South African Journal of Marine Science* **17**:21-28

Jury MR, Brundrit GB (1992) Temporal organization of upwelling in the southern Benguela ecosystem by resonant coastal trapped waves in the ocean and atmosphere. In: Payne AIL, Brink KH, Mann KH, Hilborn (eds) *Benguela Trophic Functioning*. *South African Journal of Marine Science* **12**:219-224

Johnson AS, Nelson G (1999) Ekman estimates of upwelling at Cape Columbine based on measurements of longshore wind from a 35-year time-series. *South African Journal of Marine Science* **21**: 433-436

Kalnay E, Kanamitsu M, Kistler R, Collins W, Deaven D, Gandin L, Iredell M, Saha S, White G, Woollen J, Zhu Y, Leetmaa A, Reynolds B, Chelliah M, Ebisuzaki W, Higgins W, Janowiak J, Mo KC, Ropelewski C, Wang J, Jenne R, Joseph D (1996) The NCEP/NCAR 40-Year Reanalysis Project. *Bulletin of the American Meteorological Society* **77** (3): 437-471

Kemper J (2006) Heading towards extinction? Demography of the African Penguin in Namibia. PhD thesis, University of Cape Town, South Africa, 248 pp.

Mann KH and Lazier JRN (1991) *Dynamics of Marine Ecosystems: Biological-Physical Interactions in the Oceans*. Blackwell, Oxford, 466pp

Nelson G (1992) Equatorward wind and atmospheric pressure spectra as metrics for primary productivity in the Benguela system. In: Payne AIL, Brink KH, Mann KH, Hilborn R (eds). *Benguela Trophic Functioning*. *South African Journal of Marine Science* **12**: 19-28

Nelson G, Hutchings, L (1983) The Benguela upwelling area. *Progress in Oceanography* **12**: 333-356

Open University (1989) *Ocean Circulation*. Pergamon, Oxford, 238pp

Parrish RH, Bakun A, Husby DM, Nelson CS (1983) Comparative climatology of selected environmental processes in relation to eastern boundary current pelagic fish reproduction. In: Sharp GD, Csirke J (eds) Proceedings of the Expert Consultation to Examine Changes in Abundance and Species Composition of Neritic Fish Resources, San José, Costa Rica, April 1983. *FAO Fisheries Report* **291 (3)**: 731-777

Peard KR, Roux J-P (2002) Influence of upwelling dynamics on bottom dissolved oxygen in Lüderitz. Abstract, *Southern African Marine Science Symposium, SAMSS 2002*, Symposium Handbook, BENEFIT SANCOR, Swakopmund, Namibia

Reason CJC, Jury MR (1990). On the generation and propagation of the southern African coastal low. *Quarterly Journal of the Royal Meteorological Society* **116**: 1133-1151

Reason CJC, Florenchie P, Rouault M, Veitch J (2006) Influences of Large Scale Climate Modes and Agulhas System Variability on the BCLME Region. *Large Marine Ecosystems* **14**: 223-238

Roux J-P (1998) The impact of environmental variability on the seal population. *Namibia Brief* **18**:138-140

Roux J-P (2002) The Present Environmental Anomaly: Summer 2001-2002. Unpublished report, Ministry of Fisheries and Marine Resources Namibia, 3pp

Roux J-P (2003) Risks. In: Molloy F, Reinikainen T (eds) *Namibia's Marine Environment*. Directorate of Environmental Affairs of the Ministry of Environment and Tourism, Windhoek, Namibia pp 137-152

Roux J-P, Shannon LJ (2004) Ecosystem approach to fisheries management in the northern Benguela: the Namibian experience. *African Journal of Marine Science* **26**: 79-93

Roux J-P, Peard KR, Grobler CAF (2000) Seasonal Report Summer 1999 – 2000. Unpublished report, Ministry of Fisheries and Marine Resources Namibia, 17pp

Roux J-P, Kemper J, Peard KR (2007) Top predator responses to environmental variability in an intense upwelling system. Report BCLME LMR/EAF/03/02: Top Predator Project

Servain J, Dessier A. (1999) Relationship between the equatorial and meridional modes of climatic variability in the tropical Atlantic. *Geophysical Research Letters* **26** (4): 485-488

Shannon LV (1970) Oceanic circulation off South Africa. *Fisheries Bulletin* **6**: 27-33

Shannon LV (1985) The Benguela ecosystem. 1. Evolution of the Benguela, physical features and processes. In: Barnes M (ed) *Oceanography and Marine Biology. An Annual Review* **23**: 105-182

Shannon V (2006) A plan comes together. In Shannon V, Hempel G, Malanotte-Rizzoli P, Moloney C, Woods J. (eds) (2006) *Benguela: Predicting a Large Marine Ecosystem*. Elsevier, Amsterdam. *Large Marine Ecosystems* **14**: 3-10

Shannon, LV, Pillar SC (1986) The Benguela ecosystem. 3. Plankton. In Barnes M (ed) *Oceanography and Marine Biology. An Annual Review* **24**: 65-170

Shannon LV, Nelson G (1996) The Benguela: Large scale features and processes and system variability. In: Wefer G, Berger WH, Siedler G, Webb DJ (eds) *The South Atlantic: Present and Past Circulation*, Springer Verlag, Berlin, pp 163-210

Shannon LV, Agenbag JJ (1990) A large-scale perspective on interannual variability in the environment in the South-East Atlantic. *South African Journal of Marine Science* **9**: 161-168

Shannon LV, O'Toole M (1999) Integrated Overview of the oceanography and environmental variability of the Benguela Current region. BCLME Thematic Report No.2. 46pp, plus 17pp figures

Shannon LV, Boyd AJ, Brundrit GB, Taunton-Clark J (1986) On the existence of an El Niño-type phenomenon in the Benguela system. *Journal of Marine Research* **44**: 495-520

Shannon LV, Lutjeharms JRE, Nelson G (1990) Causative mechanisms for intra-annual change and interannual variability in the marine environment around southern Africa. *South African Journal of Science* **86**: 356-373

Shannon LV, Crawford RJM, Pollock DE, Hutchings L, Boyd AJ, Taunton-Clark J, Badenhorst A, Melville-Smith R, Augustyn CJ, Cochrane KL, Hampton I, Nelson G, Japp DW, Tarr RJQ (1992) The 1980's - a decade of change in the Benguela ecosystem. In: Payne AIL, Brink KH, Mann KH, Hillborn (eds) *Benguela Trophic Functioning*. *South African Journal of Marine Science* **12**: 271-296

Shannon V, Hempel G, Malanotte-Rizzoli P, Moloney C, Woods J. (eds) (2006) *Benguela: Predicting a Large Marine Ecosystem*. Elsevier, Amsterdam, 410 pp and CD-ROM

Shillington FA, Reason CJC, Duncombe Rae CM, Florenchie P, Penven P (2006) Large Scale Physical Variability of the Benguela Current Large Marine Ecosystem (BCLME). In: Shannon V, Hempel G, Malanotte-Rizzoli P, Moloney C, Woods J (eds) *Large Marine Ecosystems* **14**: 49-70

Siegfried WR, Crawford RJM, Pollock DE, Payne AIL, Krohn RG (1990) Scenarios for global-warming induced change in the open-ocean environment and selected fisheries of the west coast of Southern Africa. *South African Journal of Marine Science* **86**: 281-285

Smith RL (1995) The physical processes of coastal ocean upwelling systems. In: Summerhayes CP, Emeis K-C, Angel MV, Smith RL, Zeitzschel B (eds) *Upwelling in the Ocean: Modern Processes and Ancient records*. Wiley, New York, pp 39-64

Smith TM, Reynolds RW (2004) Reconstruction of monthly mean oceanic sea level pressure based on COADS and station data (1854-1997). *Journal of Atmospheric and Oceanic Technology* **21**: 1272-1282

Stander G H (1964) The pilchard of South West Africa (*Sardinops ocellata*). The Benguela current off South West Africa. *Administration of South West Africa Marine Research Laboratory Investigational Report*: **12**:1-43, plus 77pp figures

Tomalin BJ (1993) Migrations of spiny rock-lobster, *Jasus lalandii*, at Lüderitz: environmental causes, and effects on the fishery and benthic ecology. MSc Thesis, University of Cape Town, South Africa, 99 pp

Tyson PD, Preston-Whyte RA (2000) *The Weather and Climate of Southern Africa*. Oxford University Press, Cape Town 396 pp

Van der Lingen CD, Shannon LJ, Cury P, Kreiner A, Moloney CL, Roux J-P, Vaz-Velho F (2006) In: Shannon V, Hempel G, Malanotte-Rizzoli P, Moloney C, Woods J (eds) *Large Marine Ecosystems* **14**:147-184

Venegas SA, Mysak LA and Straub DN (1996) Evidence for interannual and interdecadal climate variability in the South Atlantic. *Geophysical Research Letters* **23** (19): 2673-2676

Walker ND (1987) Interannual sea surface temperature variability and associated atmospheric forcing within the Benguela system. In Payne ALL, Gulland, JA, Brink KH (eds) *The Benguela and Comparable Ecosystems*. *South African Journal of Marine Science* **5**: 121-132

Zar JH (1996) *Biostatistical Analysis*. Third edition. Prentice-Hall, London 662pp  
Appendix 205pp